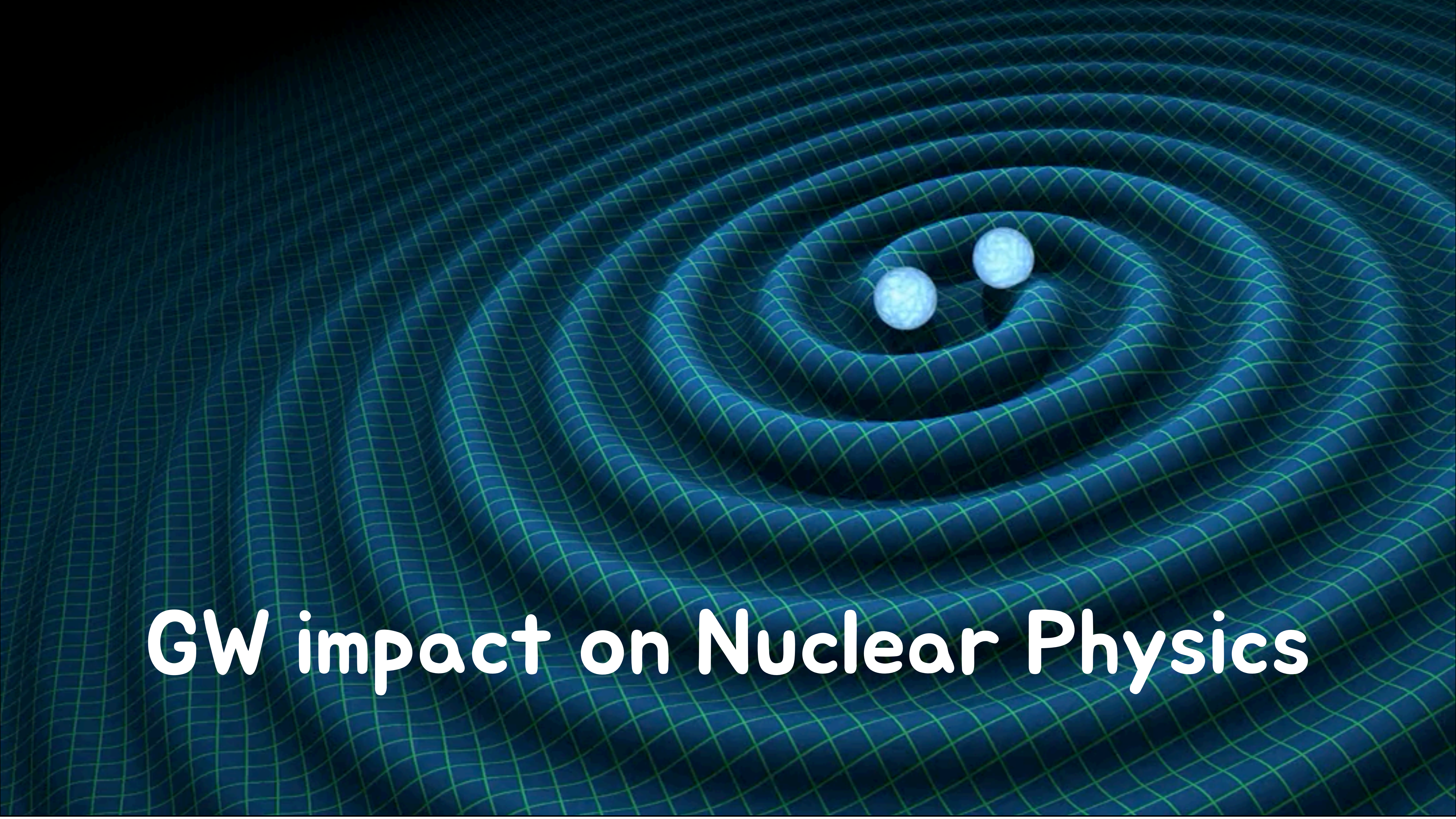

GW impact on Nuclear Physics

Kim, Young-Min (김영민)
Korea Astronomy and
Space Science Institute
(KASI)

Contact: ymkim@kasi.re.kr

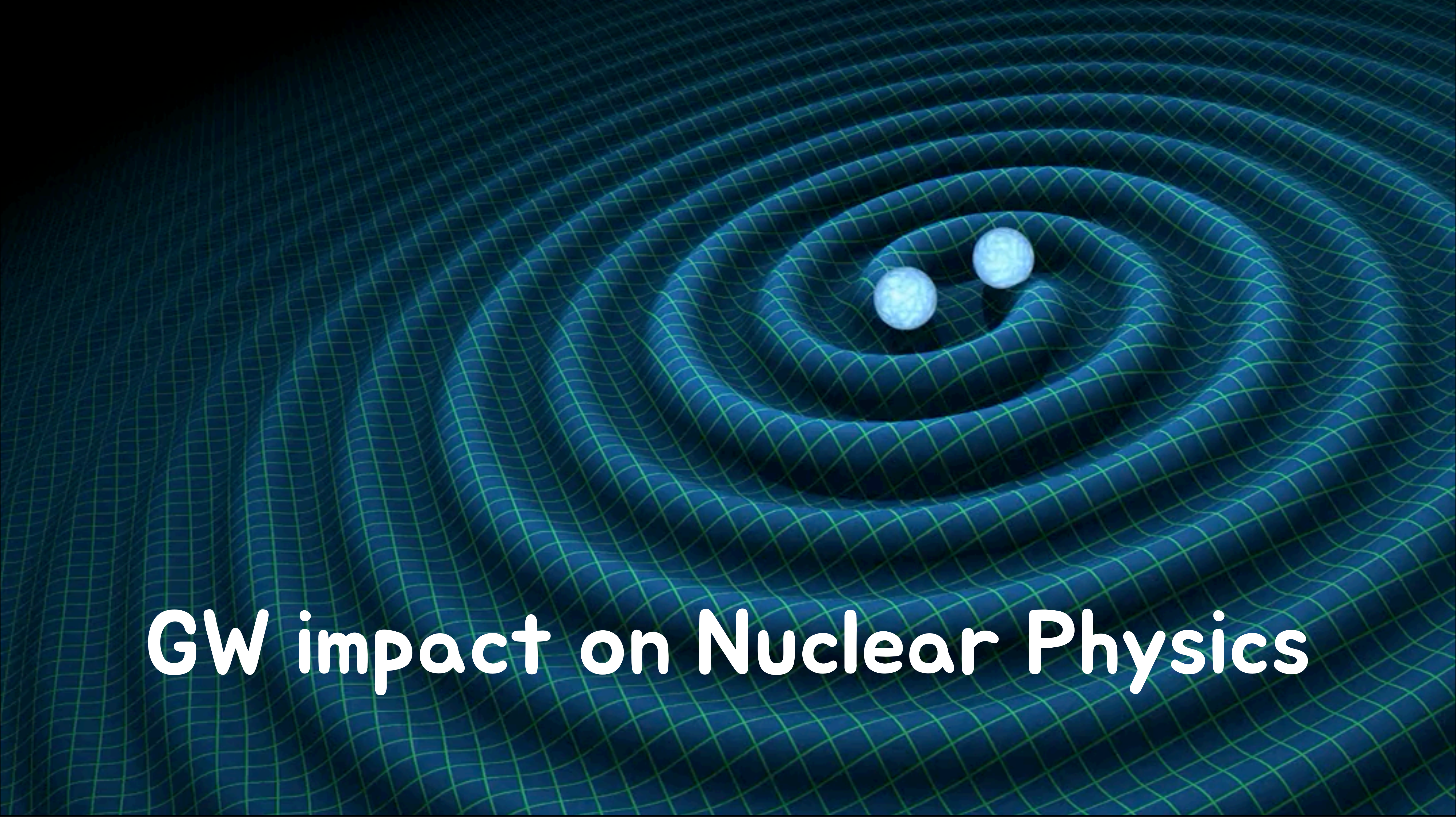

GW impact on Nuclear Physics

Kim, Young-Min (김영민)
Korea Astronomy and
Space Science Institute
(KASI)

Contact: ymkim@kasi.re.kr

Neutron Star

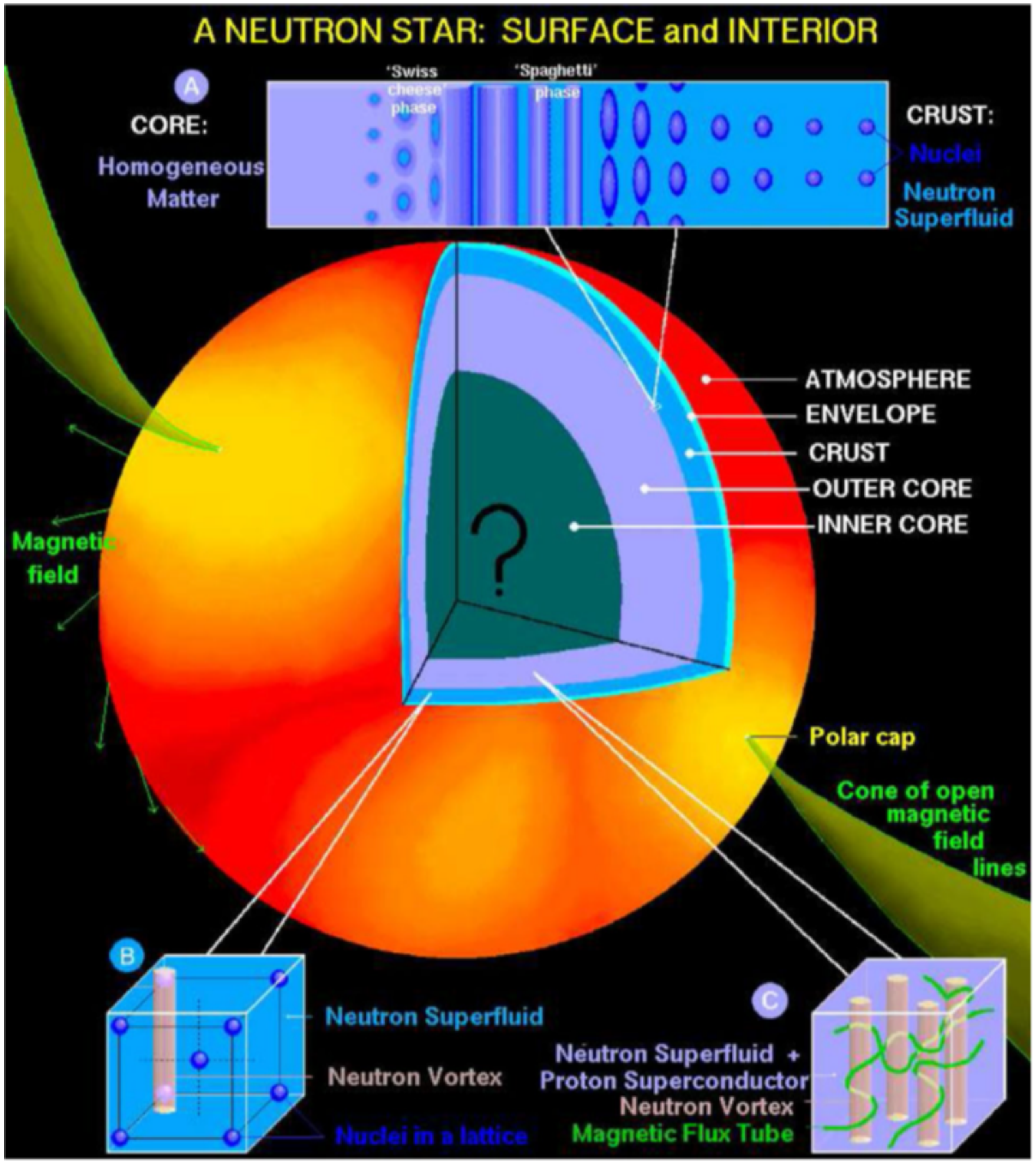

courtesy of D. Page

M= 1.4~2.0M$_\odot$

R=10~15km

A~ 10^{57} nucleons

$$\rho_{\text{center}} \approx \text{several} \times \rho_0$$

$$n_0 \approx 0.16\ \text{fm}^{-3} \approx 1.6 \times 10^{44}\text{m}^{-3}$$

$$\rho_0 \approx 2.04 \times 10^{17}\text{kg} \cdot \text{m}^{-3}$$

GW170817 : The Golden Binary

ApJL, 848:L12 (2017)

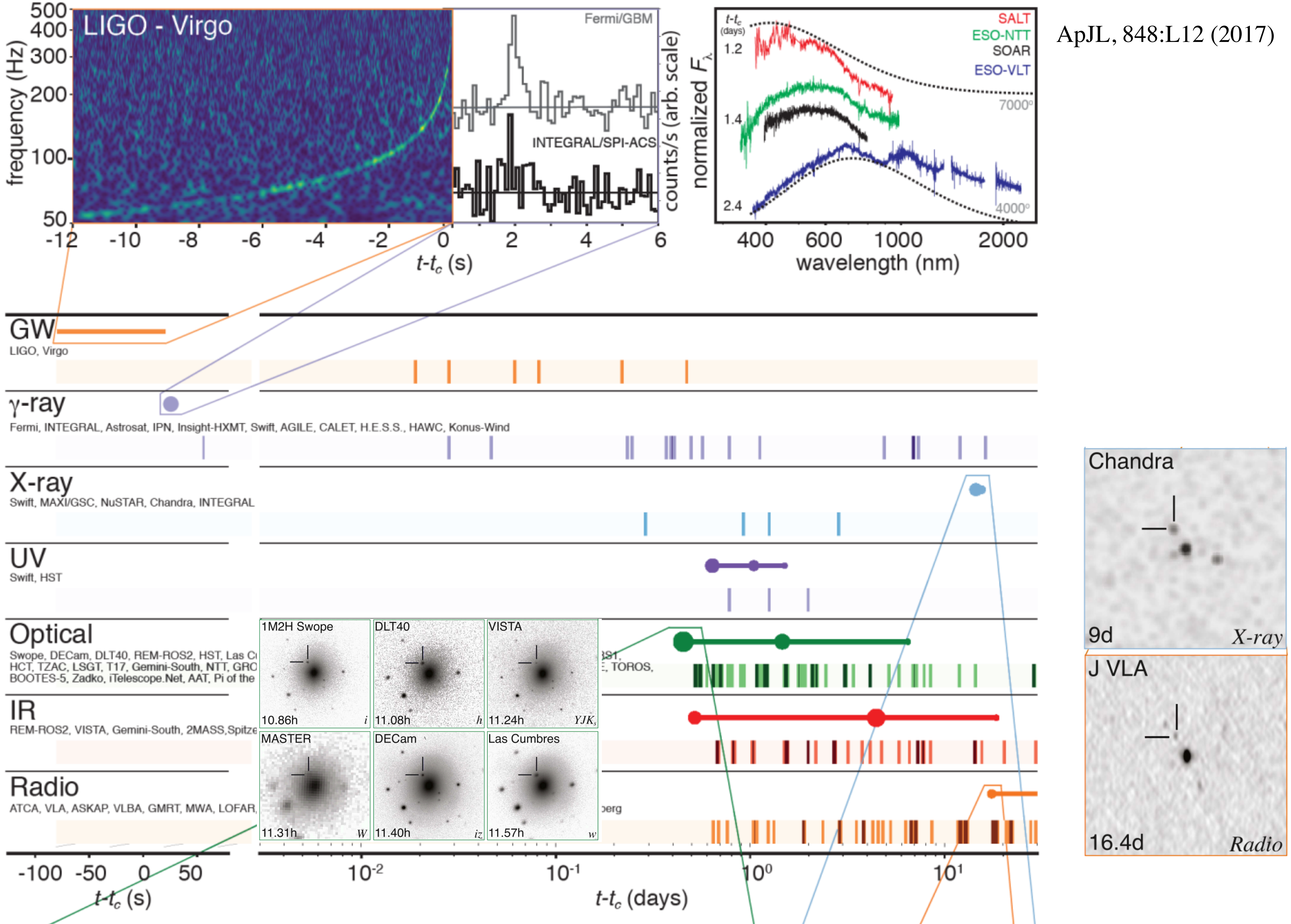

Dynamics of BNS merger, GW170817

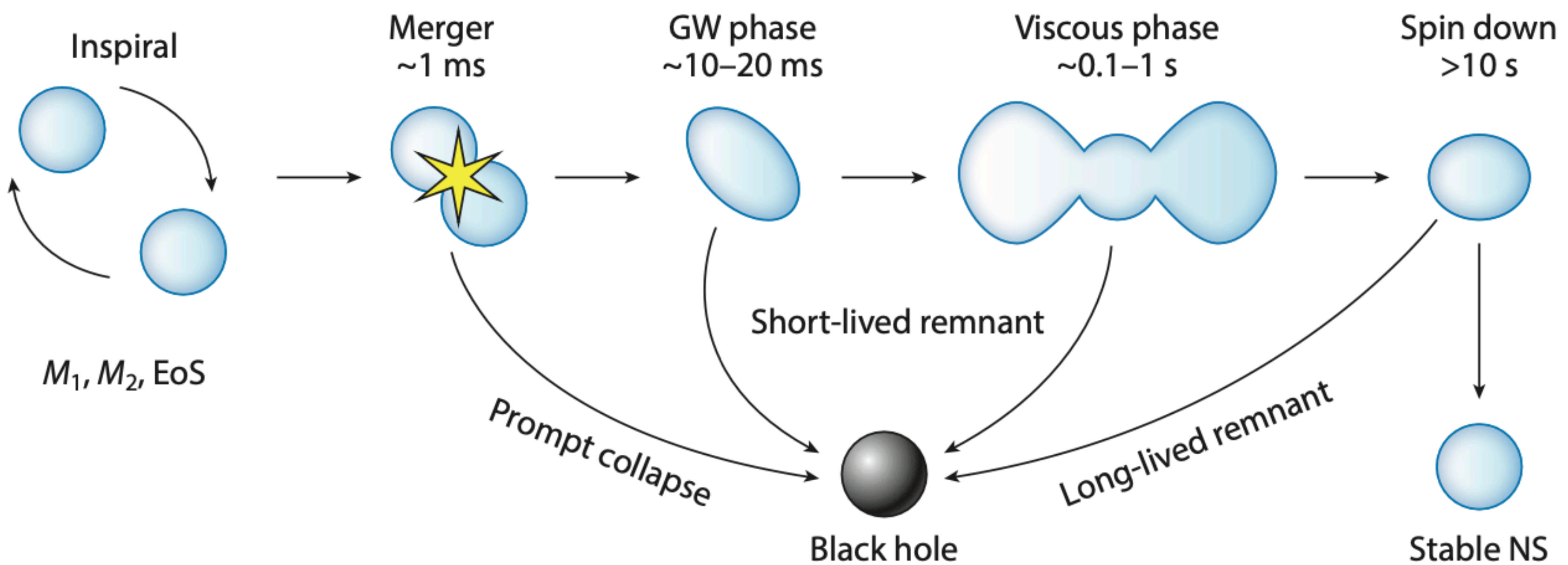

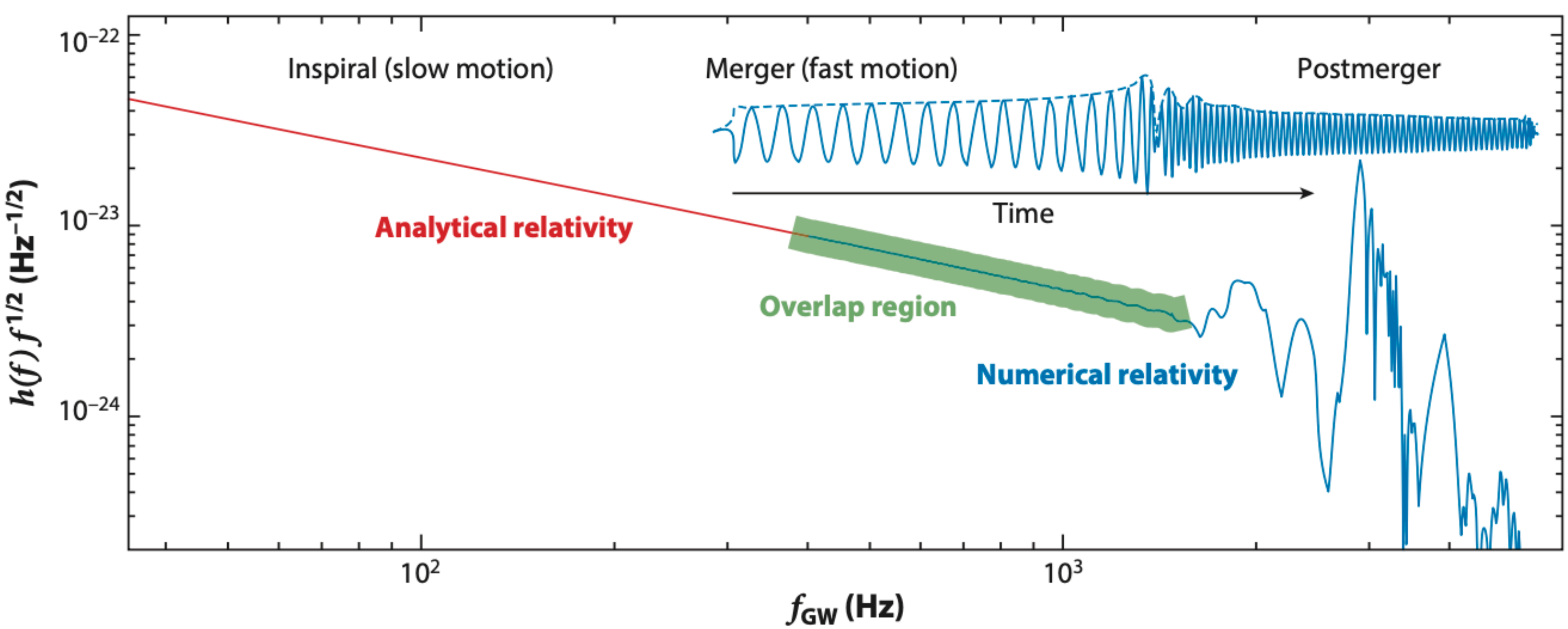

Radice et al. , Annu. Rev. Nucl. Part. Sci. 70, 95–119 (2020)

Dynamics of BNS merger, GW170817

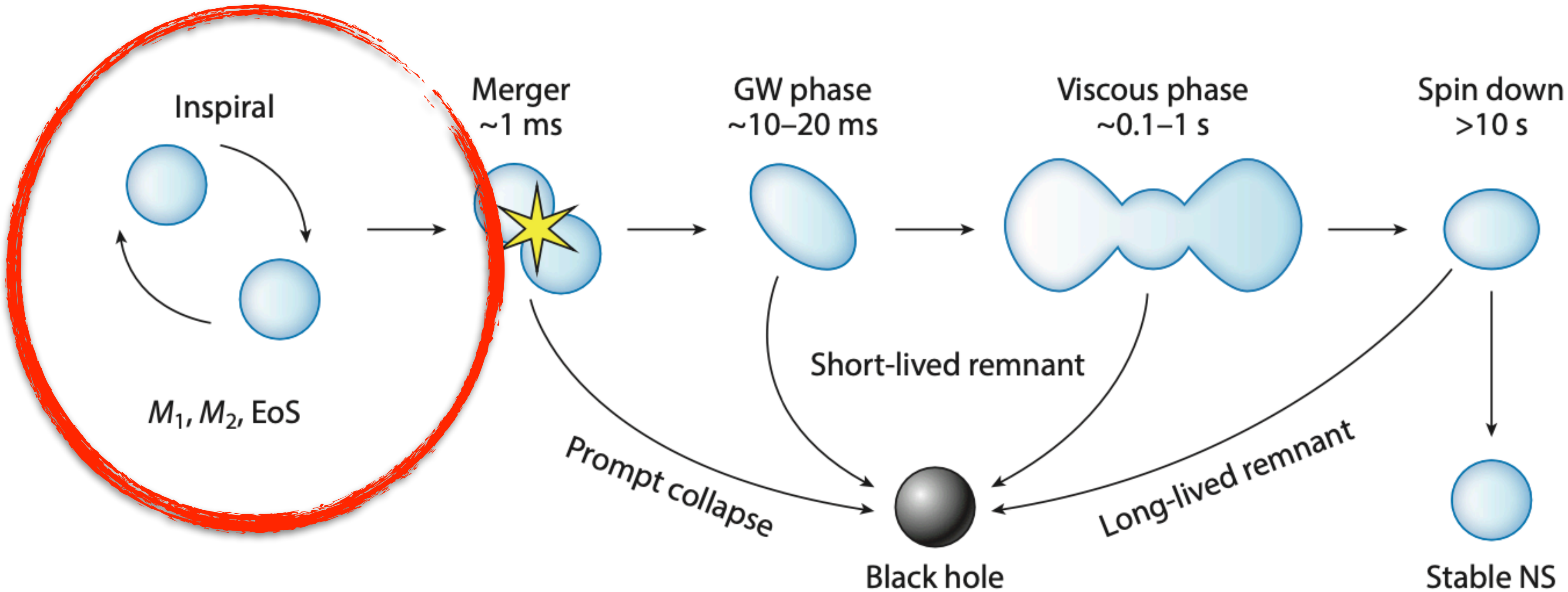

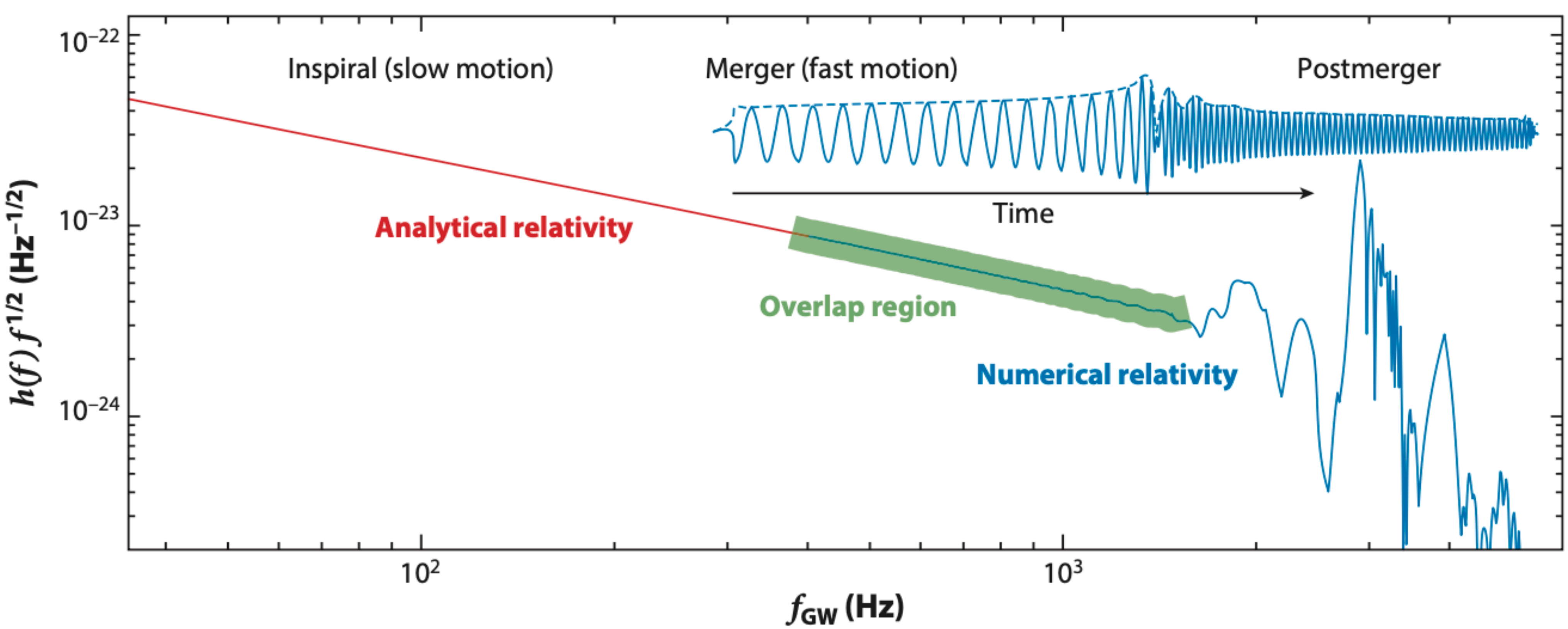

Radice et al. , Annu. Rev. Nucl. Part. Sci. 70, 95–119 (2020)

Properties of GW170817

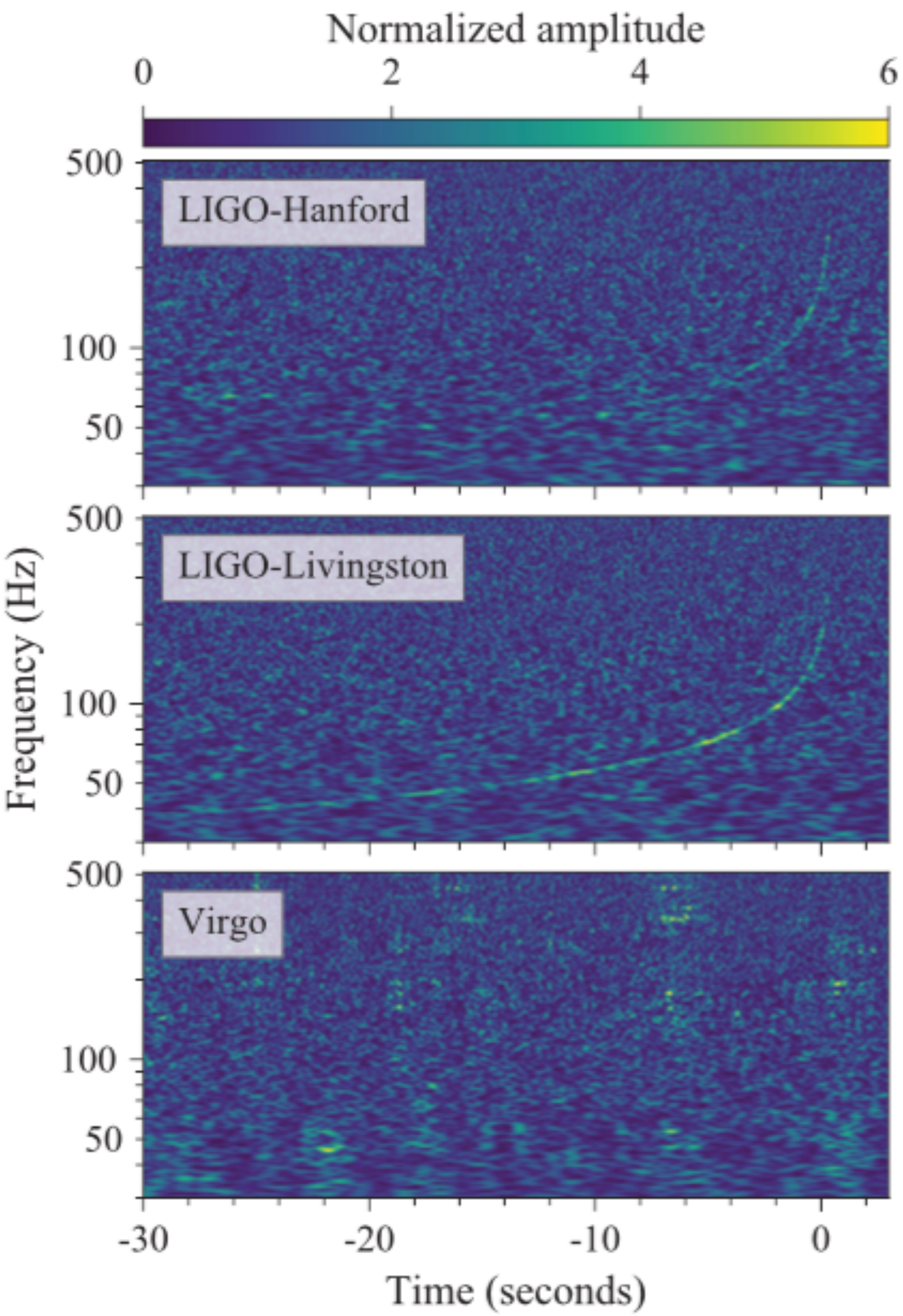

PRL 119, 161101 (2017)

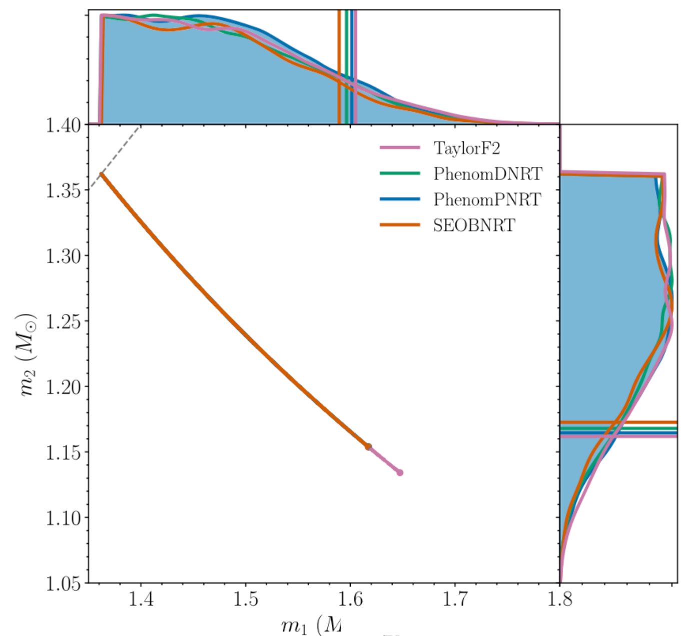

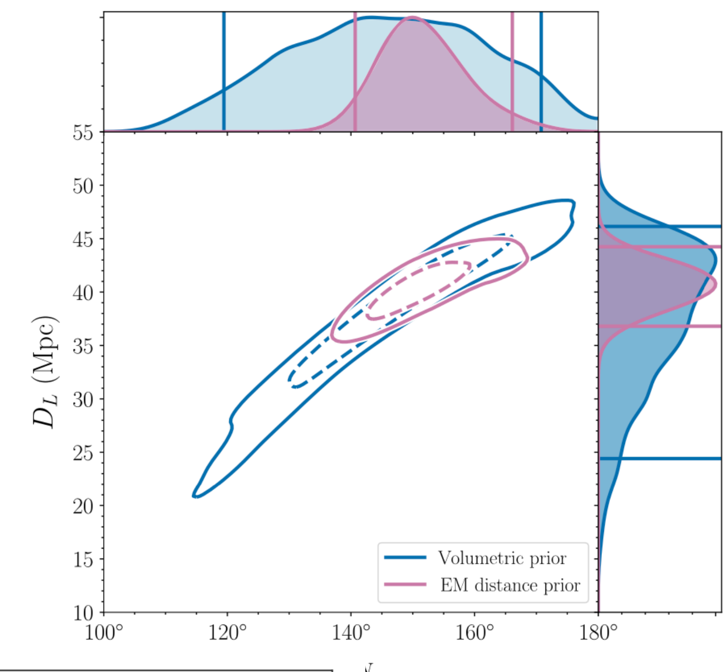

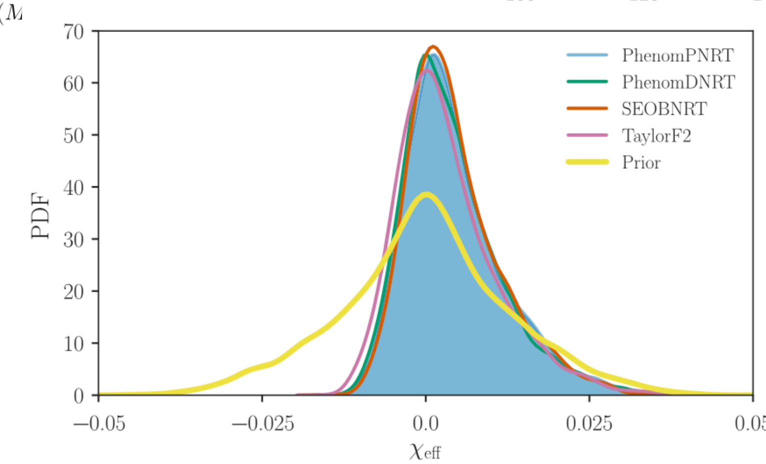

	Low-spin prior ($\chi \leq 0.05$)	High-spin prior ($\chi \leq 0.89$)
Binary inclination θ_{JN}	146^{+25}_{-27} deg	152^{+21}_{-27} deg
Binary inclination θ_{JN} using EM distance constraint [108]	151^{+15}_{-11} deg	153^{+15}_{-11} deg
Detector-frame chirp mass $\mathcal{M}^{\rm det}$	$1.1975^{+0.0001}_{-0.0001}$ $M_\odot$	$1.1976^{+0.0004}_{-0.0002}$ $M_\odot$
Chirp mass $\mathcal{M}$	$1.186^{+0.001}_{-0.001}$ $M_\odot$	$1.186^{+0.001}_{-0.001}$ $M_\odot$
Primary mass m_1	(1.36, 1.60) $M_\odot$	(1.36, 1.89) $M_\odot$
Secondary mass m_2	(1.16, 1.36) $M_\odot$	(1.00, 1.36) $M_\odot$
Total mass m	$2.73^{+0.04}_{-0.01}$ $M_\odot$	$2.77^{+0.22}_{-0.05}$ $M_\odot$
Mass ratio q	(0.73, 1.00)	(0.53, 1.00)
Effective spin $\chi_{\rm eff}$	$0.00^{+0.02}_{-0.01}$	$0.02^{+0.08}_{-0.02}$
Primary dimensionless spin χ_1	(0.00, 0.04)	(0.00, 0.50)
Secondary dimensionless spin χ_2	(0.00, 0.04)	(0.00, 0.61)
Tidal deformability $\tilde{\Lambda}$ with flat prior	300^{+500}_{-190}(symmetric)/300^{+420}_{-230}(HPD)	(0, 630)

PHYS. REV. X 9, 011001 (2019)

Response of NS to GW during inspiral

T. Hinderer, ApJ, 677, 1216 (2008)

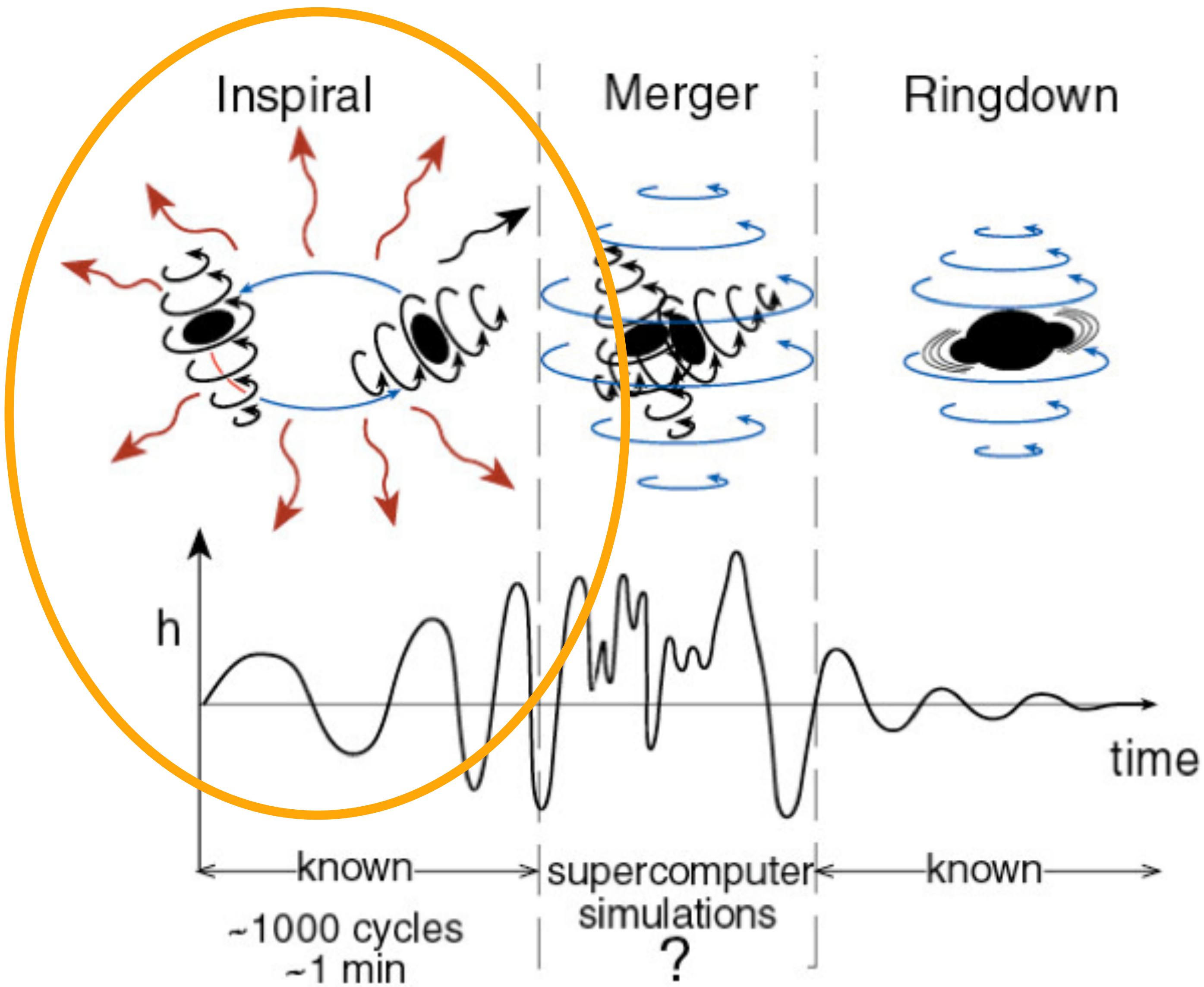

perturbative approaches

$$\frac{(1-g_{tt})}{2} = -\frac{M}{r} - \frac{3Q_{ij}}{2r^3}\left(n^i n^j - \frac{1}{3}\delta^{ij}\right) + O\left(\frac{1}{r^3}\right) + \frac{1}{2}\mathcal{E}_{ij}x^i x^j + O(r^3),$$

$$Q_{ij} = -\lambda \mathcal{E}_{ij}$$

$$\lambda = \frac{2}{3}\frac{R^5}{G}k_2$$

λ : Tidal deformability

Q_{ij} : Quadrupole moment of NS

$\mathcal{E}_{ij}$: External quadrupole tidal field

k_2 : l = 2 Tidal Love number

New EoS constraint : tidal deformability

$\Lambda(1.4M_\odot)=190^{+390}_{-120}$

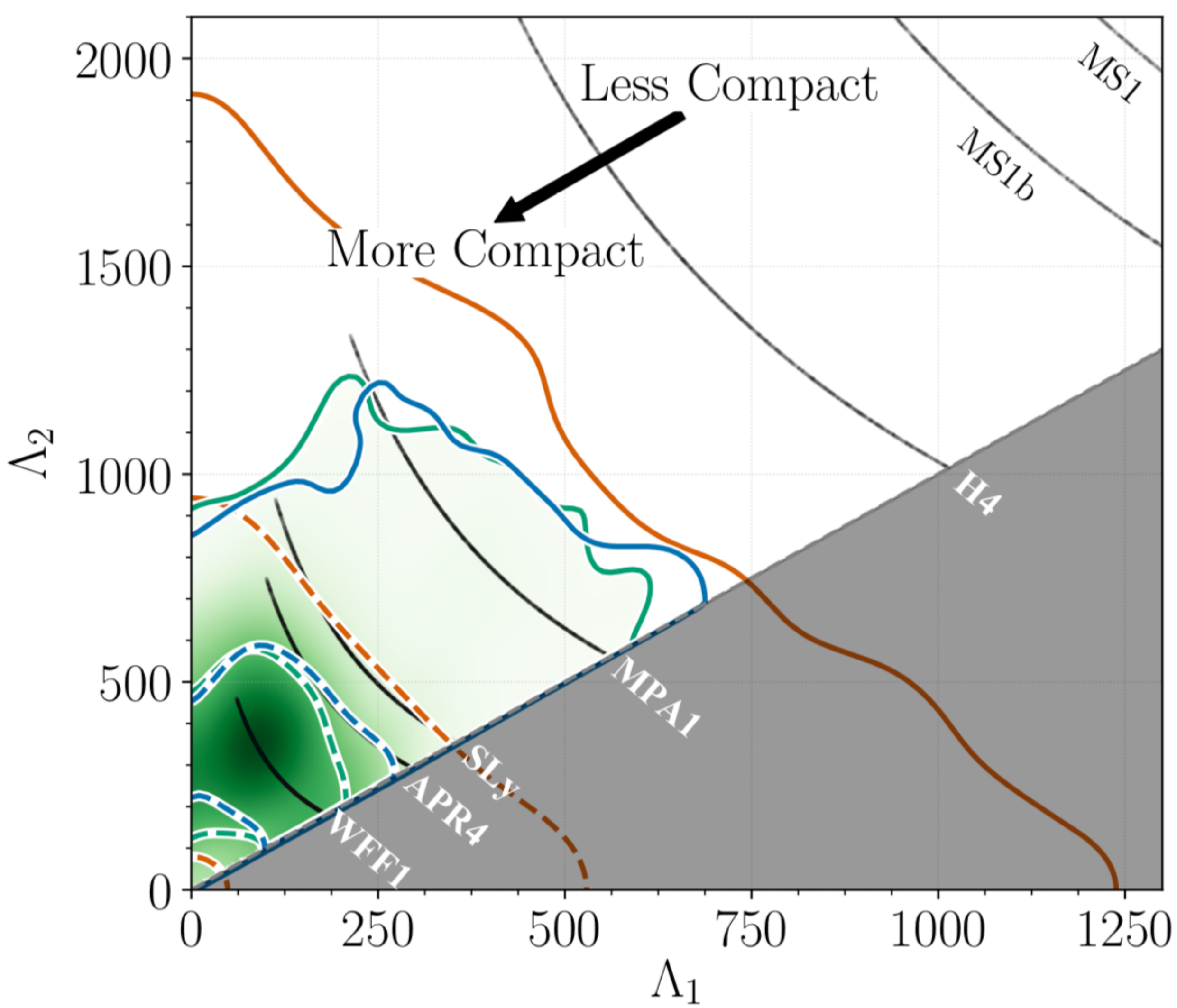

Abbott et al. (LSC and Virgo),
arxiv:1805.11581 (PhysRevLett.121.161101)

M. Favata, PRL.112.101101 (2014)

$$\tilde{h}_T(f) = \mathcal{A} f^{-7/6} e^{i\Psi_T}(f)$$

$$\Psi_\mathrm{T}(f) = \varphi_c + 2\pi f t_c + \frac{3}{128\eta v^5}\left(\Delta\Psi^{\mathrm{pp}}_{3.5\mathrm{PN}} + \Delta\Psi^{\mathrm{spin}}_{3\mathrm{PN}} + \Delta\Psi^{\mathrm{ecc.}}_{2\mathrm{PN}} + \Delta\Psi^{\mathrm{tidal}}_{6\mathrm{PN}} + \Delta\Psi^{\mathrm{tm}}_{6\mathrm{PN}}\right)$$

$$v = (\pi f M)^{1/3}$$

$$\Delta\Psi^{\mathrm{tidal}}_{6\mathrm{PN}} = -\frac{39}{2}\tilde{\Lambda} v^{10} + v^{12}\left(\frac{6595}{364}\delta\tilde{\Lambda} - \frac{3115}{64}\tilde{\Lambda}\right)$$

$$\tilde{\Lambda} = \frac{16}{13}\frac{(m_1+12m_2)m_1^4\Lambda_1 + (m_2+12m_1)m_2^4\Lambda_2}{(m_1+m_2)^5}$$

$$\Lambda = \lambda/M^5 \to G\left(\frac{c^2}{GM}\right)^5 \lambda = \frac{2}{3}\left(\frac{Rc^2}{GM}\right)^5 k_2$$

Measurement Errors of Tidal Deformability

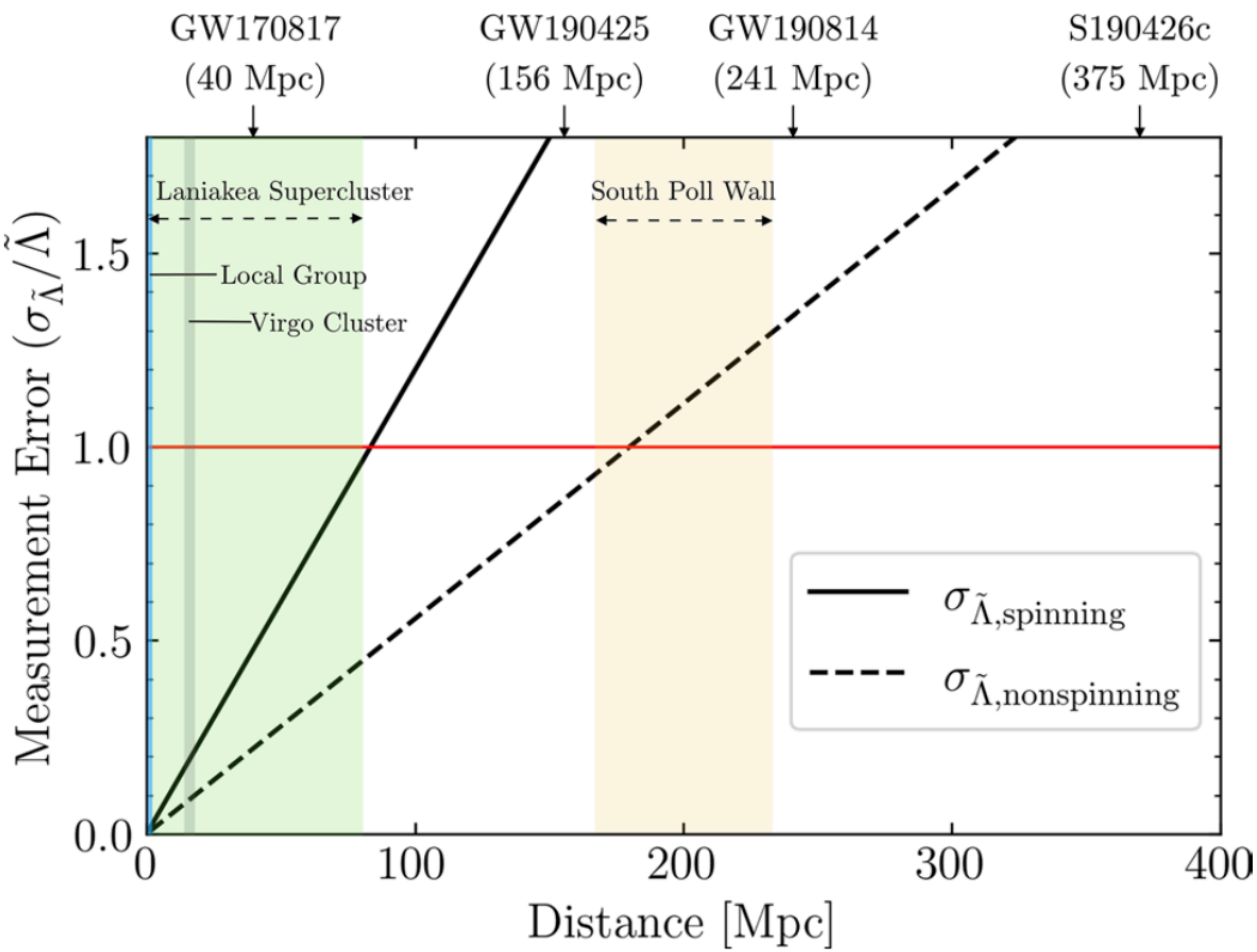

Kim, Kim, Kwak, Choi, Cho and Lee, JKPS (2021)

Calculations of Tidal Love number, k2

$$\frac{dH}{dr} = \beta \qquad \frac{d\beta}{dr} = 2\left(1-2\frac{M}{r}\right)^{-1} \times H\left\{-2\pi\left[5\epsilon+9P+(d\epsilon/dP)(\epsilon+P)\right]\right.$$

$$\left. + \frac{3}{r^2} + 2\left(1-2\frac{M}{r}\right)^{-1}\left(\frac{M}{r^2}+4\pi r P\right)^2\right\}$$

$$+ \frac{2\beta}{r}\left(1-2\frac{M}{r}\right)^{-1}\left\{-1+\frac{M}{r}+2\pi r^2(\epsilon-P)\right\}$$

TOV

$$\frac{dP}{dr} = -\frac{GM\rho}{r^2}\left(1+\frac{P}{\rho c^2}\right)\left(1+\frac{4\pi P r^3}{Mc^2}\right)\left(1-\frac{2GM}{rc^2}\right)$$

$$\frac{dM}{dr} = 4\pi r^2\left(\frac{\epsilon}{c^2}\right)$$

k2 (λ,Λ) depends on NS EoS !!

Compositions of a NS

F. Weber 2005

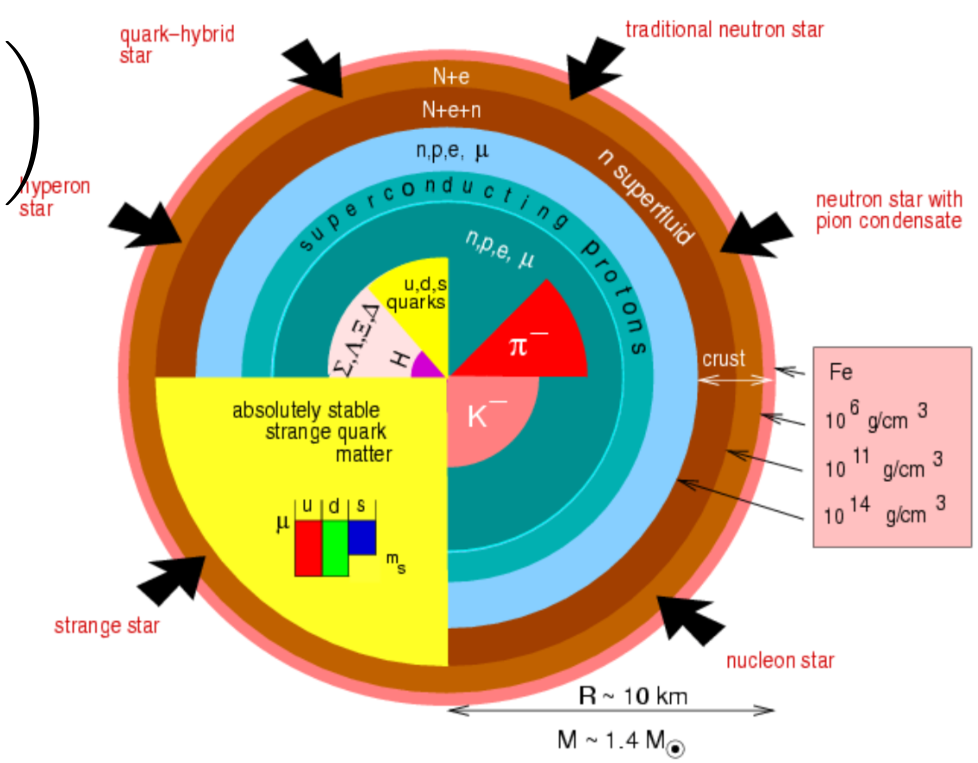

Calculations of Tidal Love number, k2

$$k_2 = \frac{8C^5}{5}(1-2C)^2[2+2C(y-1)-y] \times \left\{ 2C[6-3y+3C(5y-8)] + 4C^3[13-11y+C(3y-2)+2C^2(1+y)] + 3(1-2C)^2[2-y+2C(y-1)]\ln(1-2C) \right\}^{-1}$$

$$y = \frac{R\beta(R)}{H(R)}$$

$$\Lambda = \lambda/M^5 \to G\left(\frac{c^2}{GM}\right)^5 \lambda = \frac{2}{3}\left(\frac{Rc^2}{GM}\right)^5 k_2$$

TOV

$$\frac{dP}{dr} = -\frac{GM\rho}{r^2}\left(1+\frac{P}{\rho c^2}\right)\left(1+\frac{4\pi P r^3}{Mc^2}\right)\left(1-\frac{2GM}{rc^2}\right)$$

$$\frac{dM}{dr} = 4\pi r^2\left(\frac{\epsilon}{c^2}\right)$$

k2 (λ,Λ) depends on NS EoS !!

Compositions of a NS

F. Weber 2005

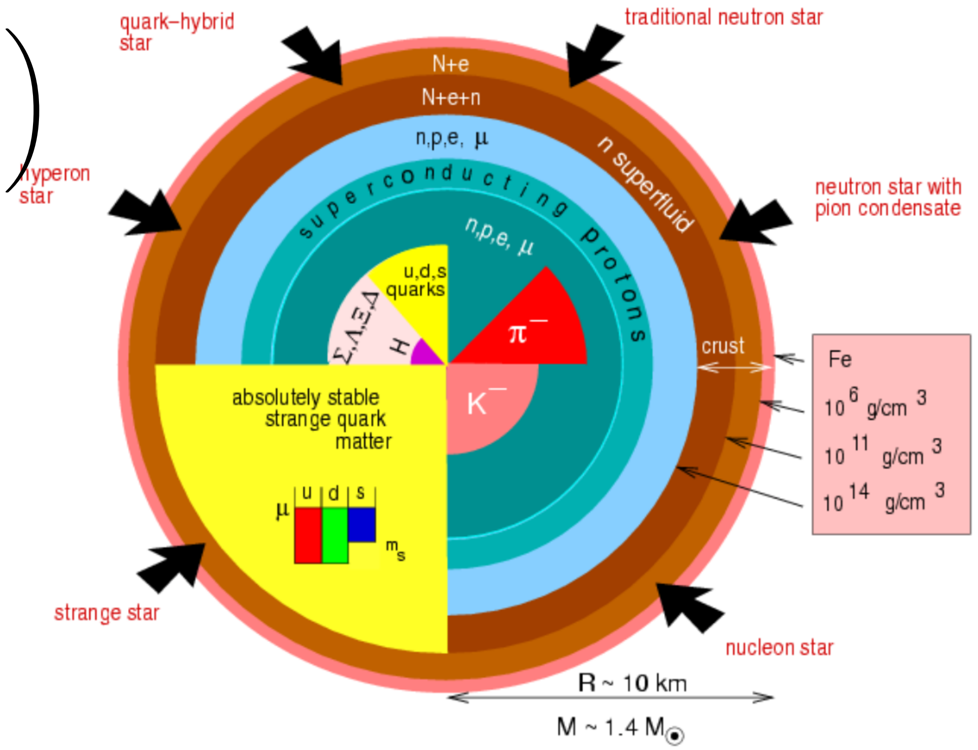

EoS : Nucleus and Strong force

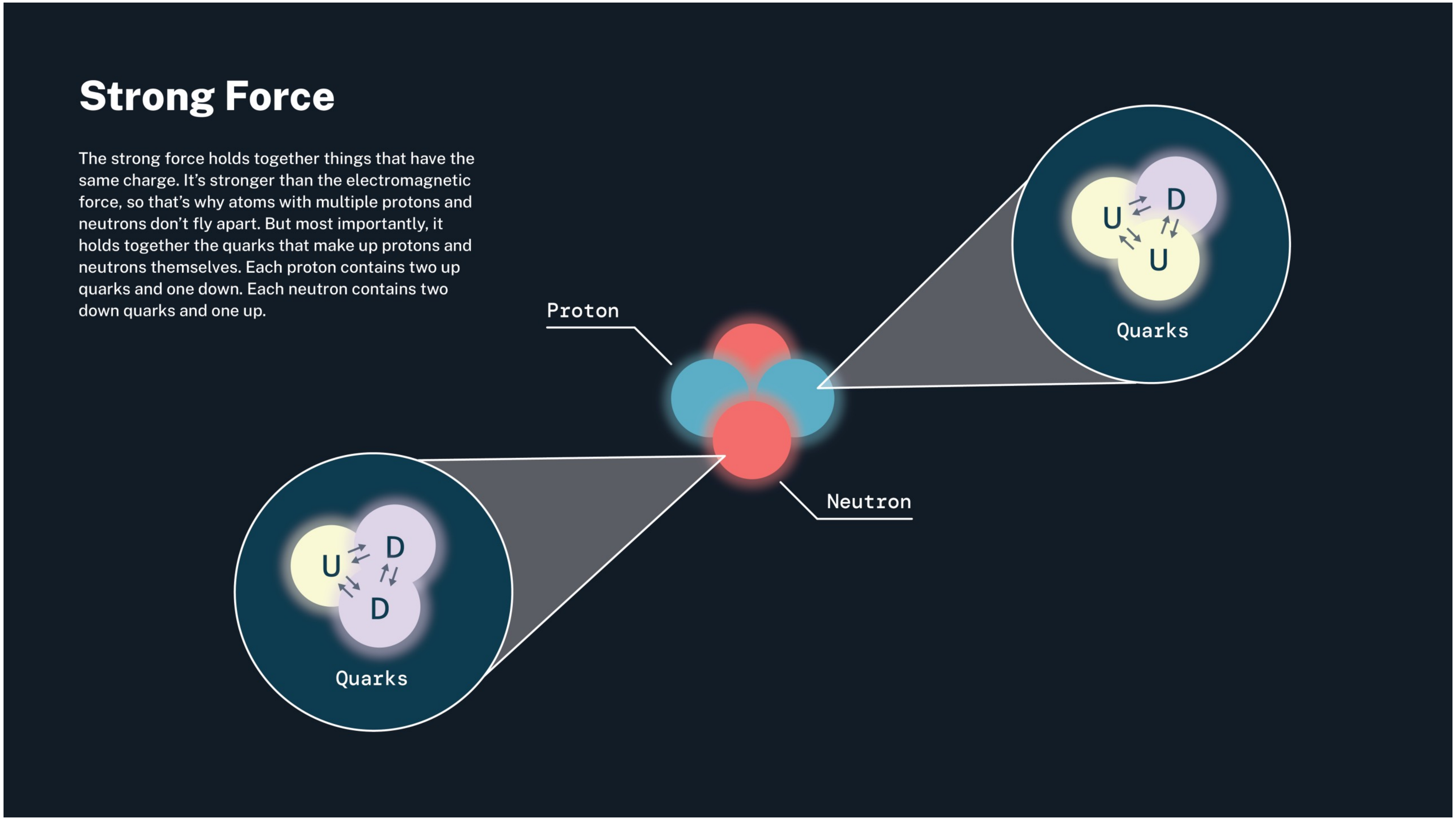

Image: NASA

Effective field theories and energy scales

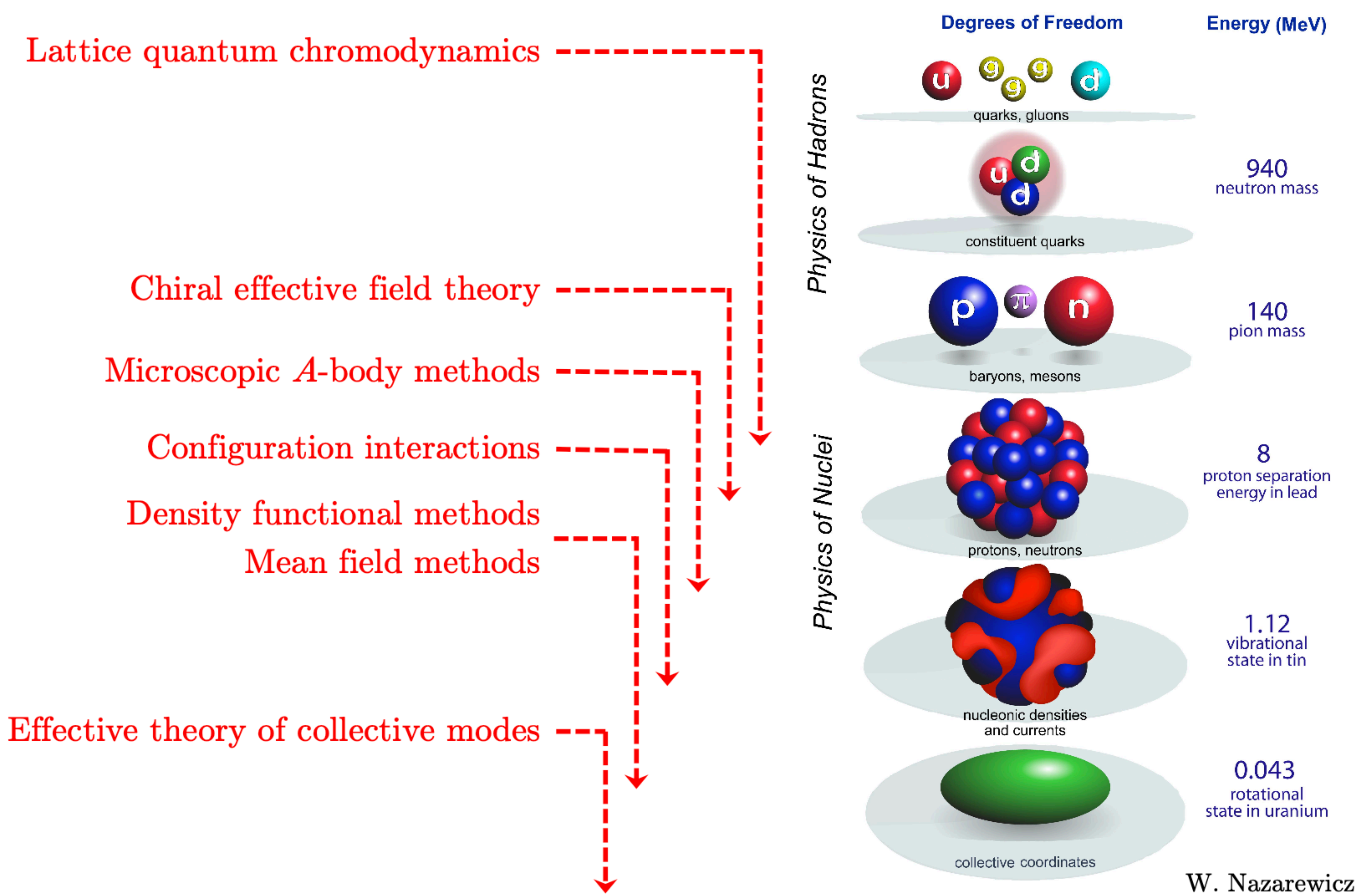

Slide from Dean Lee' lecture in Nuclear Physics School 2020

Nuclei properties

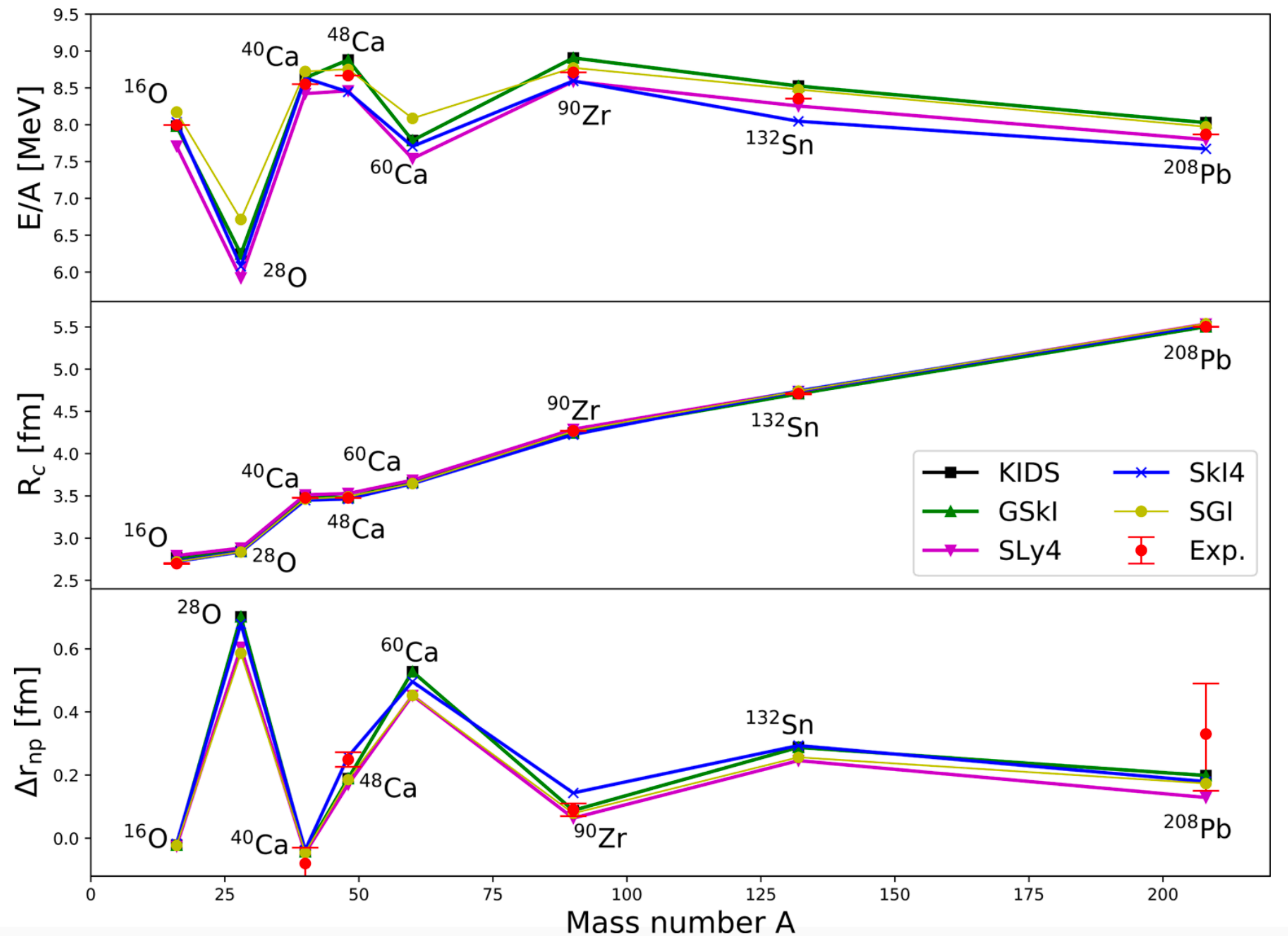

Kim et al. (IJMPE 2020)

Equations of States

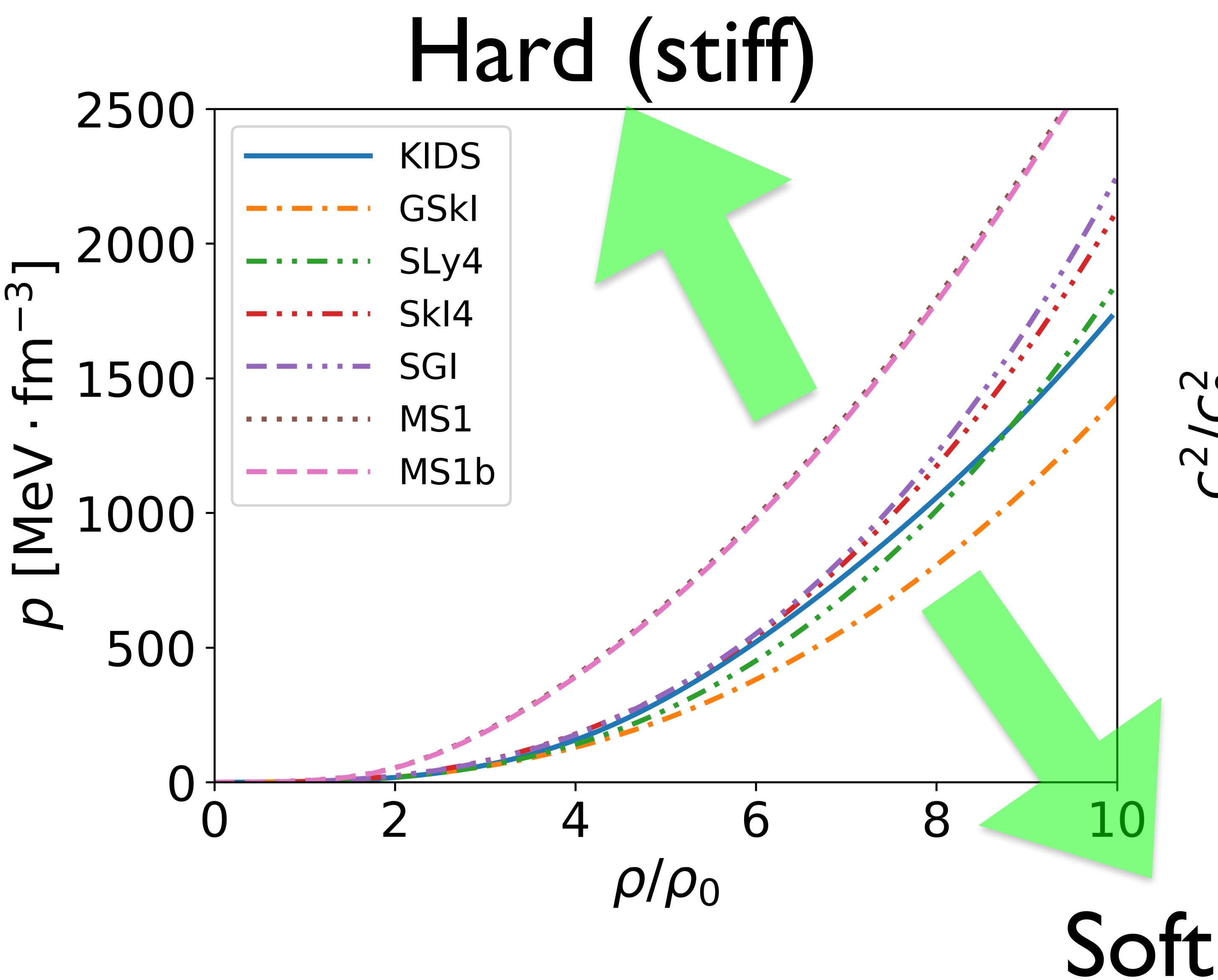

Y.-M. Kim et al. (EPJA 2020)

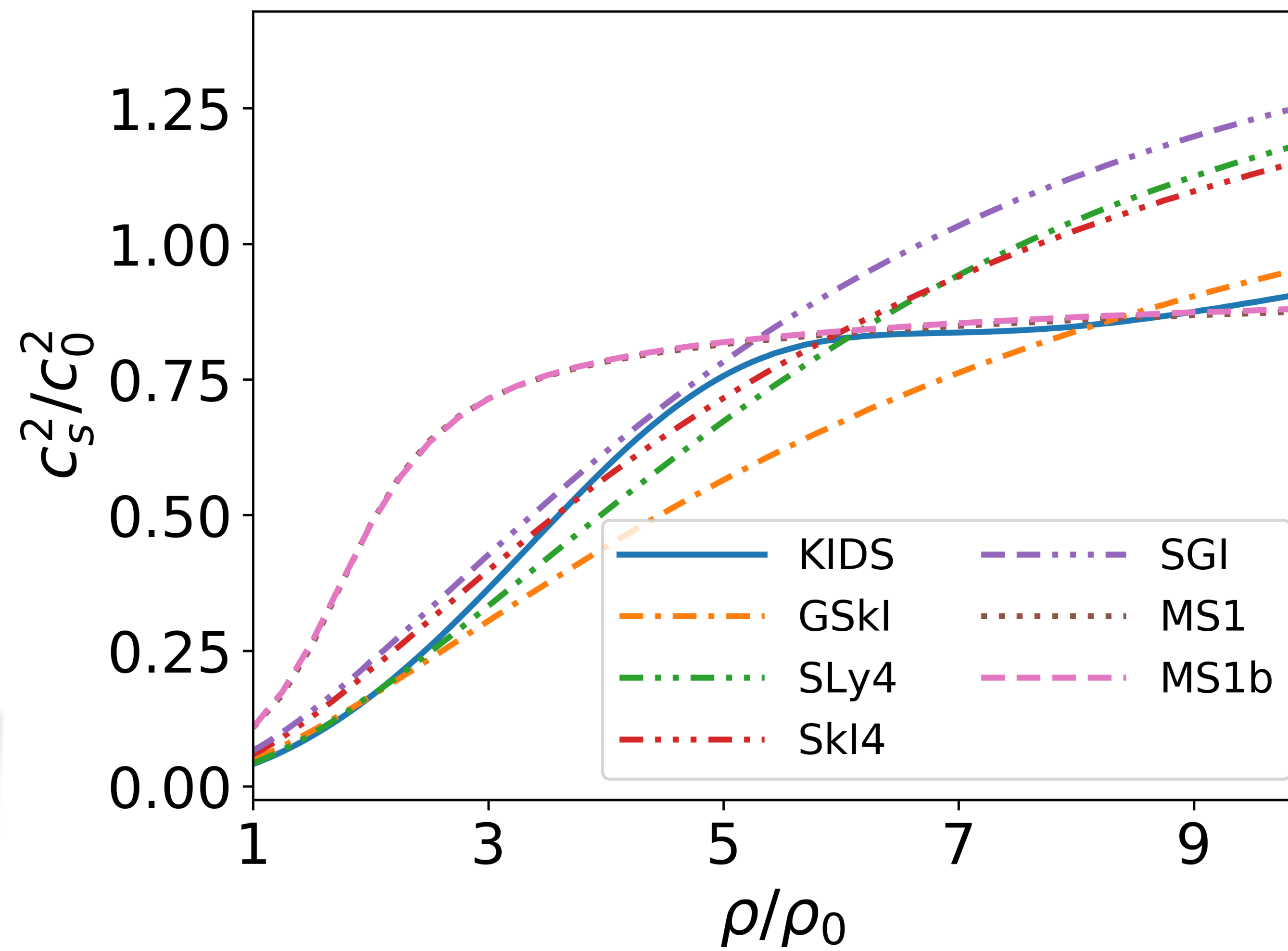

Tidal Love number, k2

Y.-M. Kim et al. (EPJA 2020)

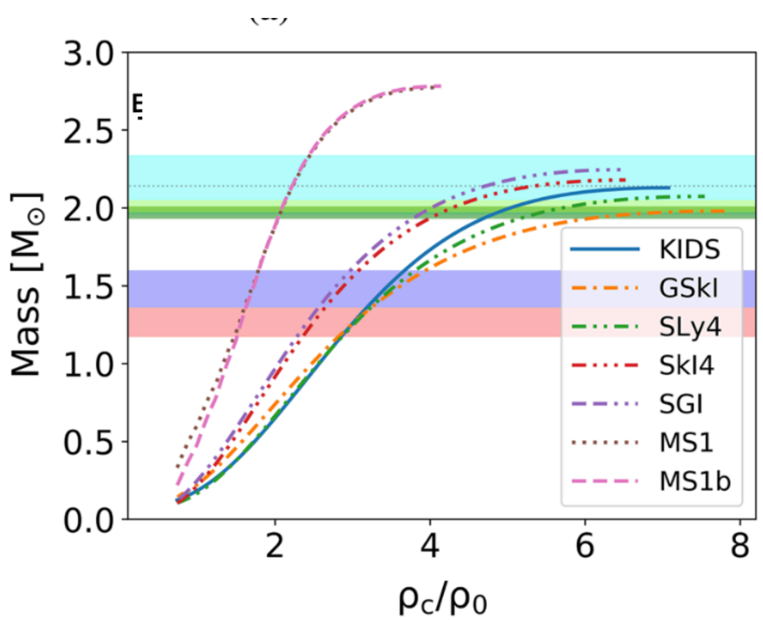

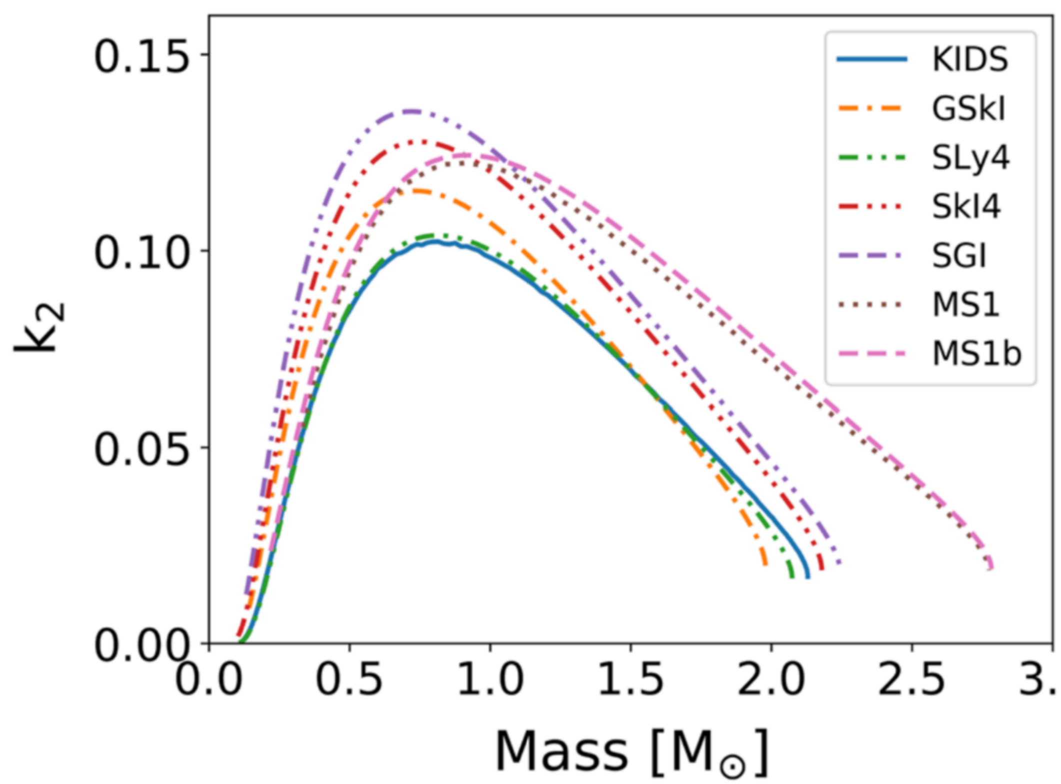

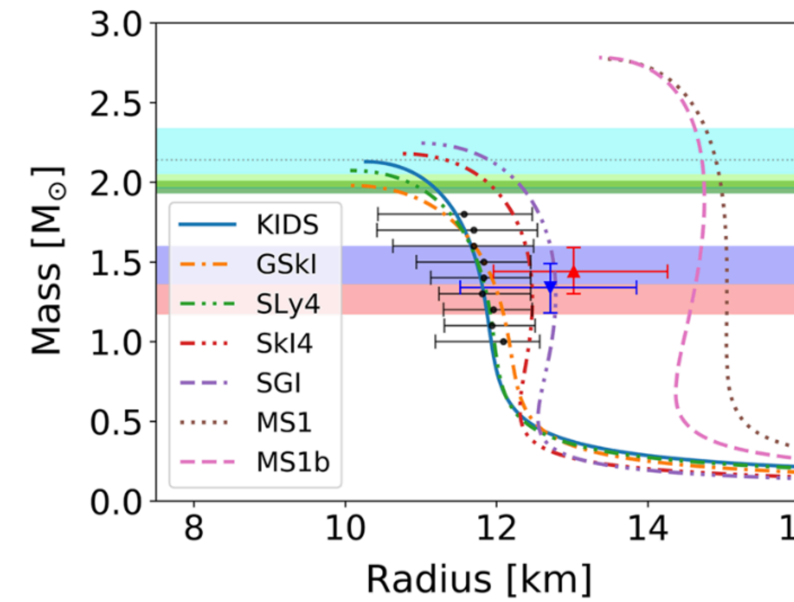

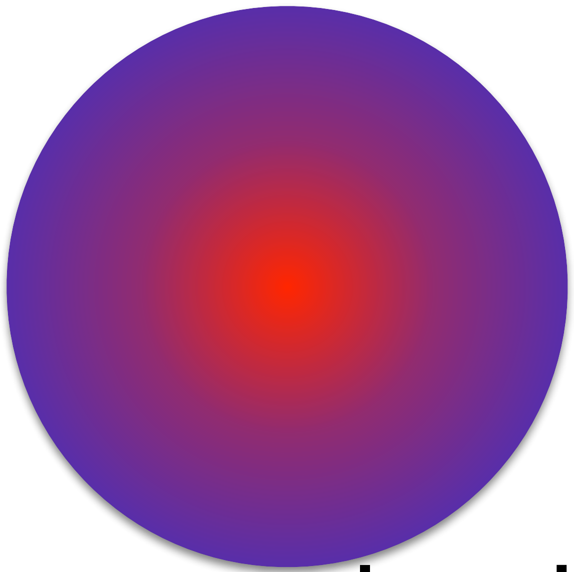

low k2

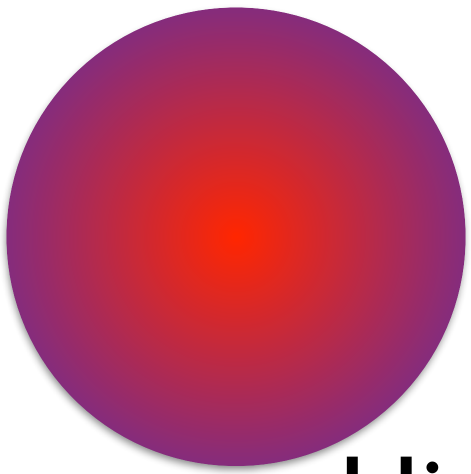

High k2

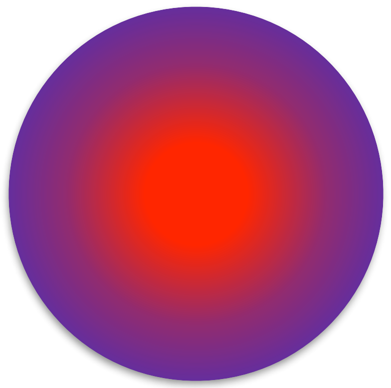

low k2

Tidal deformability of GW170817

$\Lambda(1.4M_\odot)=190^{+390}_{-120}$

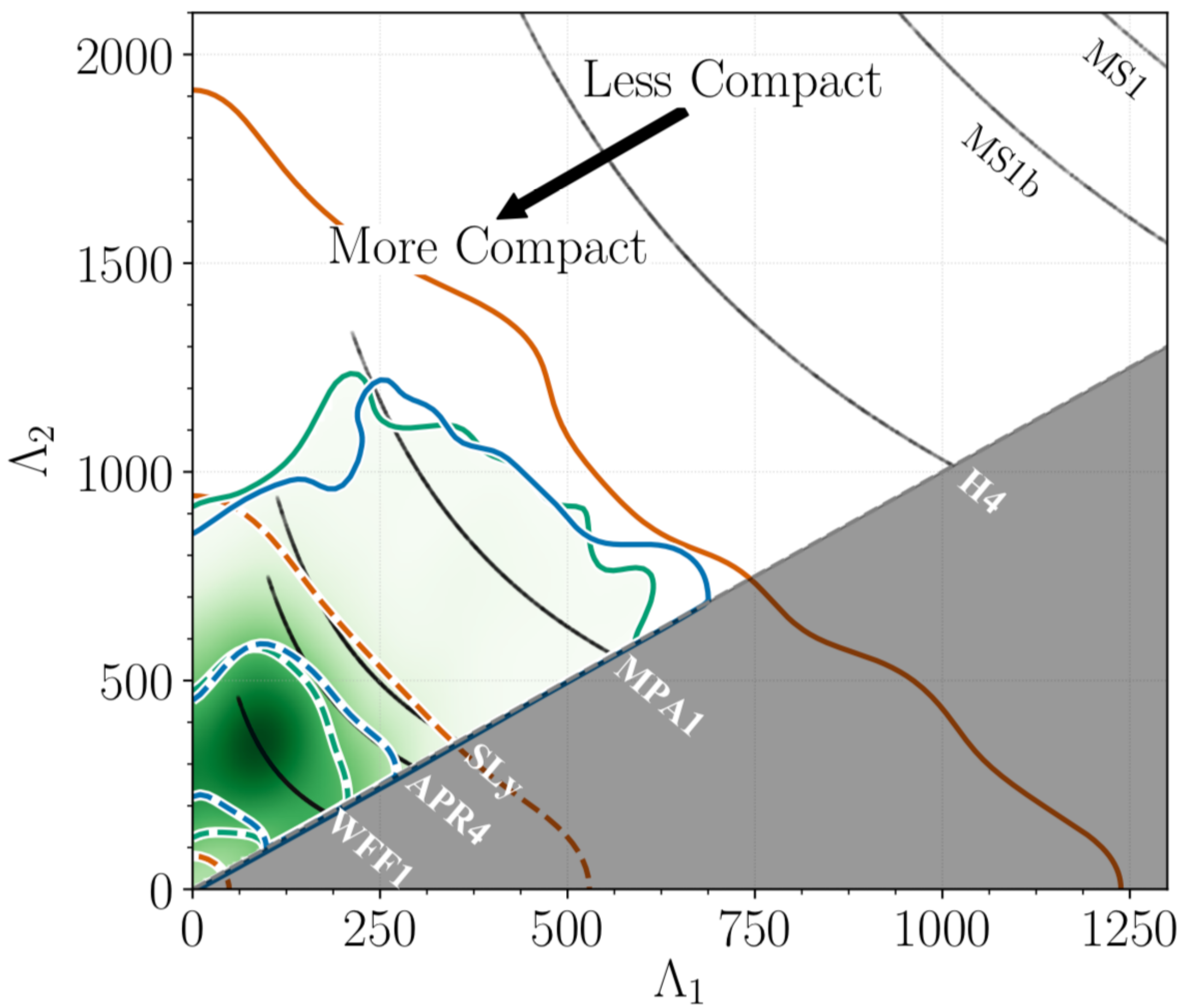

$P(2\ \rho_{nuc})= 3.5^{+2.7}_{-1.7}\ x10^{34}$ dyne/cm^2
$P(6\ \rho_{nuc})= 9.0^{+7.9}_{-2.6}\ x10^{35}$ dyne/cm^2

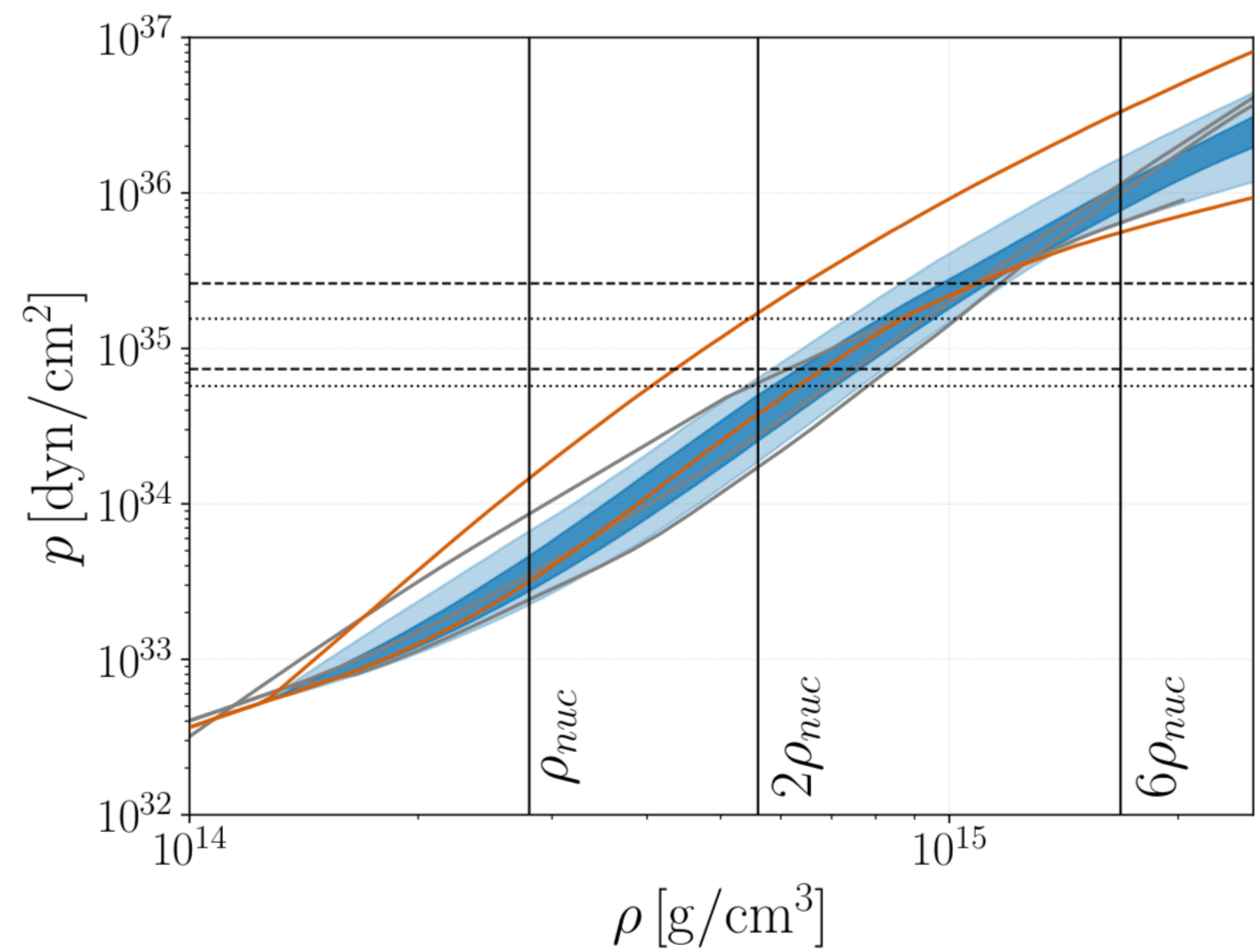

Abbott et al. (LSC and Virgo), arxiv:1805.11581 (PhysRevLett.121.161101)

ρ_{nuc}= 2.8 x10^{14} g/cm^3

Eos-insensitive relation

Y.-M. Kim et al. (EPJA 2020)

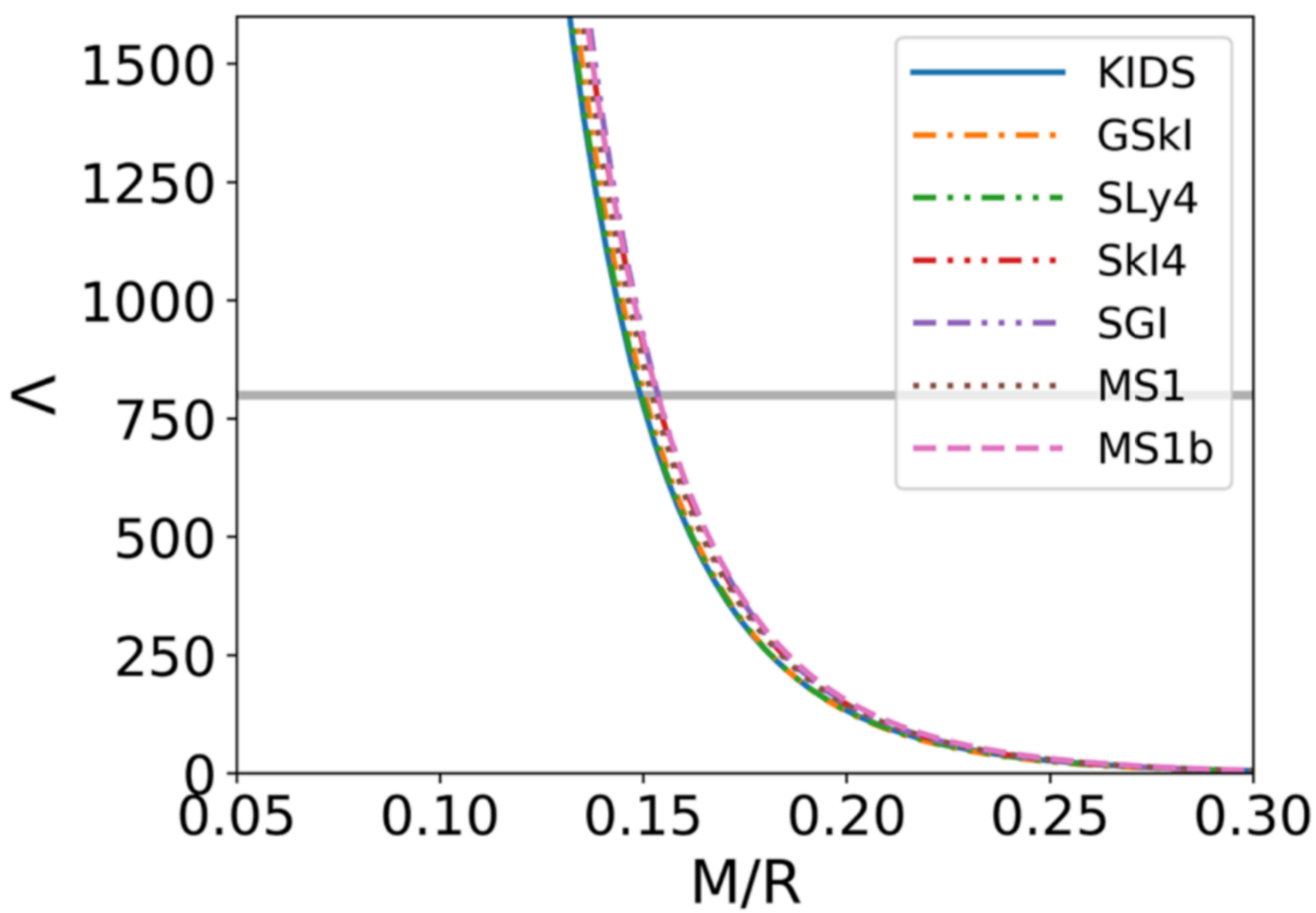

Insensitive to EoS

K. Yagi and N. Yunes, Phys. Rep. 681 (2017) 1

$$C = a_0 + a_1(\ln\Lambda) + a_2(\ln\Lambda)^2$$

a_0=0.360, a_1= - 0.0355, a_2= 0.000705

C=GM/Rc^2

Eos-insensitive relation

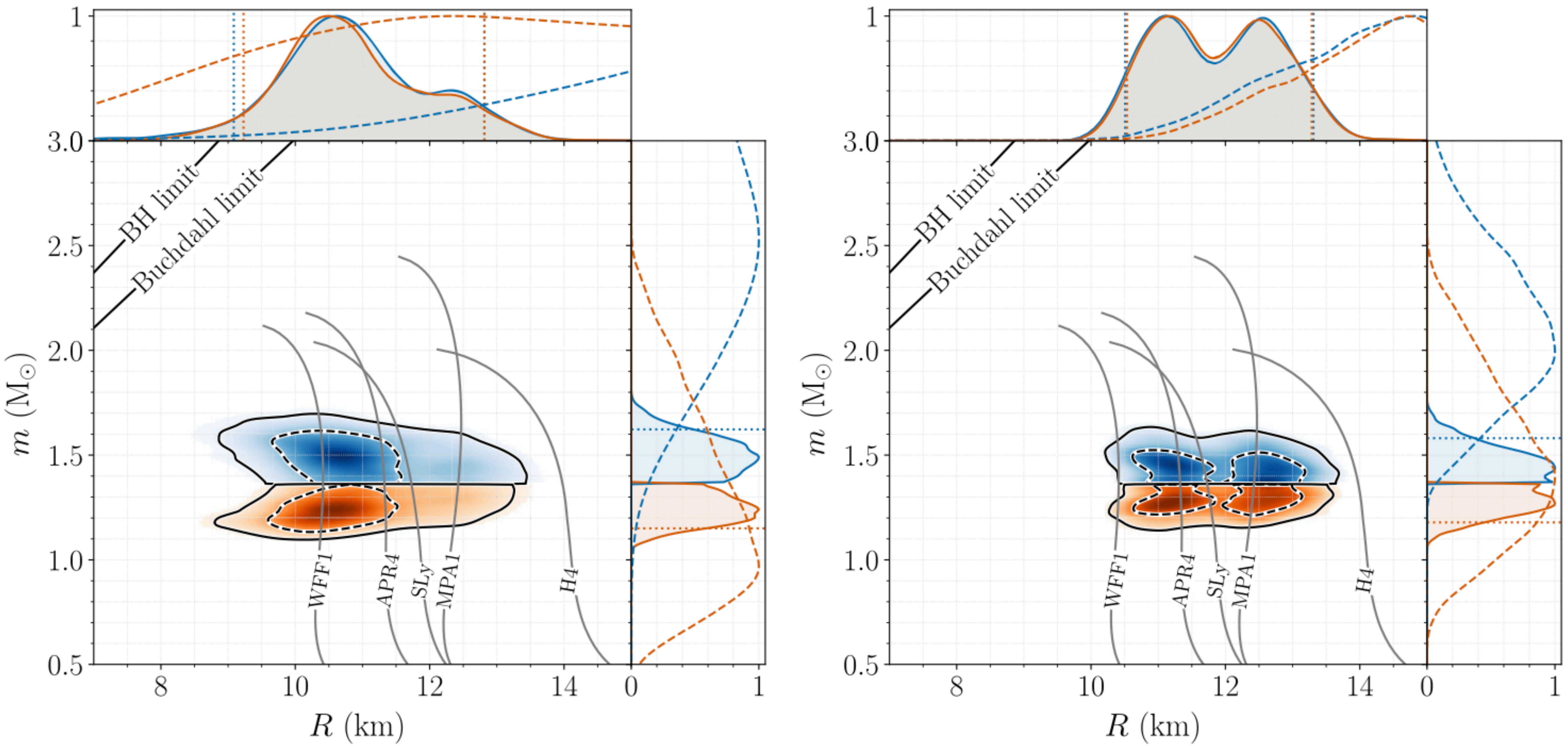

Abbott et al. (LSC and Virgo), arxiv:1805.11581 (PhysRevLett.121.161101)

Lambda-Radius relation

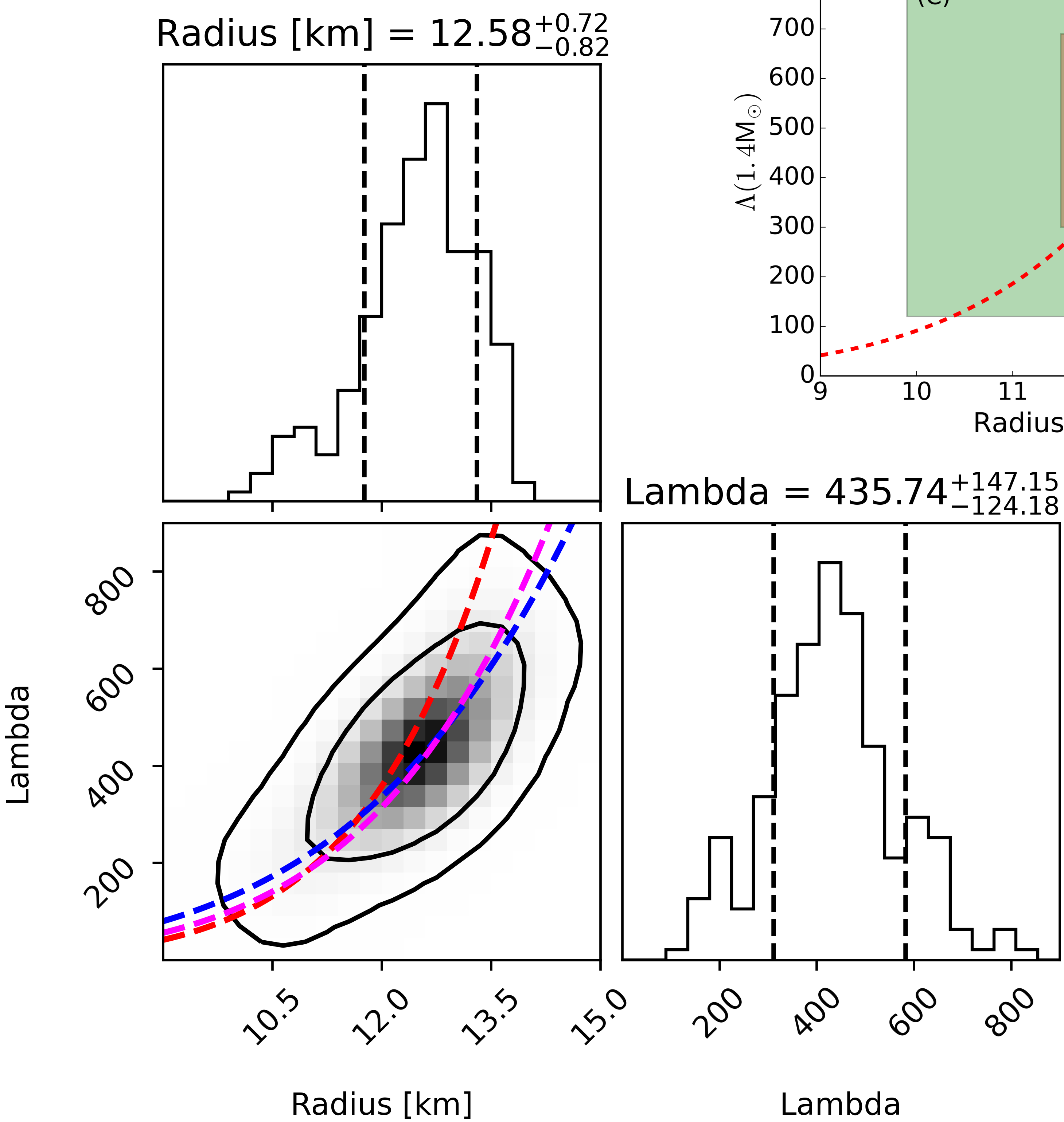

Kim et al., PhysRevC.98.065805 (2018)

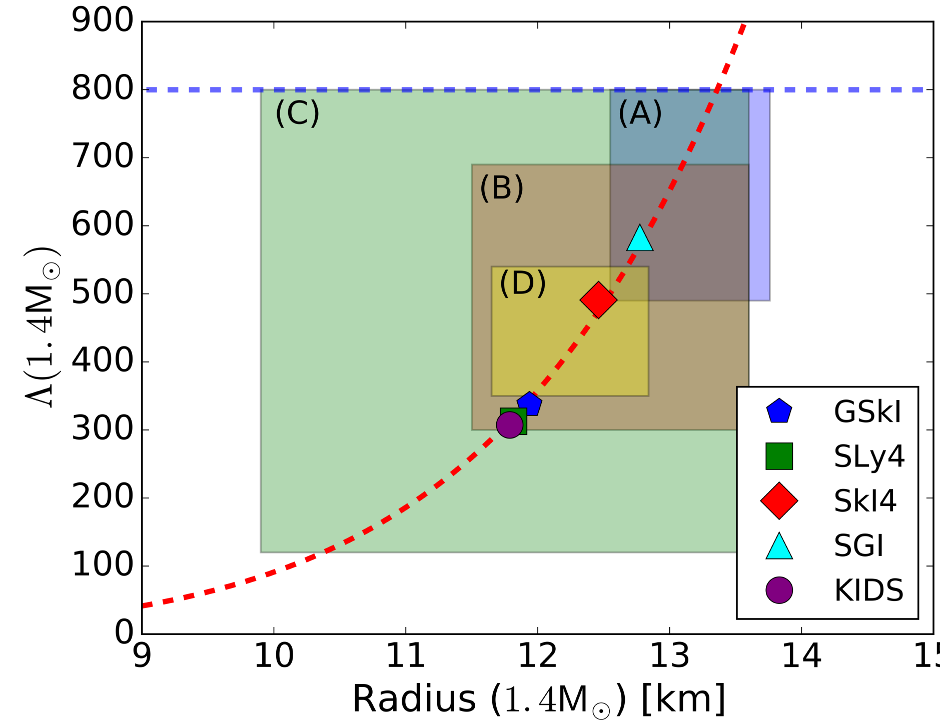

Implication of PREX 2 -
PhysRevLett.126.172503 (2021)

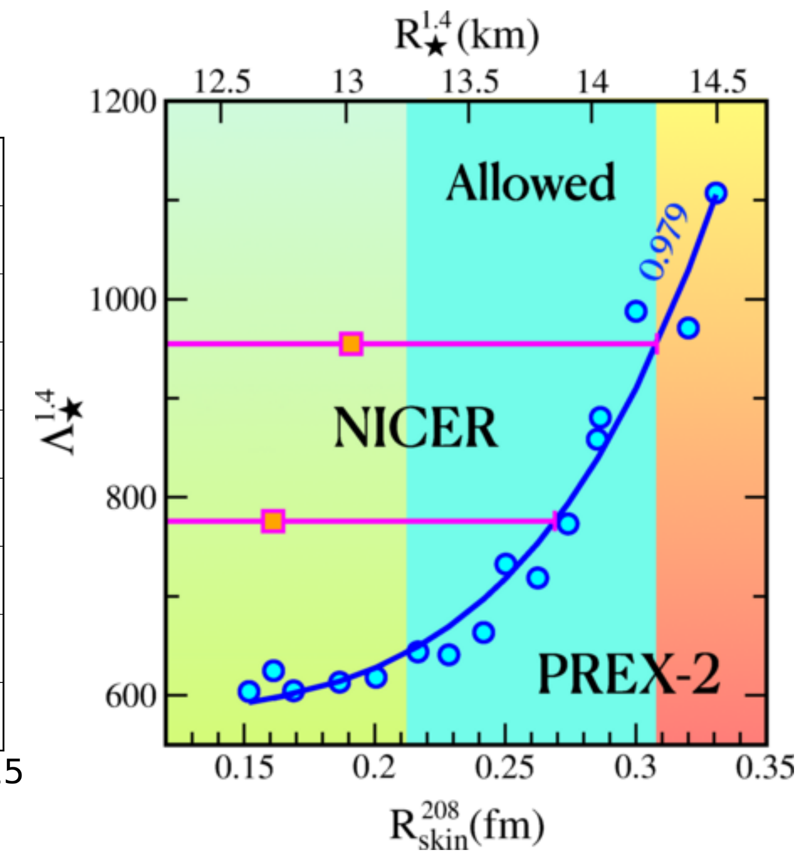

Red line: $\Lambda(1.4M_\odot) = 2.88 * 10^{-6}\,(R/km)^{7.5}$

[C] PhysRevLett.120.172703.pdf

Blue line: $\Lambda(1.4M_\odot) = 1.35 * 10^{-3}\,(R/km)^{5.0}$

Implication of PREX 2 - PhysRevLett.126.172503 (2021)

=> $\Lambda \sim R^{4.8}$

Magenta line: $\Lambda(1.4M_\odot) = 1.05 * 10^{-4}\,(R/km)^{6.0}$

Y.-M. Kim, in progress

Nuclear Symmetry Energy

$$\frac{E}{A}(\rho,\delta) = \frac{V}{A}\epsilon(\rho,\delta) = \epsilon(\rho,\delta)/\rho \equiv \mathscr{E}(\rho,\delta) \qquad \delta = \frac{\rho_n - \rho_p}{\rho}$$

$$= E(\rho,\delta=0) + E_{sym}(\rho)\delta^2 + \mathcal{O}(\delta^4) + \ldots,$$

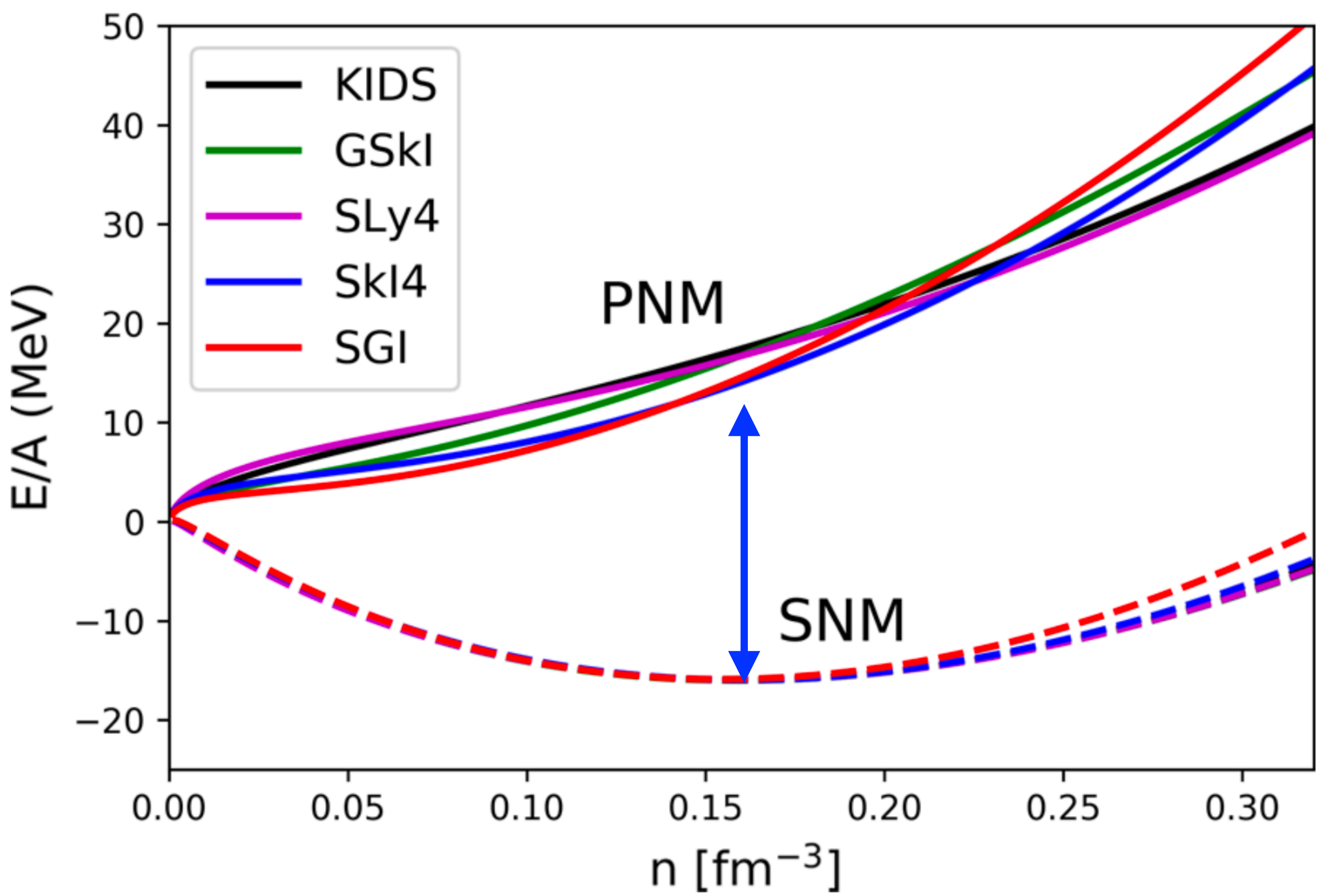

Kim et al. (IJMPE 2020)

$$\mathscr{E}(\rho,0) = E_0 + \tfrac{1}{2}K_0x^2 + \tfrac{1}{6}Q_0x^3 + O(x^4),$$

$$\mathcal{S}(\rho) = J + Lx + \tfrac{1}{2}K_{\rm sym}x^2 + \tfrac{1}{6}Q_{\rm sym}x^3 + \tfrac{1}{24}R_{\rm sym}x^4 + O(x^5),$$

$\rho_0 \sim 0.16$: saturation density

Nuclear Symmetry Energy

J.M. Lattimer / Nuclear Physics A 928 (2014) 276–295

Gandolfi and Steiner (2016)

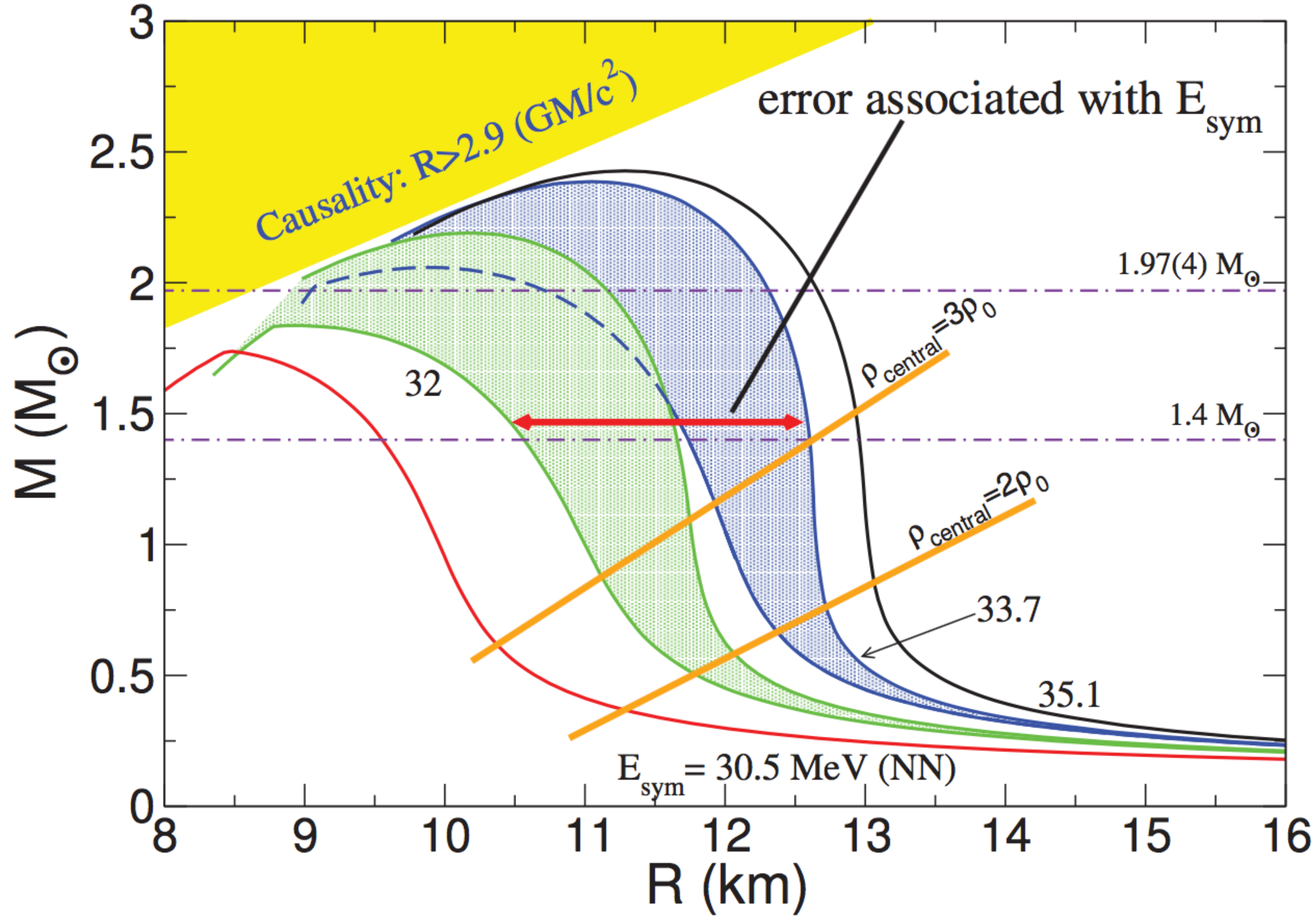

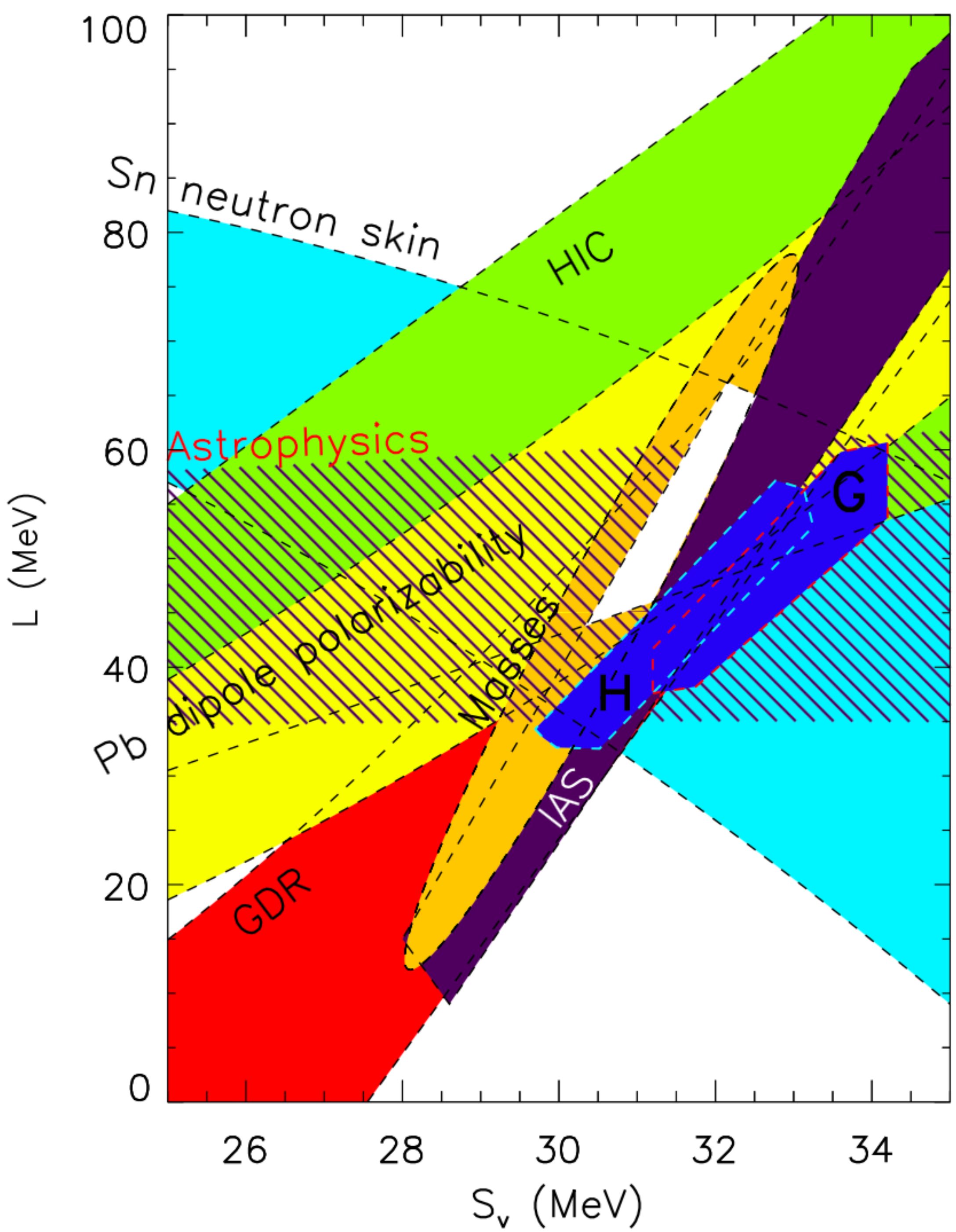

Symmetry Energy from GW observation

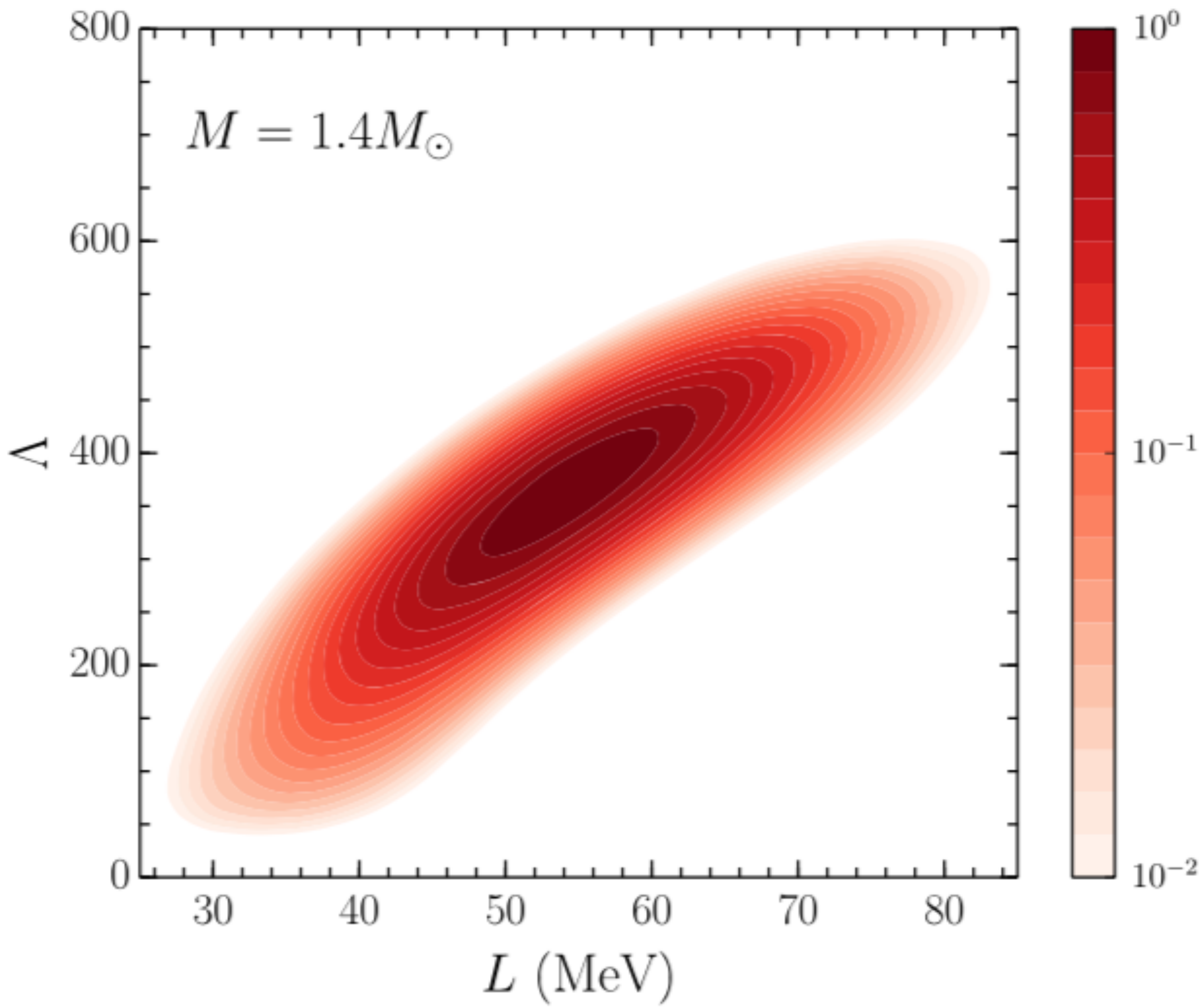

isospin-asymmetry energy slope parameter L

Yeunhwan Lim and J. Holt, PRL.121.062701 (arXiv:1803.02803v2)

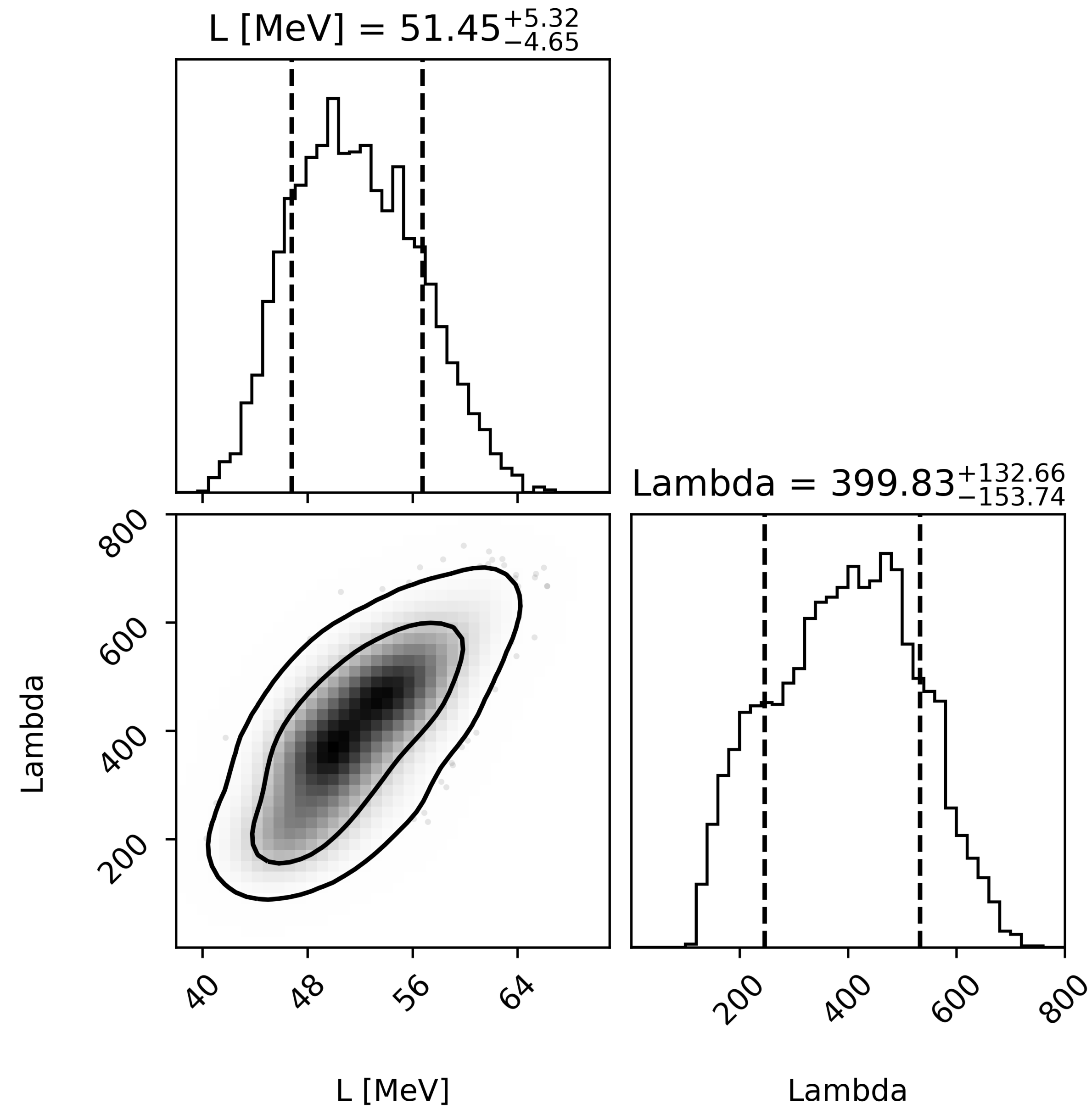

Y.-M. Kim, in progress

Implication of PREX 2 and NICER Obs.

PREX 2 - PhysRevLett.126.172502 (2021) Neutron skin thickness, Rn-Rp = 0.278 +/- 0.078 (exp.) +/- 0.012 (theo.) fm

Implication of PREX 2 - PhysRevLett.126.172503 (2021)

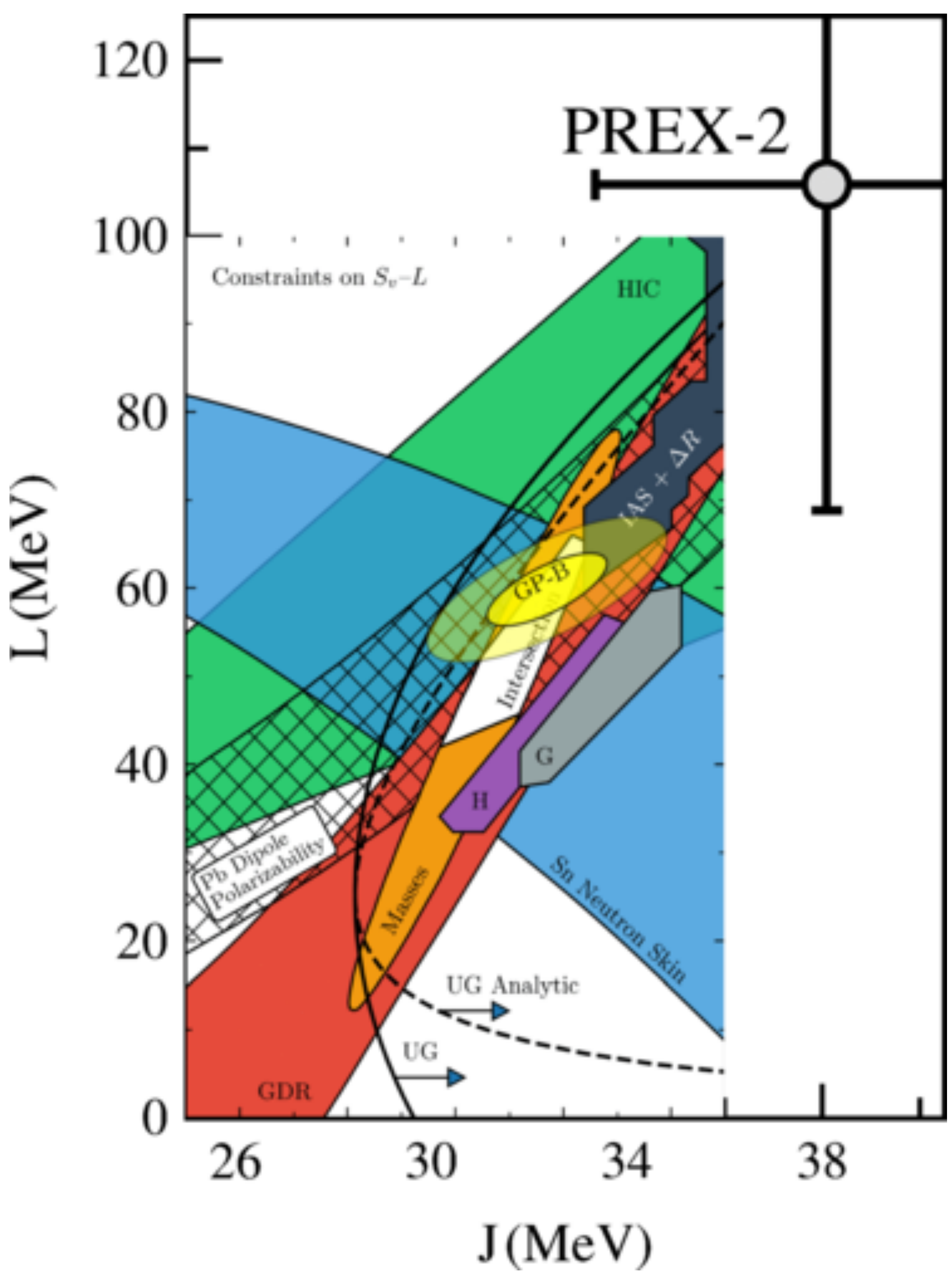

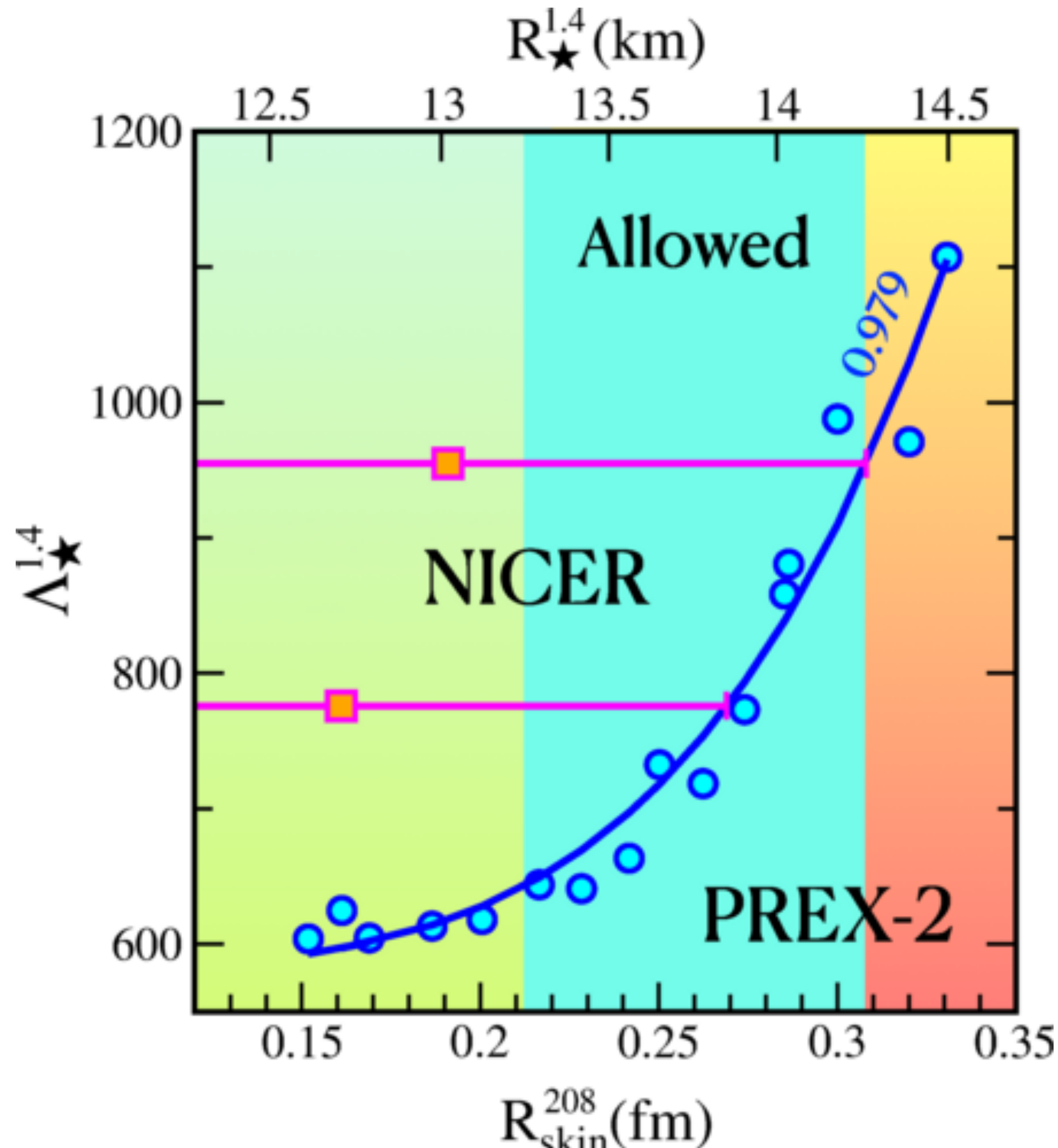

Astrophysics w/ nuclear physics

기초과학연구원 중이온가속기연구소
중이온가속기 라온(RAON)

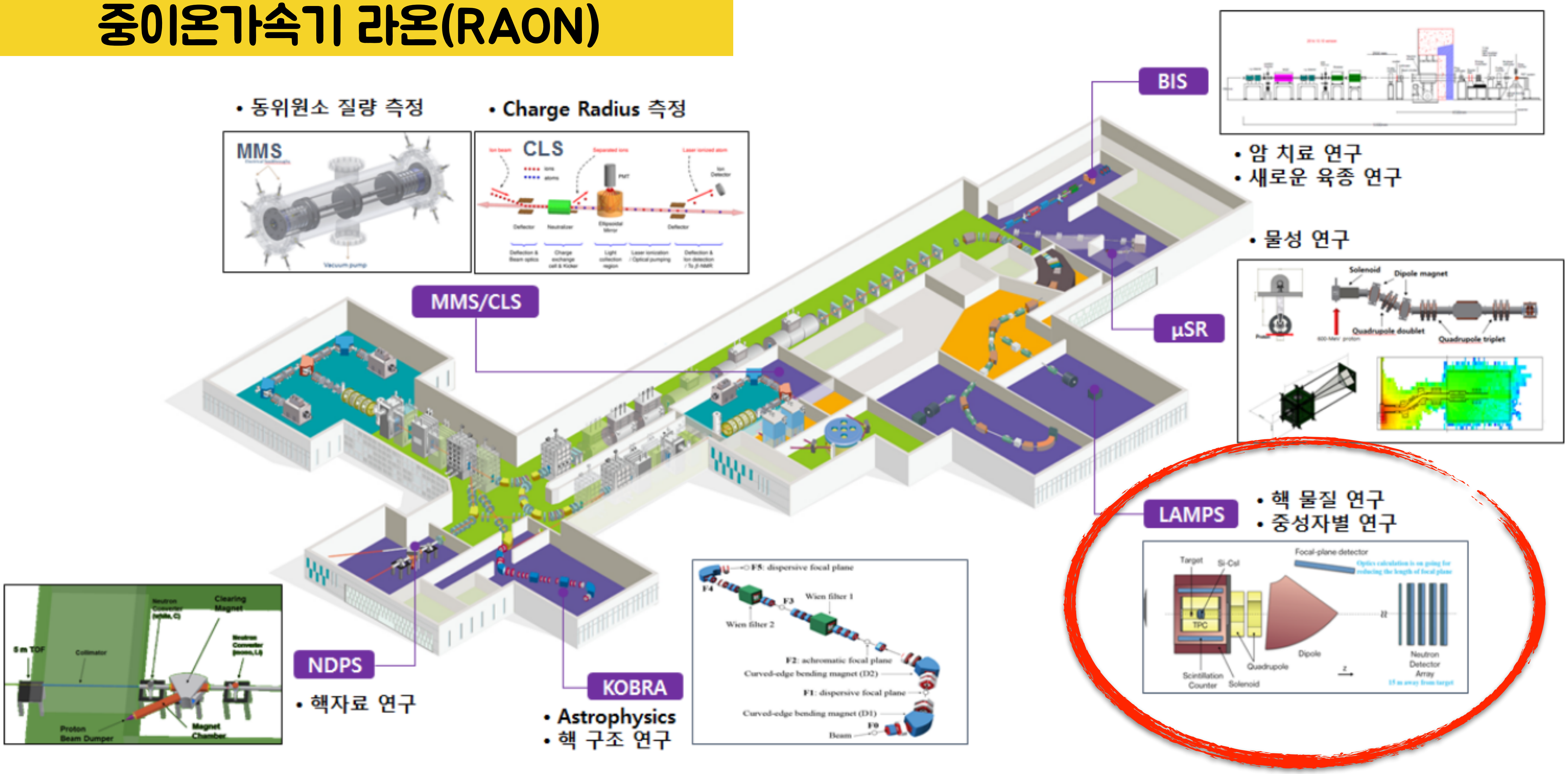

Bayesian analysis on EoS parameters

$$P(\{E_0, K_0, Q_0, J, L, K_\tau, Q_{\text{sym}}\}|\text{data})$$

Draft in preparation

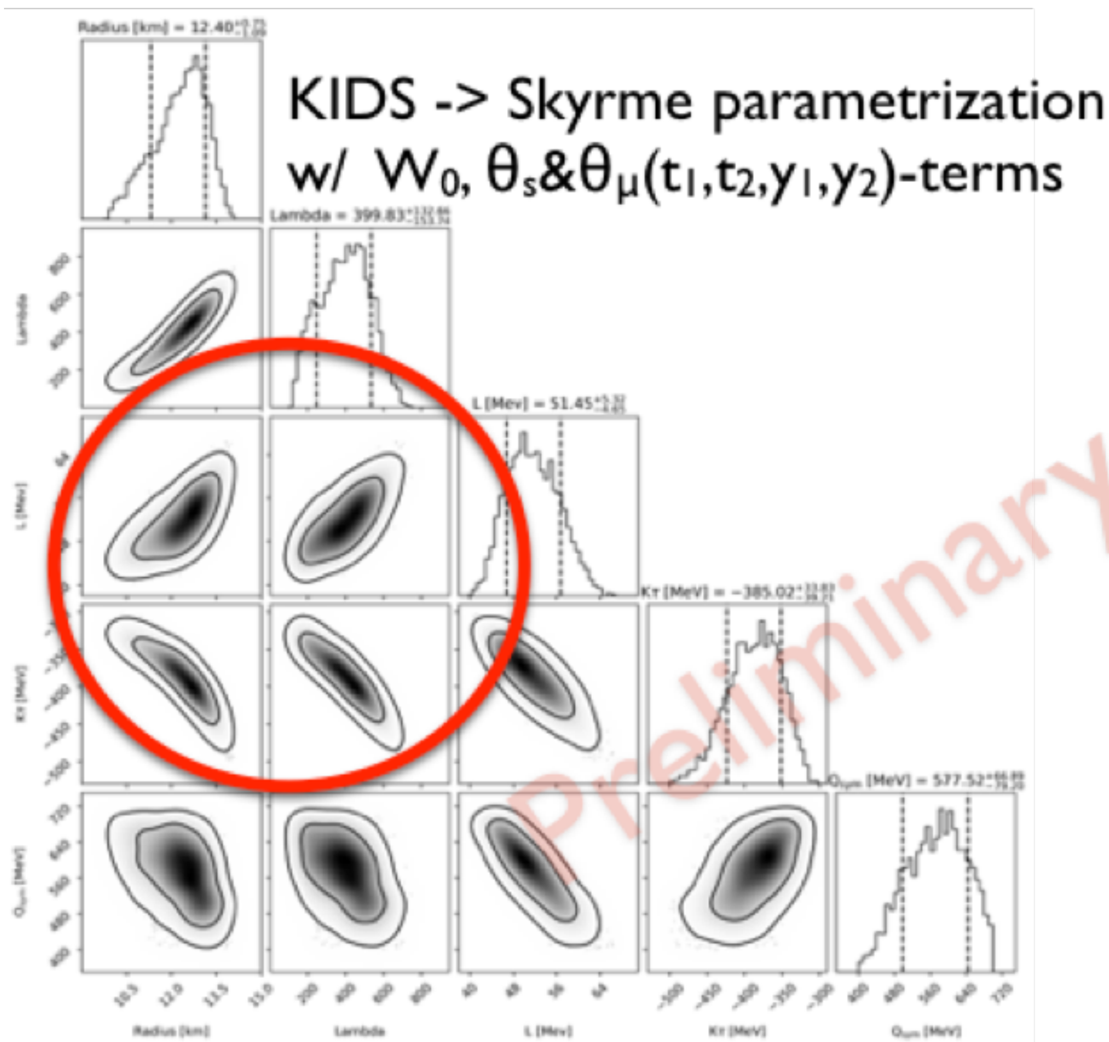

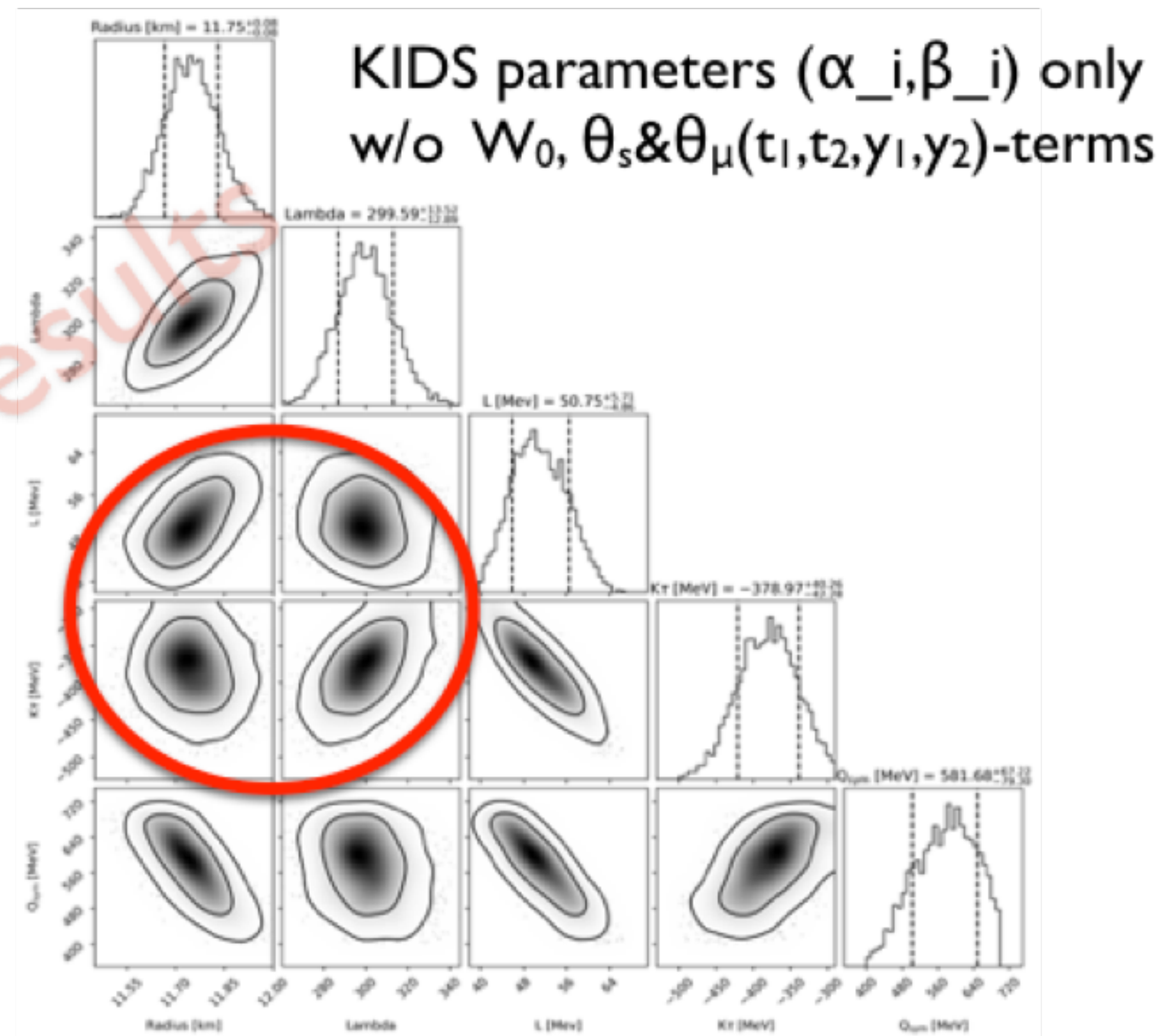

Precise measurements of R, Λ
=> constraints of EoS & Nuclei properties

Maximum mass of Neutron Stars

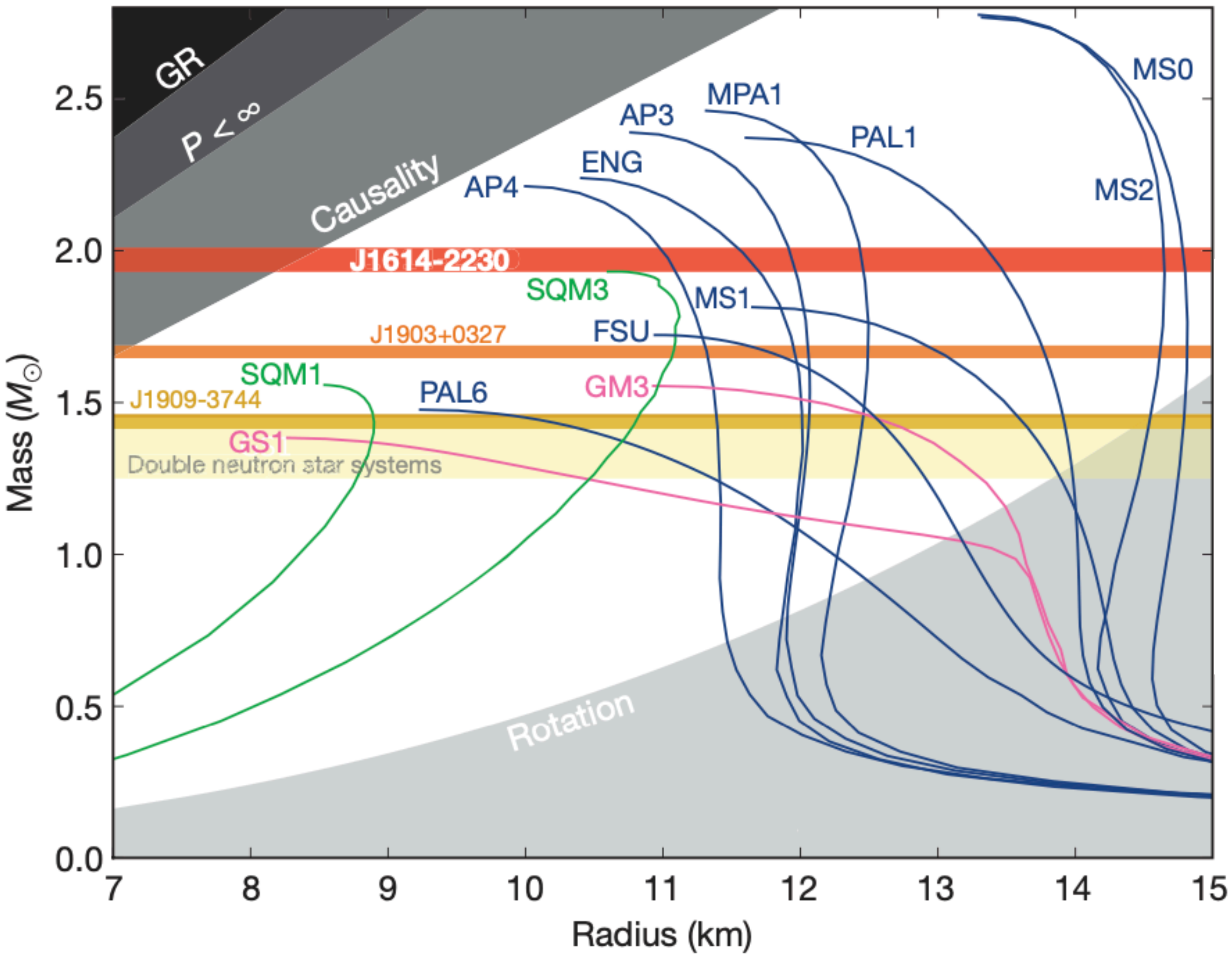

Shapiro delay

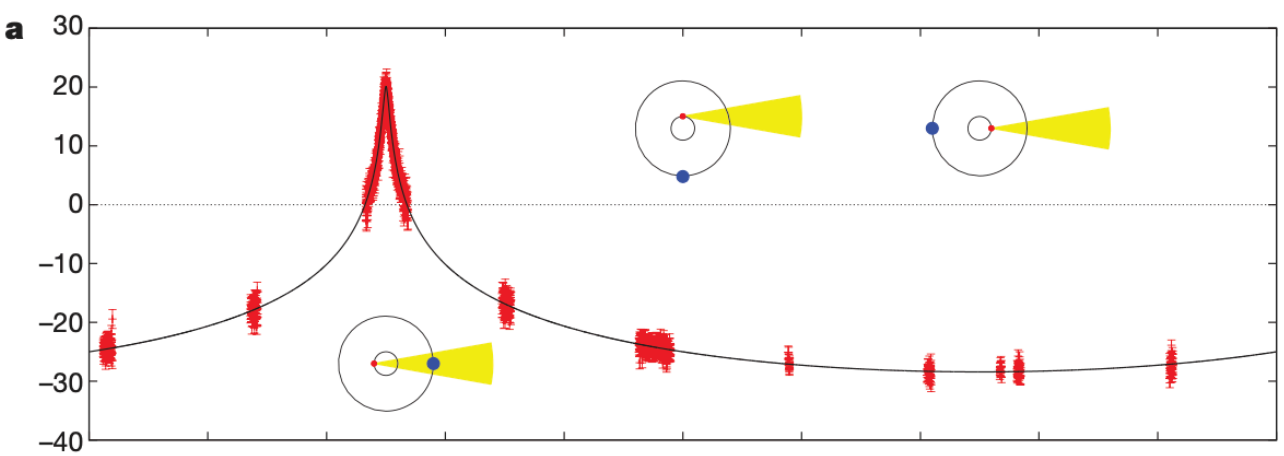

Demorest et al. Nature (2010)

NICER observations

PSR J0030+0451

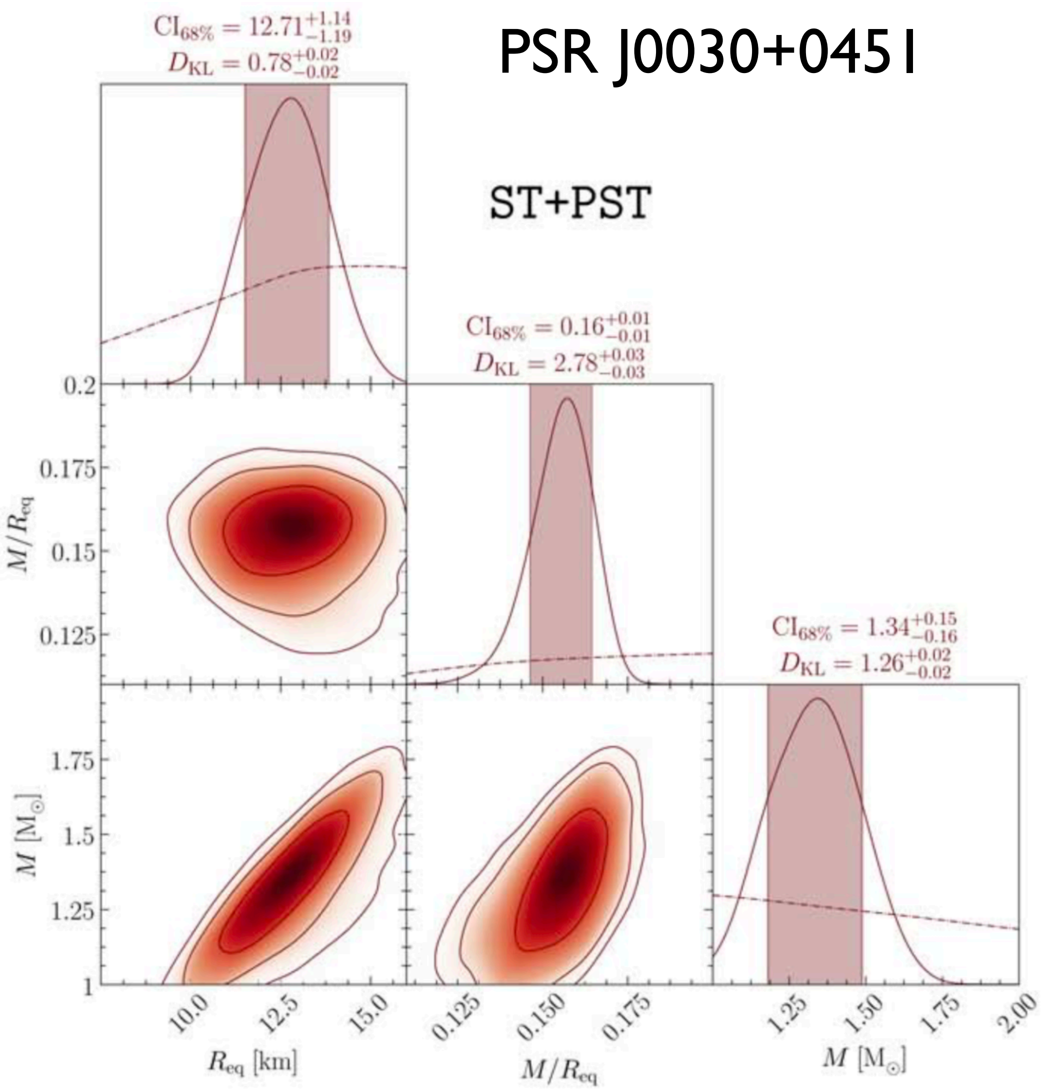

Riley_2019_ApJL_887_L21

PSR J0740+6620

arxiv:2105.06979

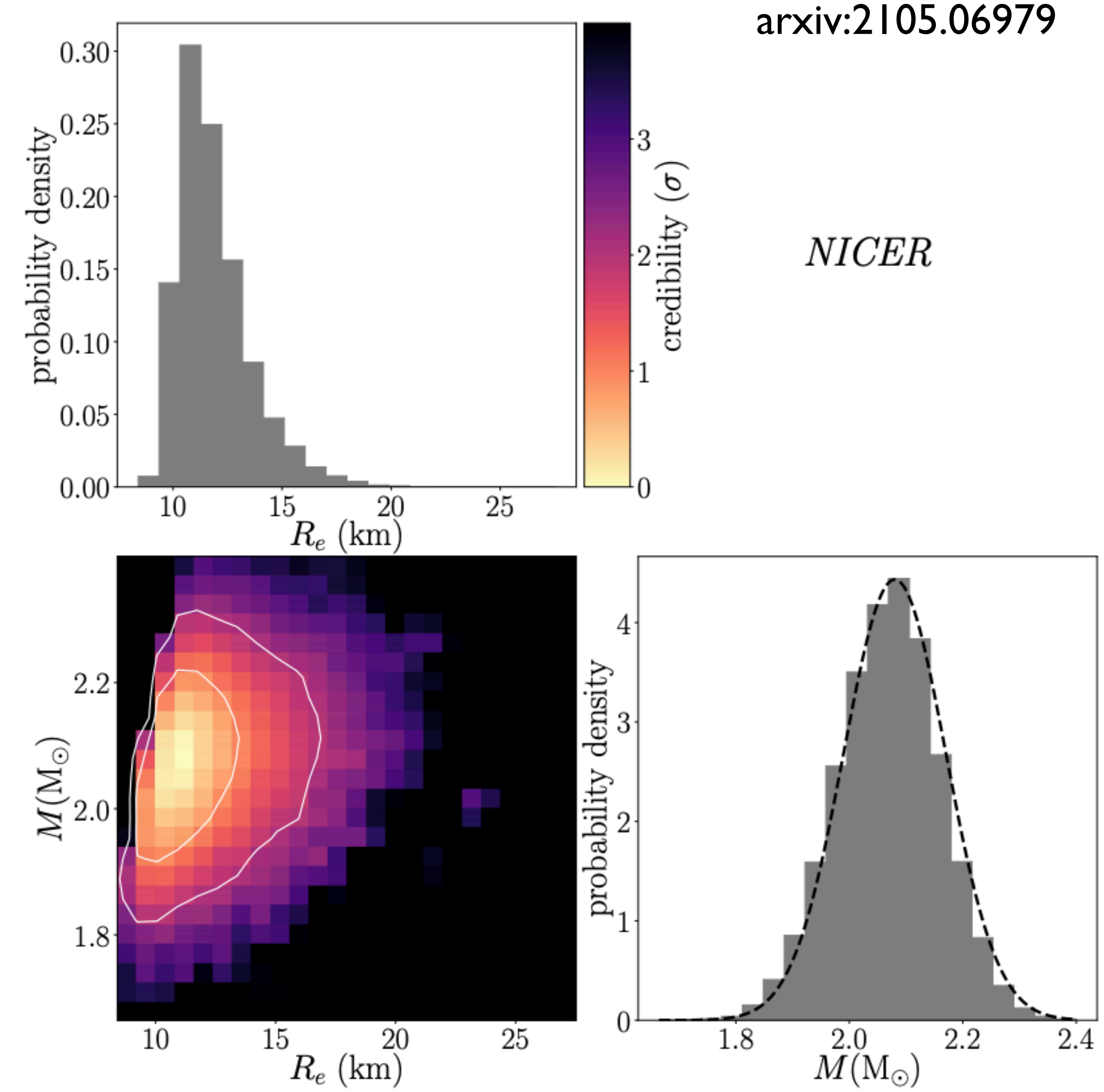

	Mass (M_{sun})	Radius (km)
Riley *et al.*[25]	$1.34^{+0.15}_{-0.16}$	$12.71^{+1.14}_{-1.19}$
Miller *et al.*[26]	$1.44^{+0.15}_{-0.14}$	$13.02^{+1.24}_{-1.06}$

Constraints on EoS from M, R, L

prefer soft EoS: GW170817,strangeness

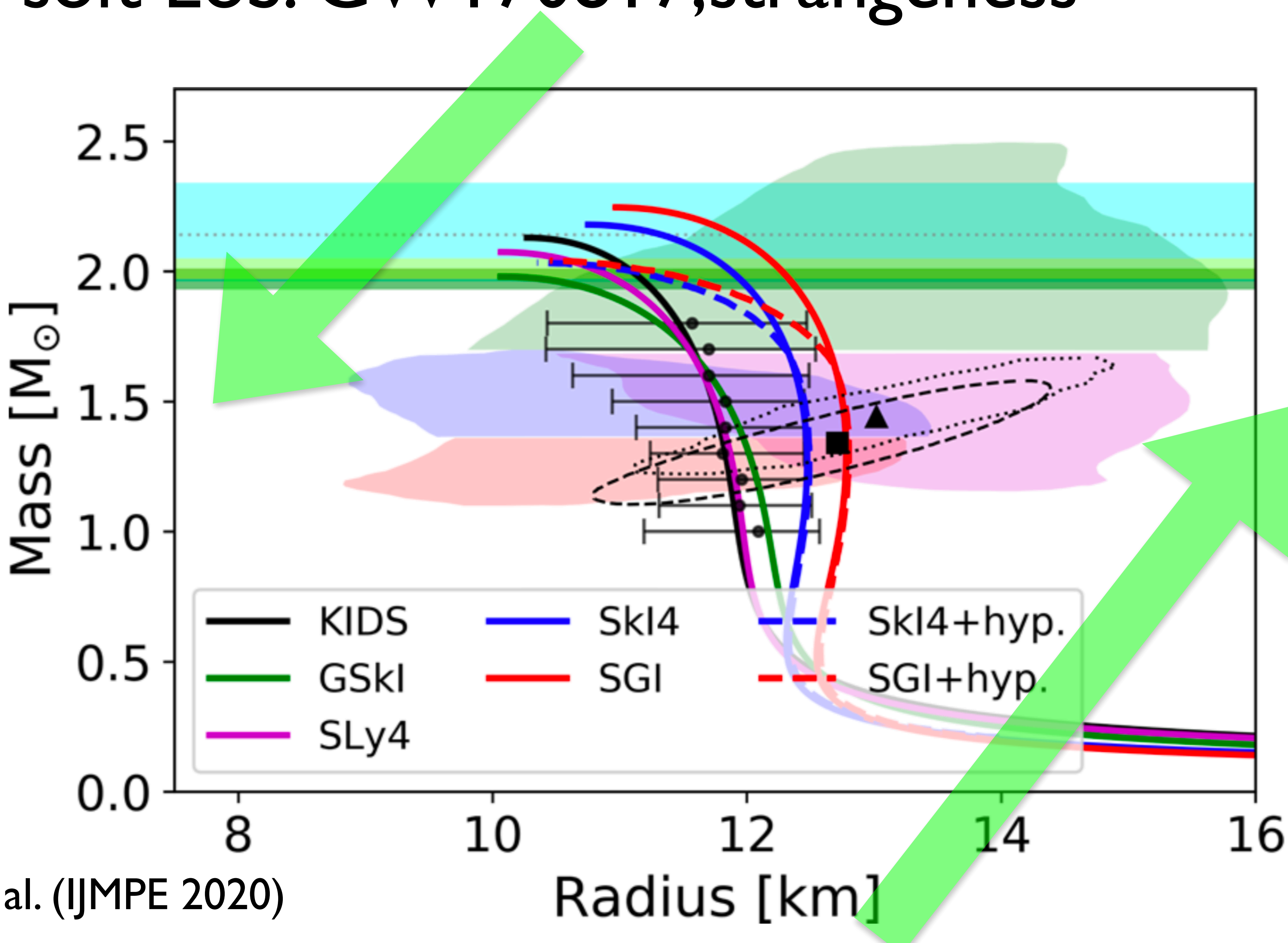

M. Kim et al. (IJMPE 2020)

prefer harder EoS: M_max, NICER

Combined Results

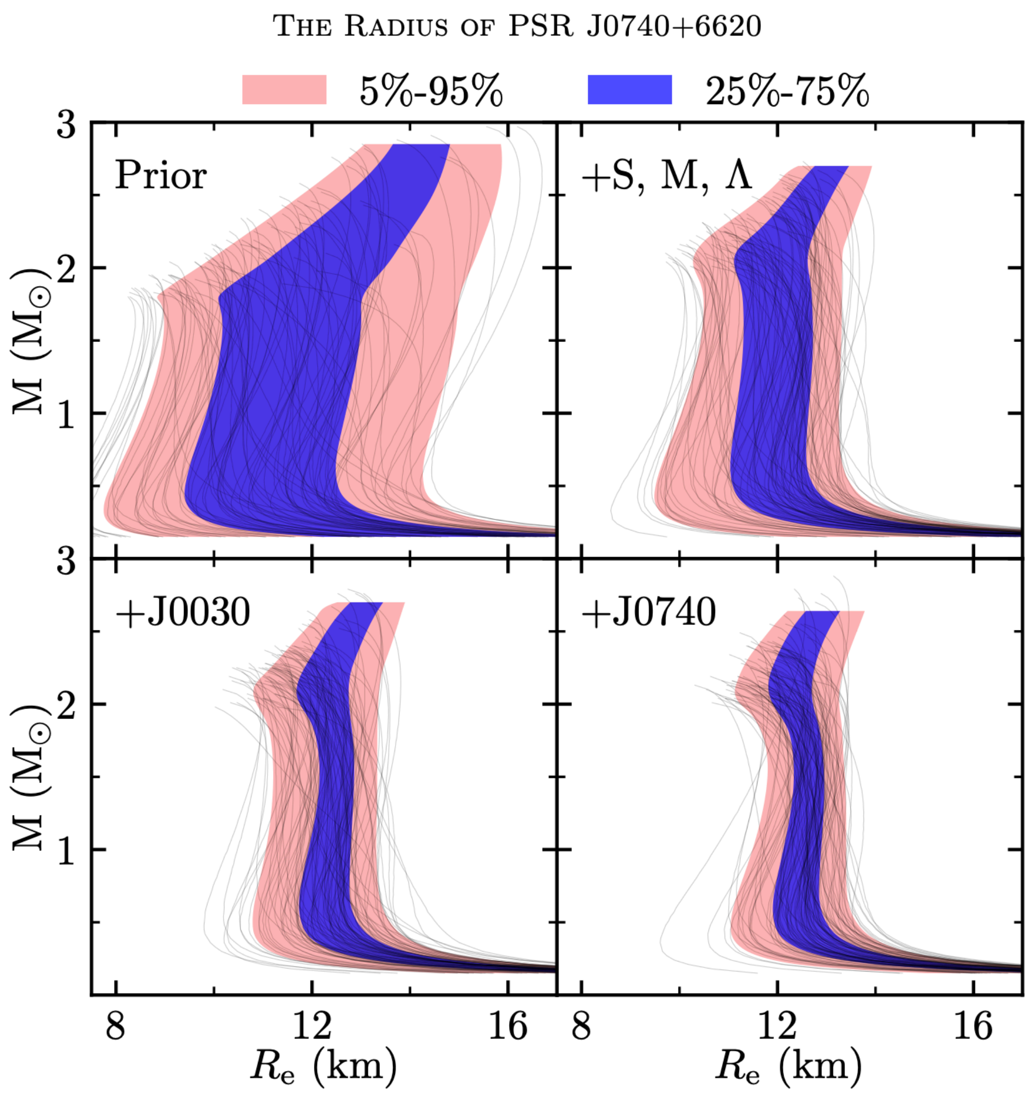

Miller_2021_ApJL_918_L28

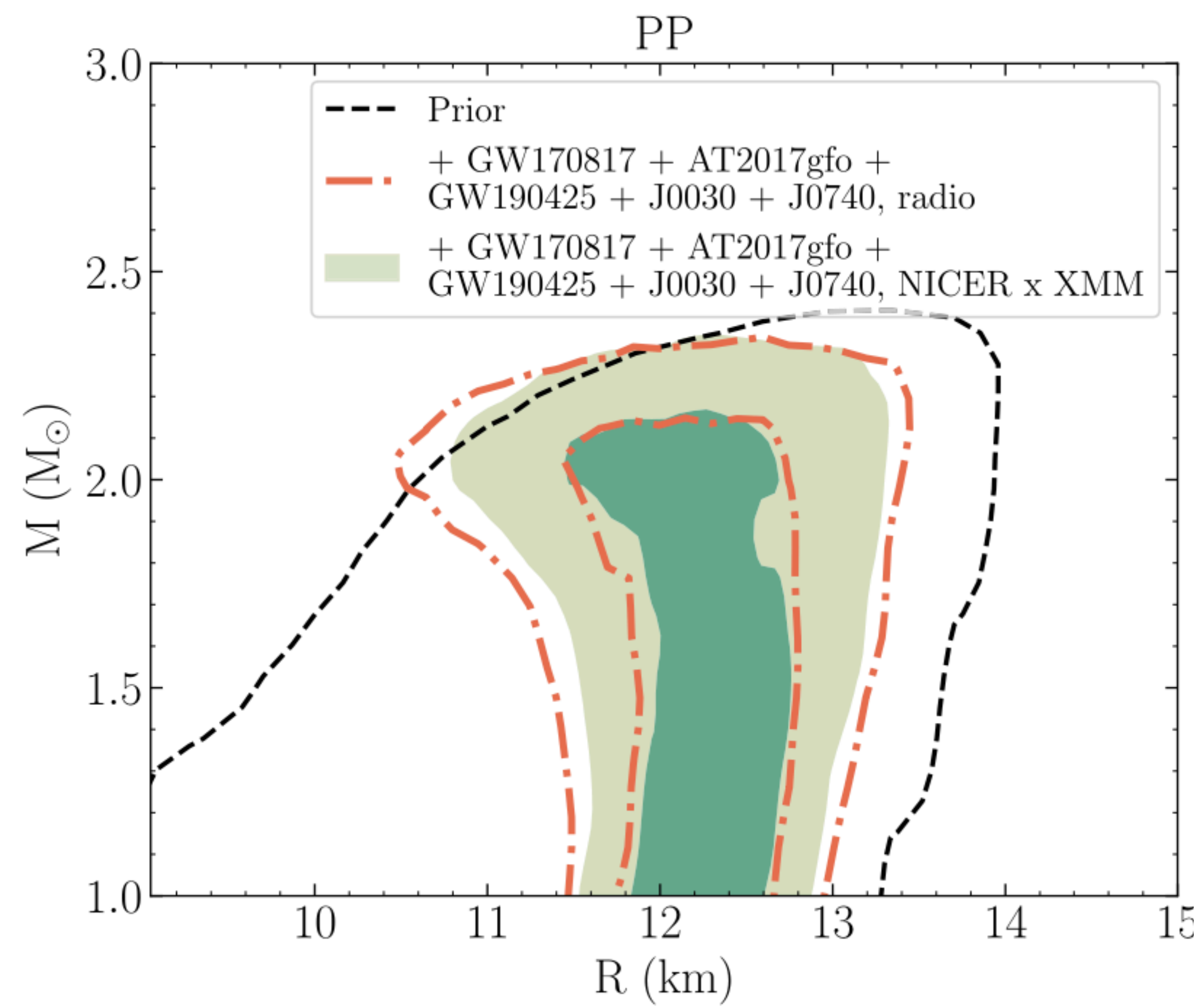

Raaijmakers_2021_ApJL_918_L29

Constraints

- S : Symmetry Energy
- M : high mass of pulsars
- Λ : tidal deformability of GW170817 and GW190425

TOV Eq. vs. Diff. Eq. for Tidal deformability

A static solution of a spherical symmetric star in hydrostatic equilibrium

$$G_{\mu\nu} = 8\pi T_{\mu\nu}$$

$$\begin{aligned} ds_0^2 &= g^{(0)}_{\alpha\beta}\, dx^\alpha\, dx^\beta \\ &= -e^{\nu(r)}\, dt^2 + e^{\lambda(r)}\, dr^2 + r^2 \left(d\theta^2 + \sin^2\theta\, d\phi^2\right). \end{aligned}$$

$$T_{\alpha\beta} = (\rho + p) u_\alpha u_\beta + p g^{(0)}_{\alpha\beta},$$

TOV eq.

$$\frac{dP}{dr} = -\frac{GM\rho}{r^2}\left(1 + \frac{P}{\rho c^2}\right)\left(1 + \frac{4\pi P r^3}{Mc^2}\right)\left(1 - \frac{2GM}{rc^2}\right)$$

$$\frac{dM}{dr} = 4\pi r^2 \left(\frac{\epsilon}{c^2}\right)$$

Mass & Radius

TOV Eq. vs. Diff. Eq. for Tidal deformability

A static (adiabatic) solution from the linearized perturbations due to an external tidal field

$$\delta G_{\mu\nu} = 8\pi \delta T_{\mu\nu}$$

$$g_{\alpha\beta} = g^{(0)}_{\alpha\beta} + h_{\alpha\beta},$$

T. Hinderer (2008), K. Thorne and A. Campolattaro (1967)

$$h_{\alpha\beta} = \mathrm{diag}\left[-e^{\nu(r)}H_0(r), e^{\lambda(r)}H_2(r), r^2K(r), r^2\sin^2\theta K(r)\right] Y_{2m}(\theta,\varphi).$$

$$\delta T^0_0 = -\delta\rho = -(dp/d\rho)^{-1}\delta p \qquad \delta T^i_i = \delta p$$

$$H'' + H'\left\{\frac{2}{r} + e^{\lambda}\left[\frac{2m(r)}{r^2} + 4\pi r(p-\rho)\right]\right\} + H\left[-\frac{6e^{\lambda}}{r^2} + 4\pi e^{\lambda}\left(5\rho + 9p + \frac{\rho+p}{dp/d\rho}\right) - \nu'^2\right] = 0,$$

k2 or λ

Linear Stability Analysis

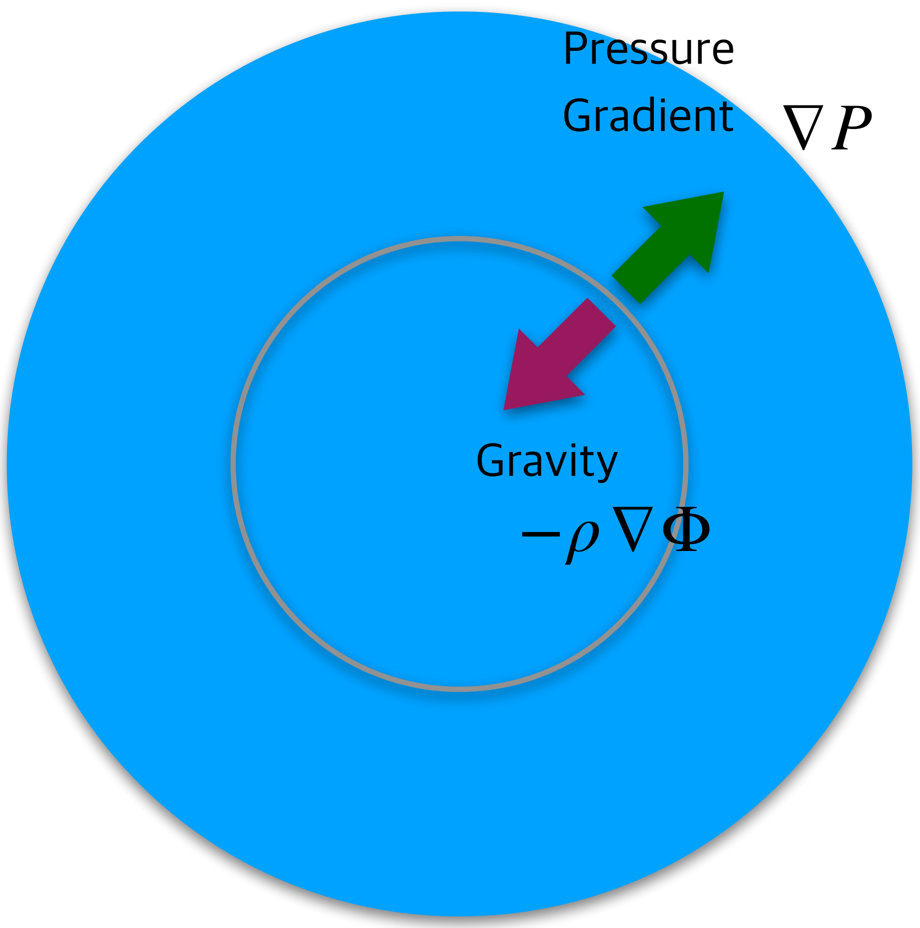

Let us revisit hydrodynamic (Euler) equation in spherical coordinates

1. Continuity Equation

$$\frac{\partial \rho}{\partial t} + \frac{1}{r^2}\frac{\partial}{\partial r}\left(r^2 \rho v\right) = 0,$$

2. Momentum Equation

$$\rho \frac{\partial v}{\partial t} + \rho v \frac{\partial v}{\partial r} + \frac{\partial P}{\partial r} = -\rho \frac{\partial \Phi}{\partial r},$$

3. Equation of State

$$P = K\rho^{\Gamma},$$

4. Poisson Equation

$$\frac{1}{r^2}\frac{\partial}{\partial r}\left(r^2 \frac{\partial \Phi}{\partial r}\right) = 4\pi G\rho.$$

Jinho Kim's slide

Linear Stability Analysis

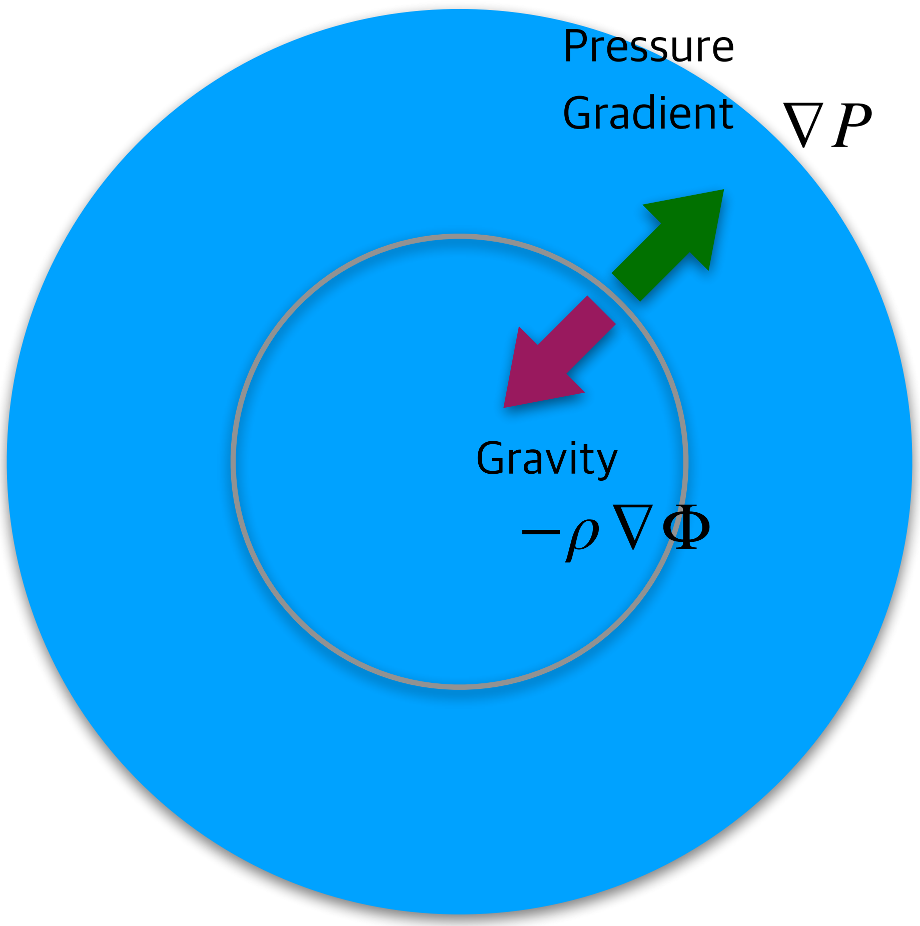

Equilibrium (background) solution

$$\frac{\partial P_0}{\partial r} = -\rho_0 \frac{\partial \Phi_0}{\partial r}.$$

Assume,

$$\rho = \rho_0 + \delta\rho,$$
$$P = P_0 + \delta P,$$
$$v = 0 + \delta v,$$
$$\Phi = \Phi_0 + \delta\Phi,$$

where subscript 0 denotes background (equilibrium) solution while δ-ed variables represents Eulerian perturbations.

We can define radial displacement, ζ, then the perturbation of velocity can be written as

$$\delta v = \frac{\partial \zeta}{\partial t}.$$

Jinho Kim's slide

Linear Stability Analysis

the linearized equations

1. Continuity Equation

$$\delta\rho + \frac{1}{r^2}\frac{\partial}{\partial r}\left(r^2\rho_0\zeta\right) = 0,$$

2. Momentum Equation

$$\rho_0\frac{\partial^2\zeta}{\partial t^2} + \frac{\partial\delta P}{\partial r} = -\rho_0\frac{\partial\delta\Phi}{\partial r} - \delta\rho\frac{\partial\Phi_0}{\partial r},$$

3. Equation of State

$$\frac{\delta P}{P_0} = \Gamma\frac{\delta\rho}{\rho_0},$$

4. Poisson Equation

$$\frac{1}{r^2}\frac{\partial}{\partial r}\left(r^2\frac{\partial\delta\Phi}{\partial r}\right) = 4\pi G\delta\rho.$$

We assume that the perturbation has a form as follows,

$$\zeta(t,r) = \xi(r)e^{i\omega t}.$$

All other δ-ed variables also follow the above form. Then the continuity and momentum equation become

$$\delta\rho + \frac{1}{r^2}\frac{\partial}{\partial r}\left(r^2\rho_0\xi\right) = 0,$$

$$-\rho_0\omega^2\xi + \frac{\partial\delta P}{\partial r} = -\rho_0\frac{\partial\delta\Phi}{\partial r} - \delta\rho\frac{\partial\Phi_0}{\partial r}.$$

Boundary condition:

1. $r = 0$: $\xi \sim r$
2. $r = r_s$: $\Delta P = 0$

Jinho Kim's slide

Mode Analysis : Non-radial Oscillations

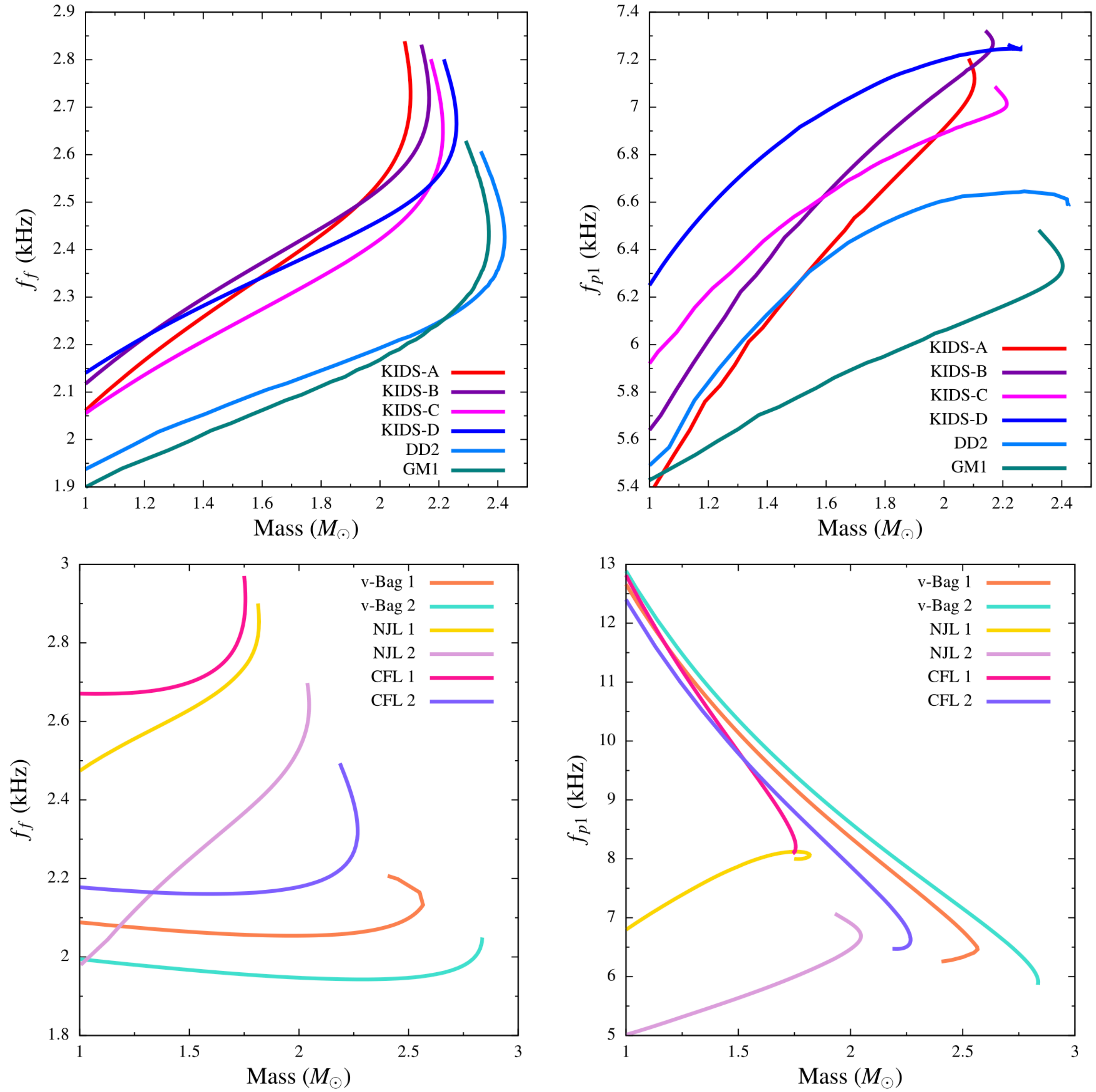

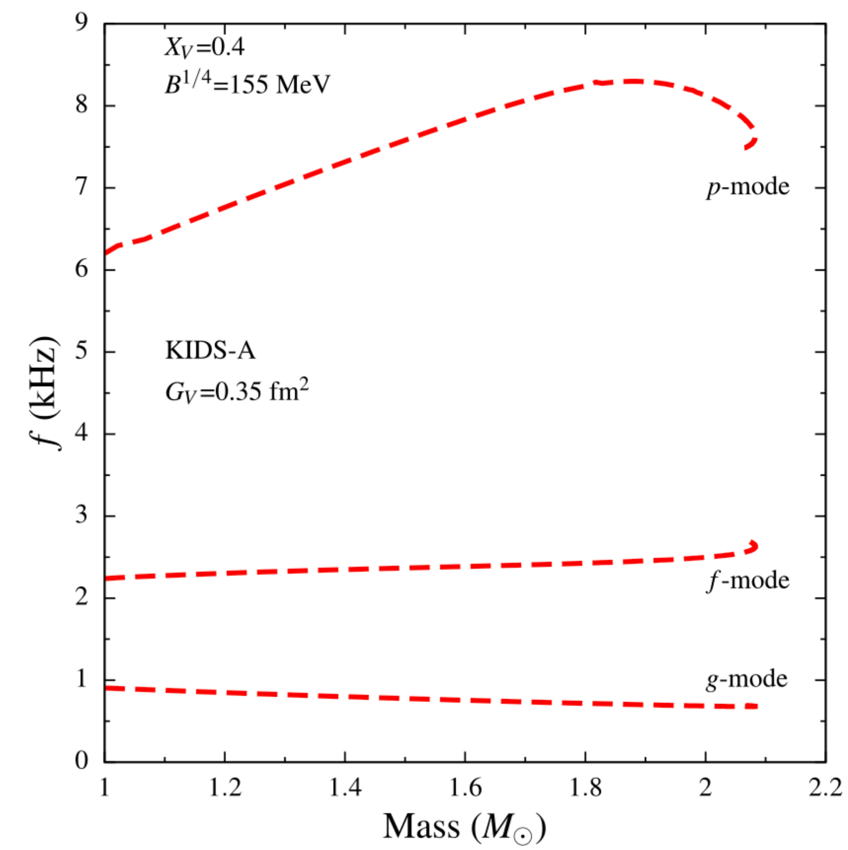

Eur. Phys. J. C (2025) 85:442

A. Guha, D. Sen, and Chang Ho Hyun

Dynamics of BNS merger

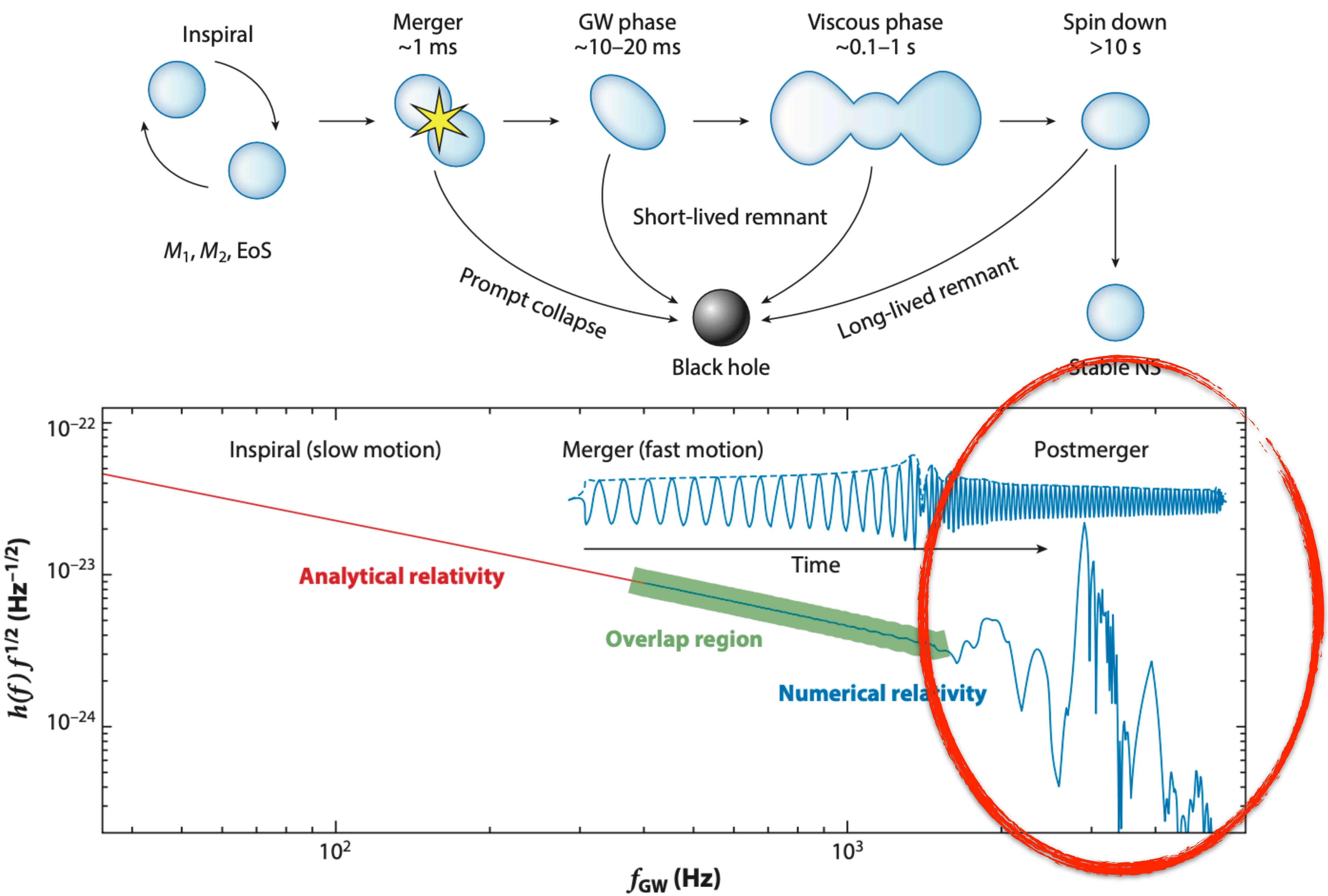

Radice et al. , Annu. Rev. Nucl. Part. Sci. 70, 95–119 (2020)

Poster-Merger signals

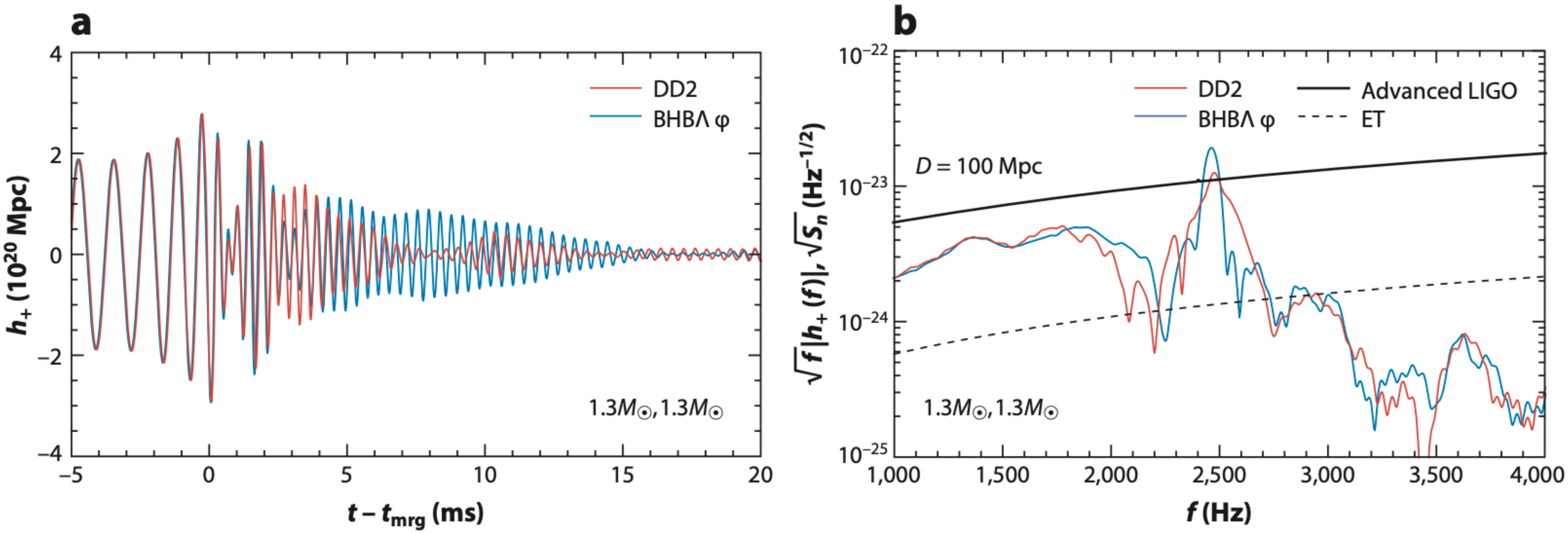

Radice et al. , Annu. Rev. Nucl. Part. Sci. 70, 95–119 (2020)

CW from rotating NS

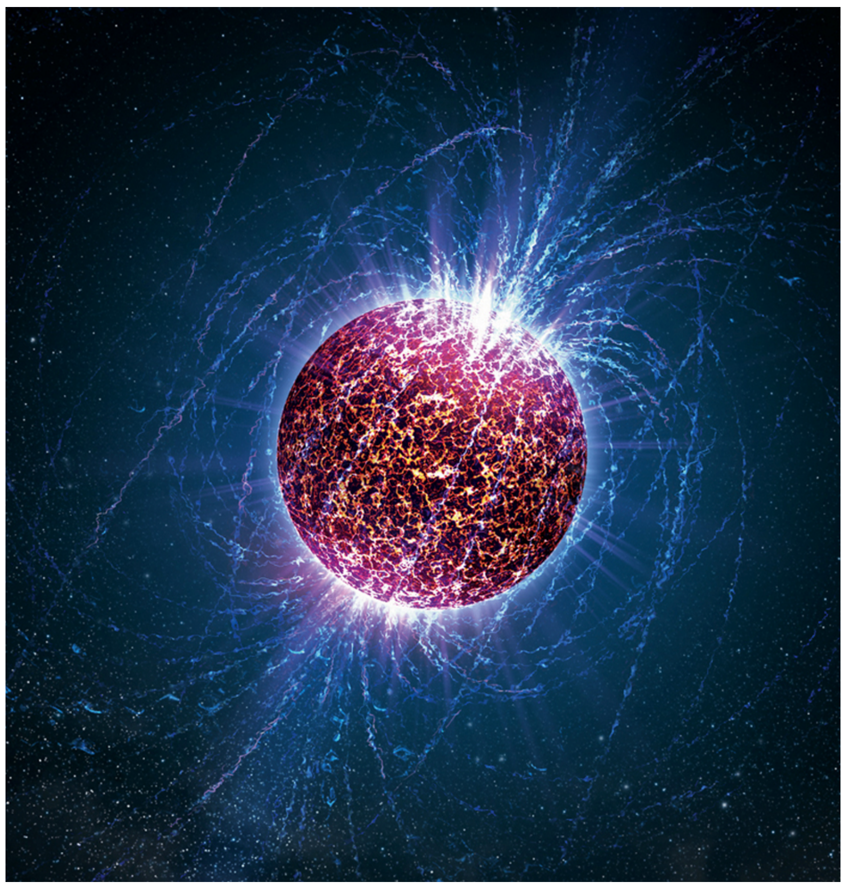

Credit: Casey Reed, Penn State

credit: A. Stuver/ LIGO

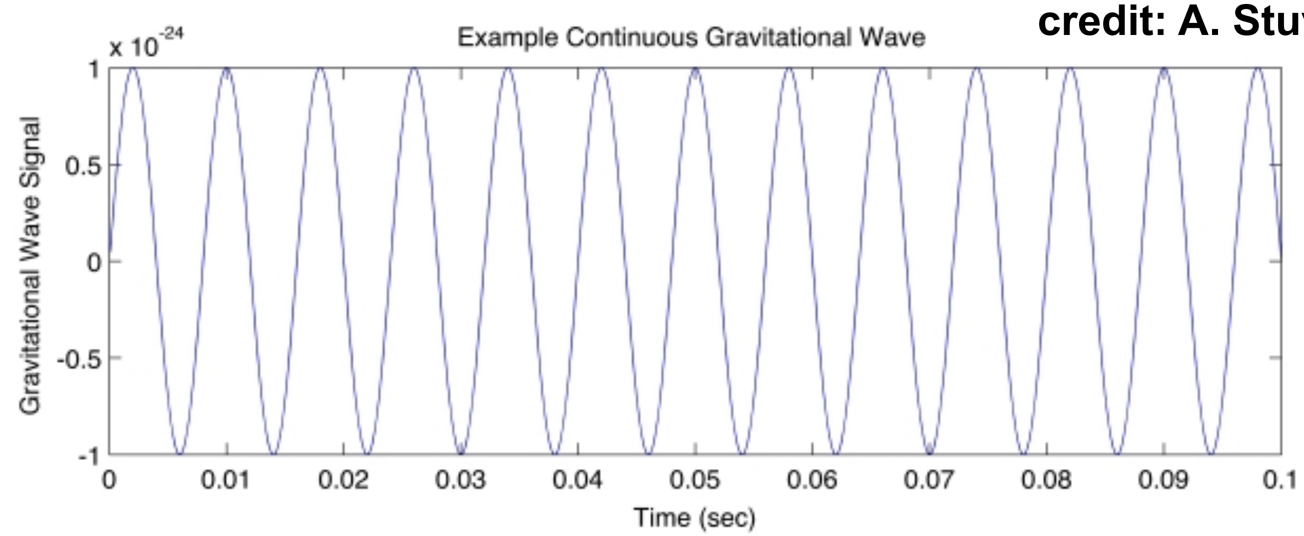

Phenomenological model

Keith Riles, Living. Rev. Rel. 26, 3(2023)

$$\dot{f} = K f^n$$

Breaking index

- $n = 1$—"Pulsar wind" (extreme model)
- $n = 3$—Magnetic dipole radiation
- $n = 5$—Gravitational mass quadrupole radiation ("mountain")
- $n = 7$—Gravitational mass current quadrupole radiation (r-modes).

$$h_0 = \sqrt{\frac{512\,\pi^7}{5}}\frac{G}{c^5}\frac{1}{d} f_{\rm GW}^3 \alpha M R^3 \tilde{J}$$

$$= 3.6\times 10^{-26}\left(\frac{1\,\rm kpc}{d}\right)\left(\frac{f_{\rm GW}}{100\,\rm Hz}\right)^3\left(\frac{\alpha}{10^{-3}}\right)\left(\frac{R}{11.7\,\rm km}\right)^3$$

$$h_{\rm spin-down} = \frac{1}{r}\sqrt{-\frac{45}{8}\frac{G}{c^3}I_{zz}\frac{\dot{f}_{\rm GW}}{f_{\rm GW}}},$$

Dynamics of BNS merger

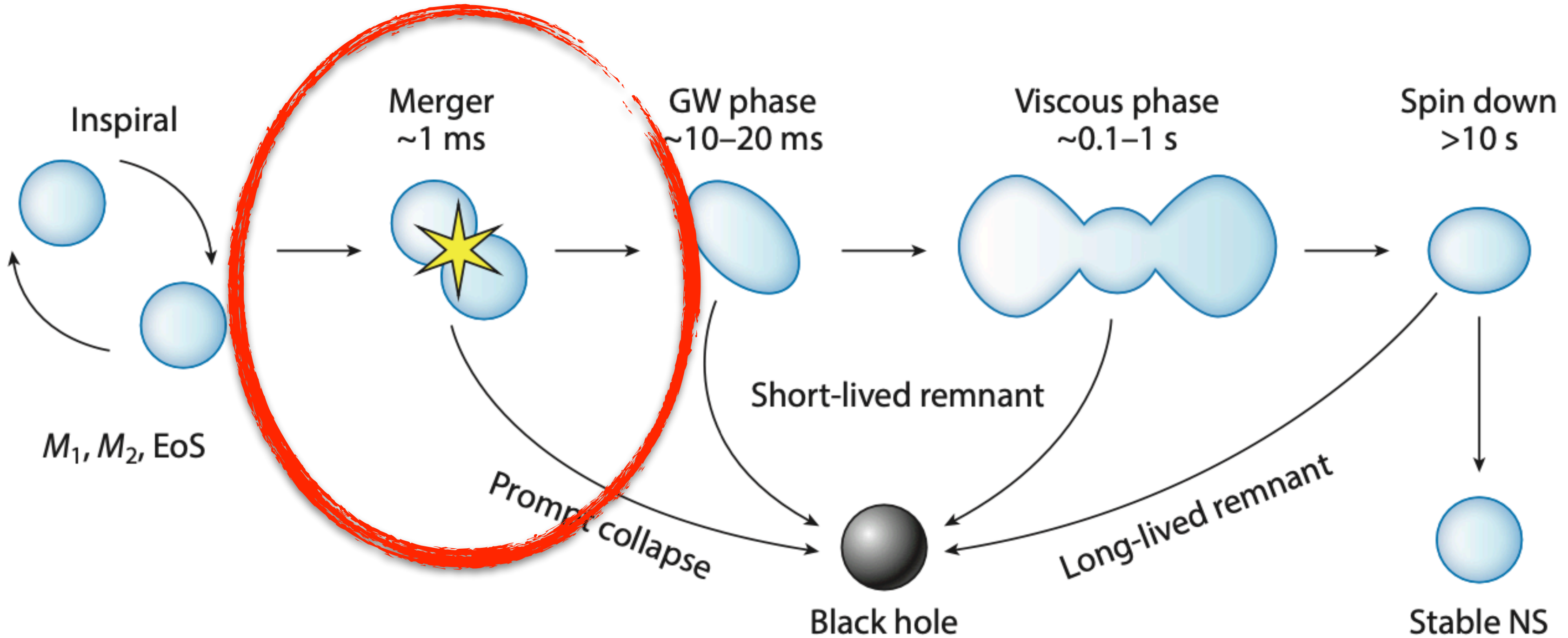

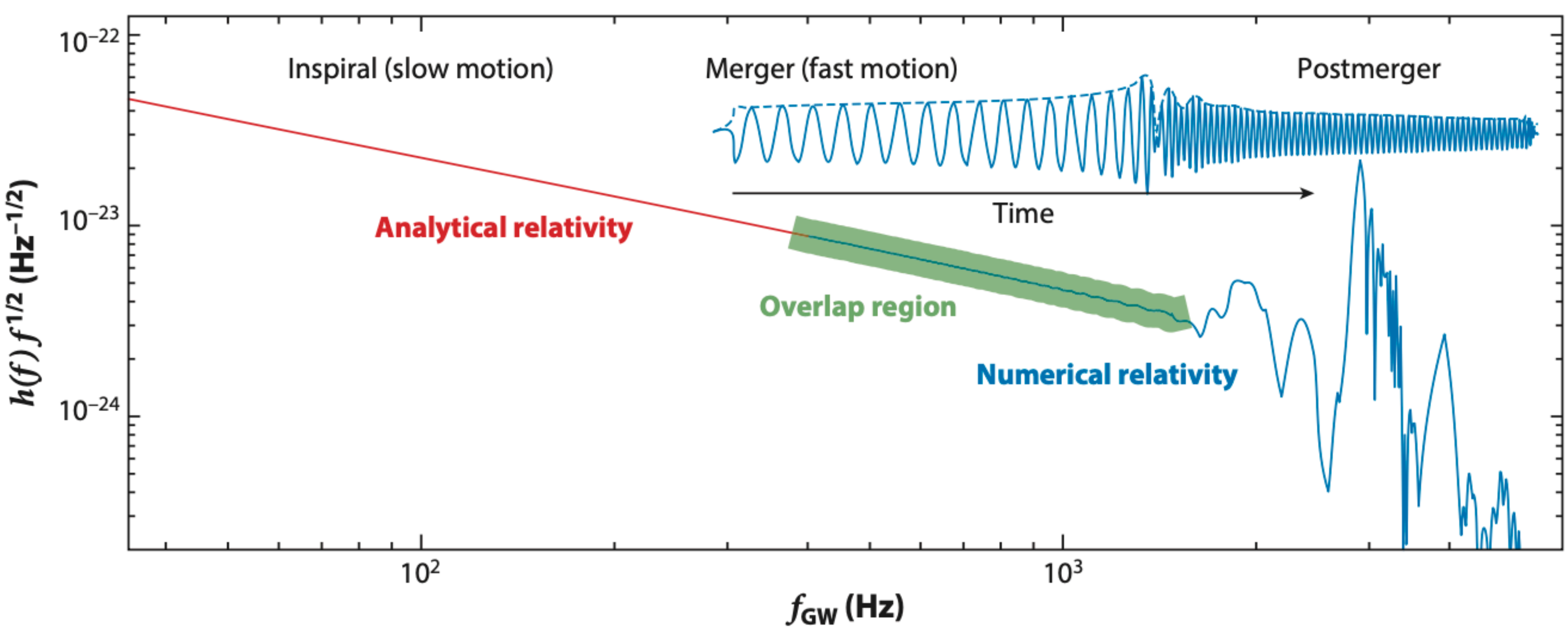

Radice et al., Annu. Rev. Nucl. Part. Sci. 70, 95–119 (2020)

EM followup of GW170817 : Kilonova

LETTER

doi:10.1038/nature24290

The X-ray counterpart to the gravitational-wave event GW170817

E. Troja[1,2], L. Piro[3], H. van Eerten[4], R. T. Wollaeger[5], M. Im[6], O. D. Fox[7], N. R. Butler[8], S. B. Cenko[2,9], T. Sakamoto[10], C. L. Fryer[5], R. Ricci[11], A. Lien[2,12], R. E. Ryan Jr[7], O. Korobkin[5], S.-K. Lee[6], J. M. Burgess[13], W. H. Lee[14], A. M. Watson[14], C. Choi[6], S. Covino[15], P. D'Avanzo[15], C. J. Fontes[5], J. Becerra González[16,17], H. G. Khandrika[7], J. Kim[6], S.-L. Kim[18], C.-U. Lee[18], H. M. Lee[19], A. Kutyrev[1,2], G. Lim[6], R. Sánchez-Ramírez[3], S. Veilleux[1,9], M. H. Wieringa[20] & Y. Yoon[6]

A long-standing paradigm in astrophysics is that collisions—or mergers—of two neutron stars form highly relativistic and collimated outflows (jets) that power γ-ray bursts of short (less than 2 seconds) duration[1–3]. The observational support for this model, however, is only indirect[4,5]. A hitherto outstanding prediction is that gravitational-wave events from such mergers should be associated with γ-ray bursts, and that a majority of these bursts should be seen off-axis, that is, they should point away from Earth[6,7]. Here we report the discovery observations of the X-ray counterpart associated with the gravitational-wave event GW170817. Although the electromagnetic counterpart at optical and infrared frequencies

On 17 August 2017 at 12:41:04 Universal Time (UT; hereafter T_0), the Advanced Laser Interferometer Gravitational-Wave Observatory (LIGO) detected a gravitational-wave transient from the merger of two neutron stars at a distance[12] of 40 ± 8 Mpc. Approximately two seconds later, a weak γ-ray burst (GRB) of short duration (<2 s) was observed by the Fermi Gamma-ray Space Telescope[13] and INTEGRAL[14]. The low luminosity of this γ-ray transient was unusual compared to the population of short GRBs at cosmological distances[15], and its physical connection with the gravitational-wave event remained unclear.

A vigorous observing campaign targeted the localization region of the gravitational-wave transient, and rapidly identified a source of

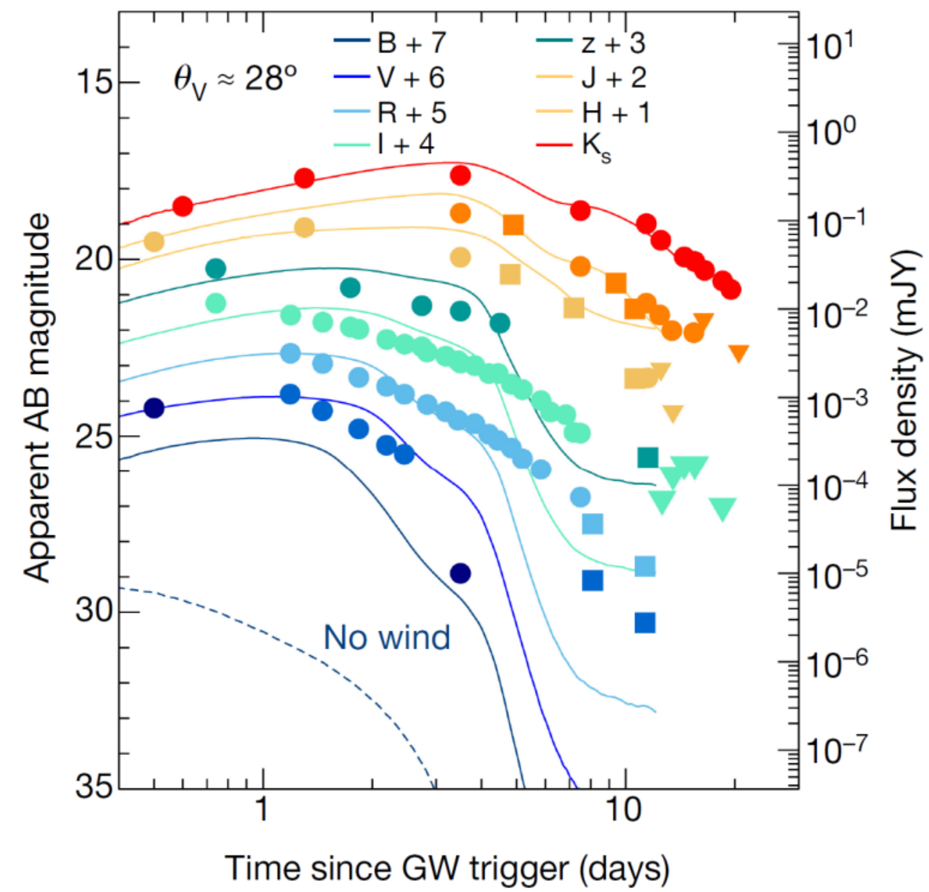

Troja et al. 2017 - Korean contributors: SNU (M. Im, S.-K. Lee, etc), and KASI

Heavy Elements from BNS mergers

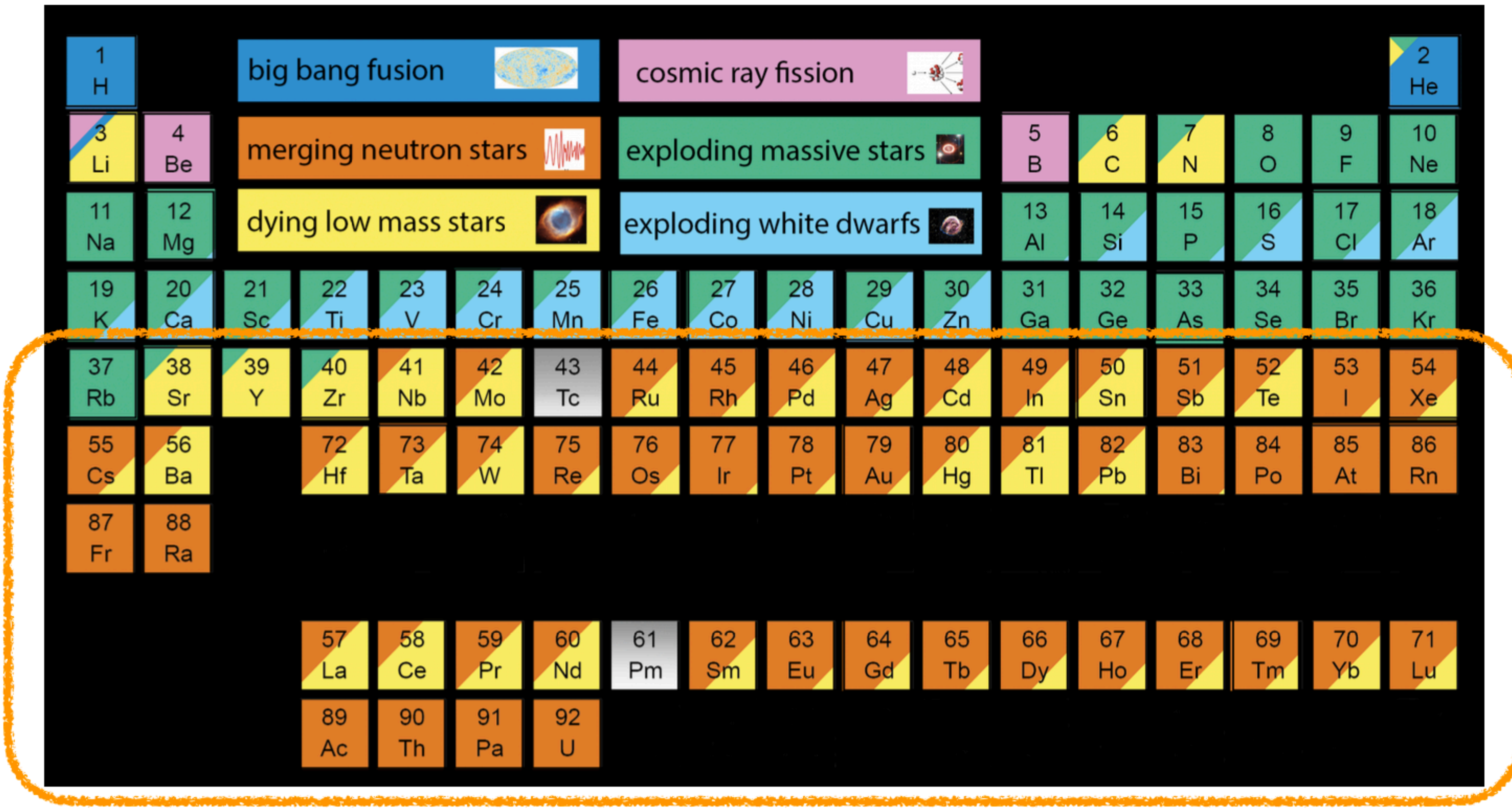

Constraints on the EoS

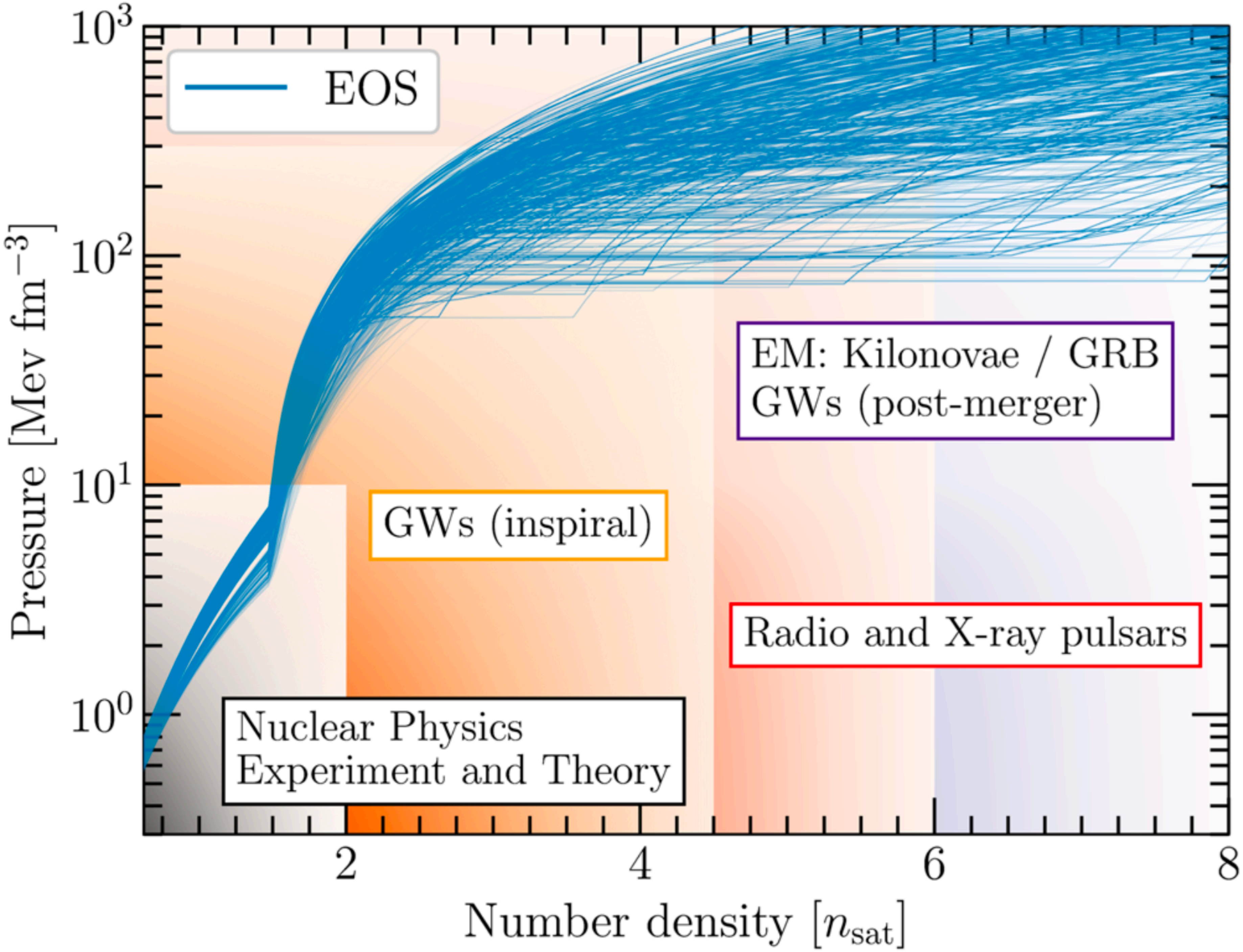

Nature Communications | (2023)14:8352

Next Generation GW detections

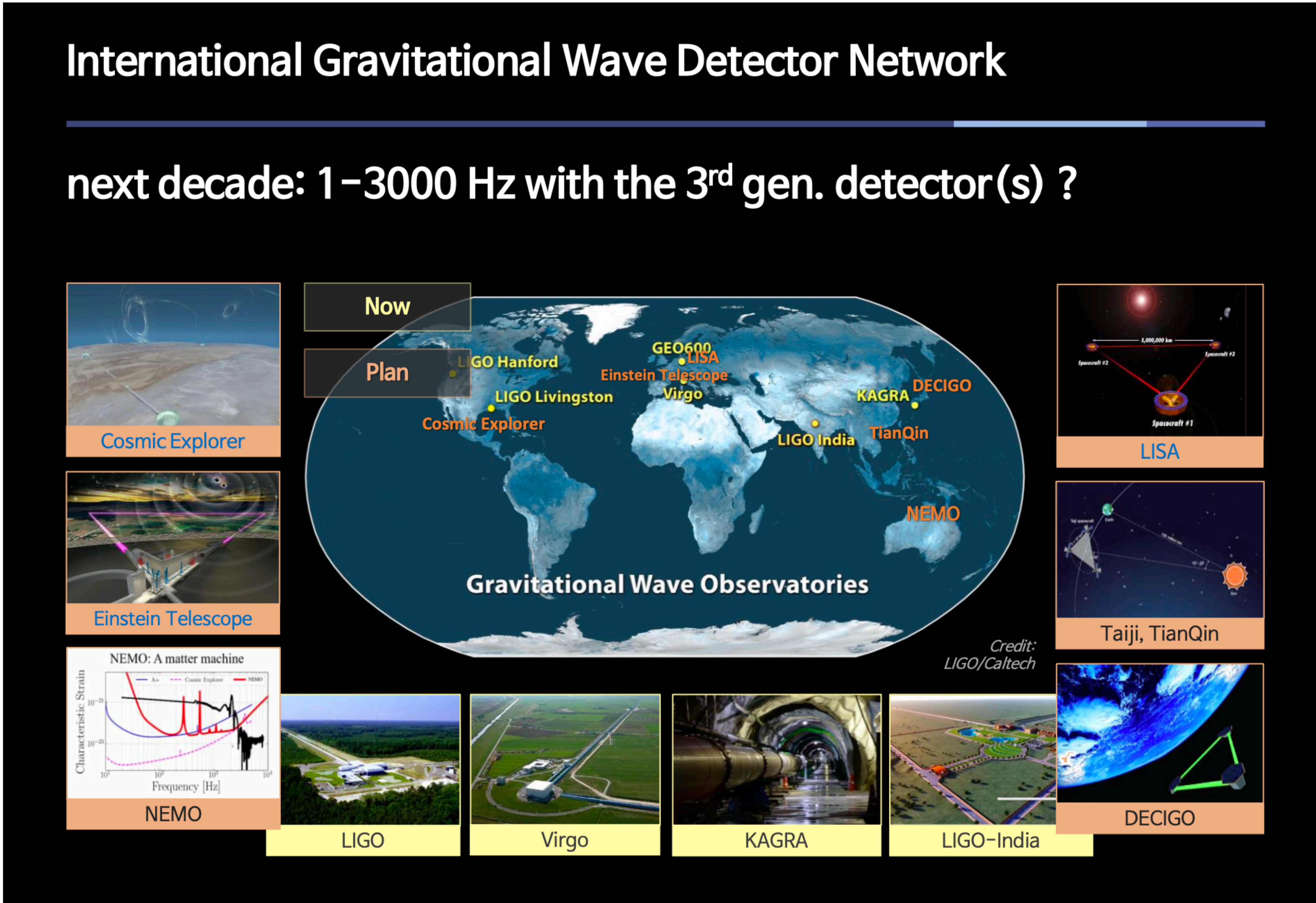

Next Generation GW detections

Einstein Telescope

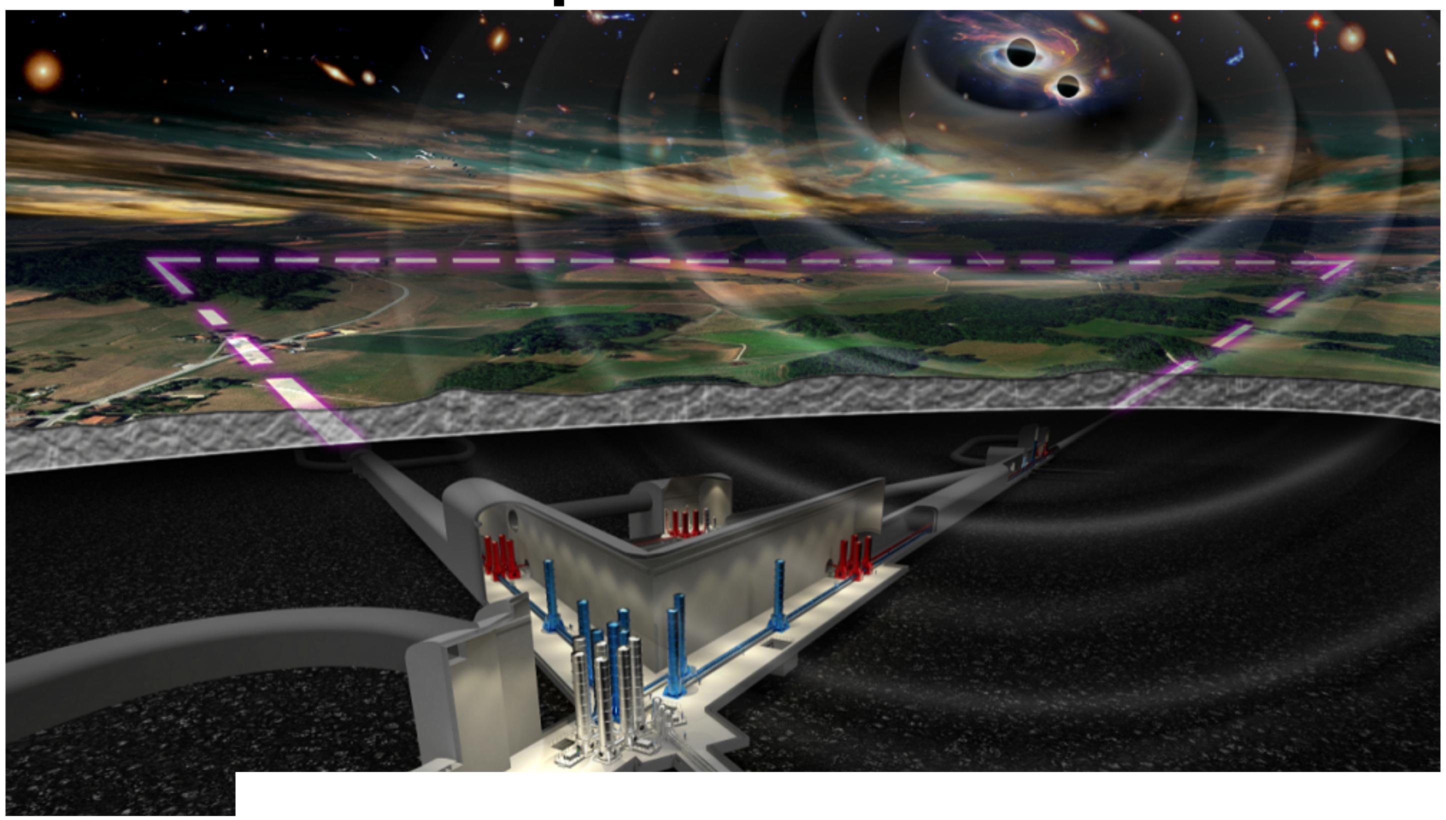

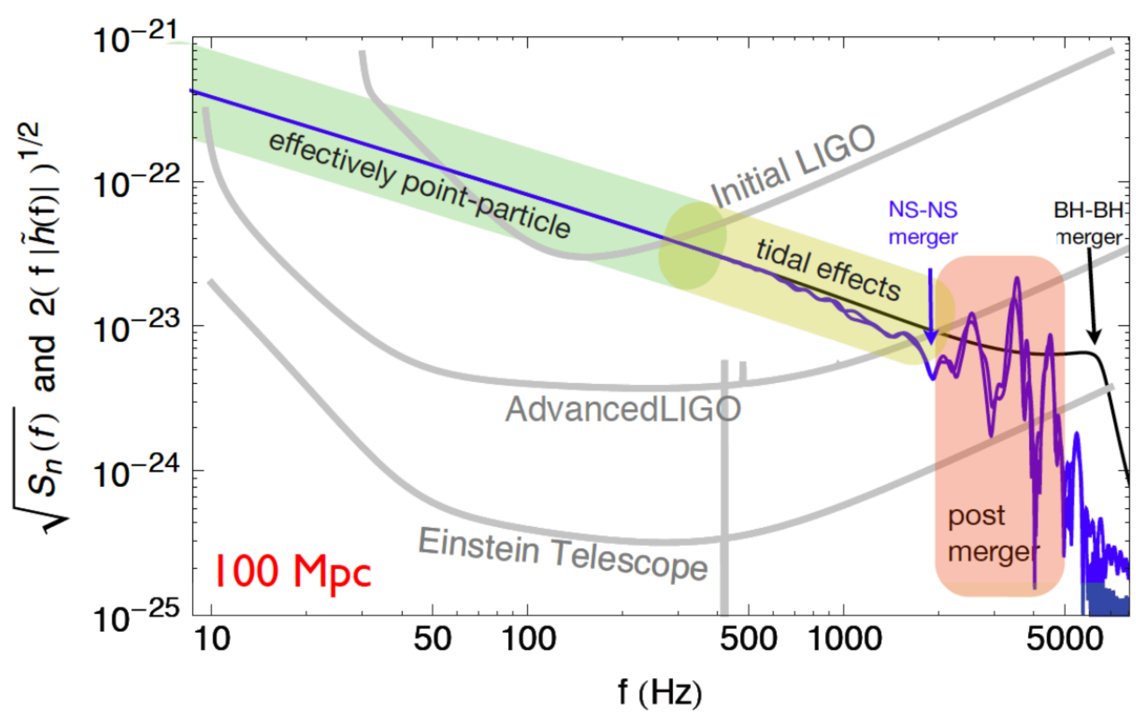

ET-bluebook

ET Korean RU

Summary

1. Through gravitational wave observations, we are detecting black hole collisions and establishing new constraints on stellar evolution.
2. By precisely measuring the physical properties of neutron stars through gravitational wave observations, we can conduct detailed studies of the internal equation of state of neutron stars.
3. Beyond measuring the mass, radius, and tidal deformability of neutron stars, studies of radial/non-radial oscillation modes enable research into the internal equations of state of neutron stars, which can be confirmed through gravitational wave observations.
4. By exploring a broader gravitational wave frequency range using next-generation gravitational wave detectors and expanding neutron star observations, research on high-density state equations can be conducted.

Thanks for your attentions

Contact : ymkim@kasi.re.kr

Tidal Love number and density profiles

PHYSICAL REVIEW D **81,** 123016 (2010)

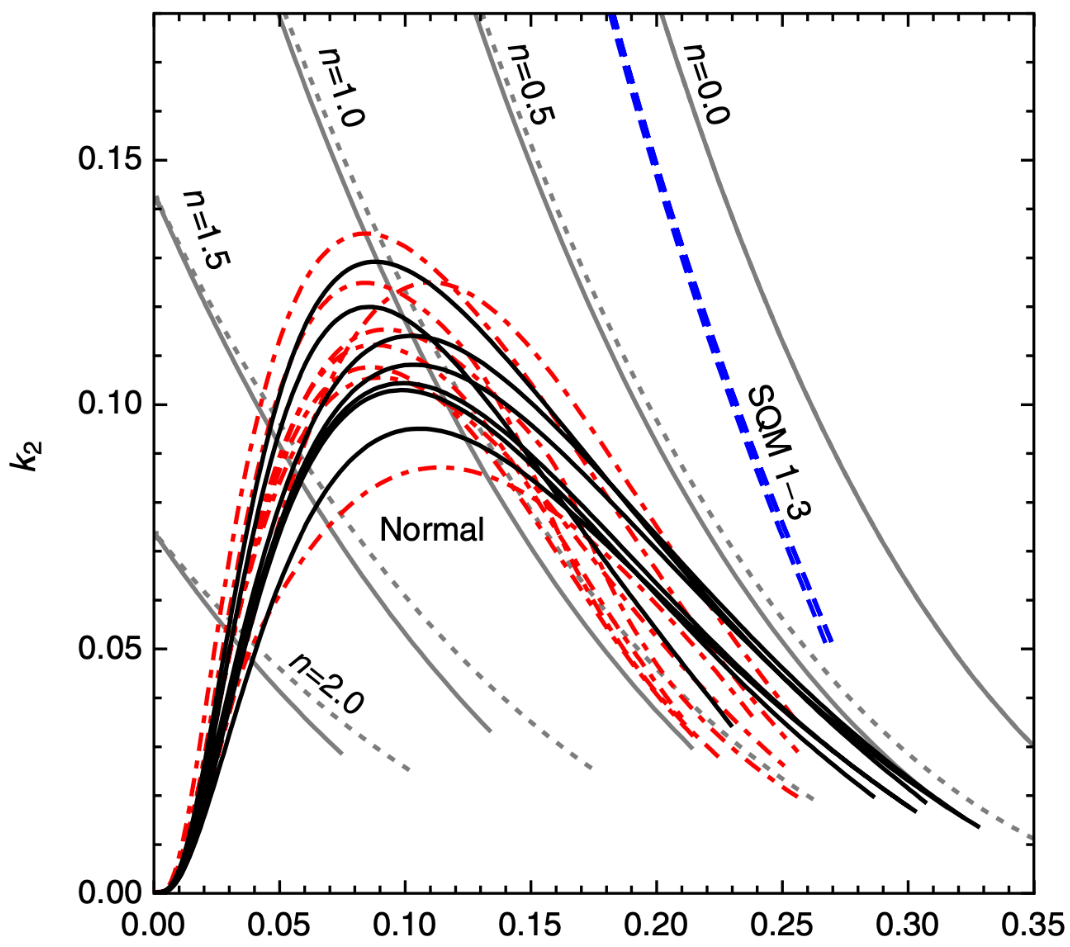

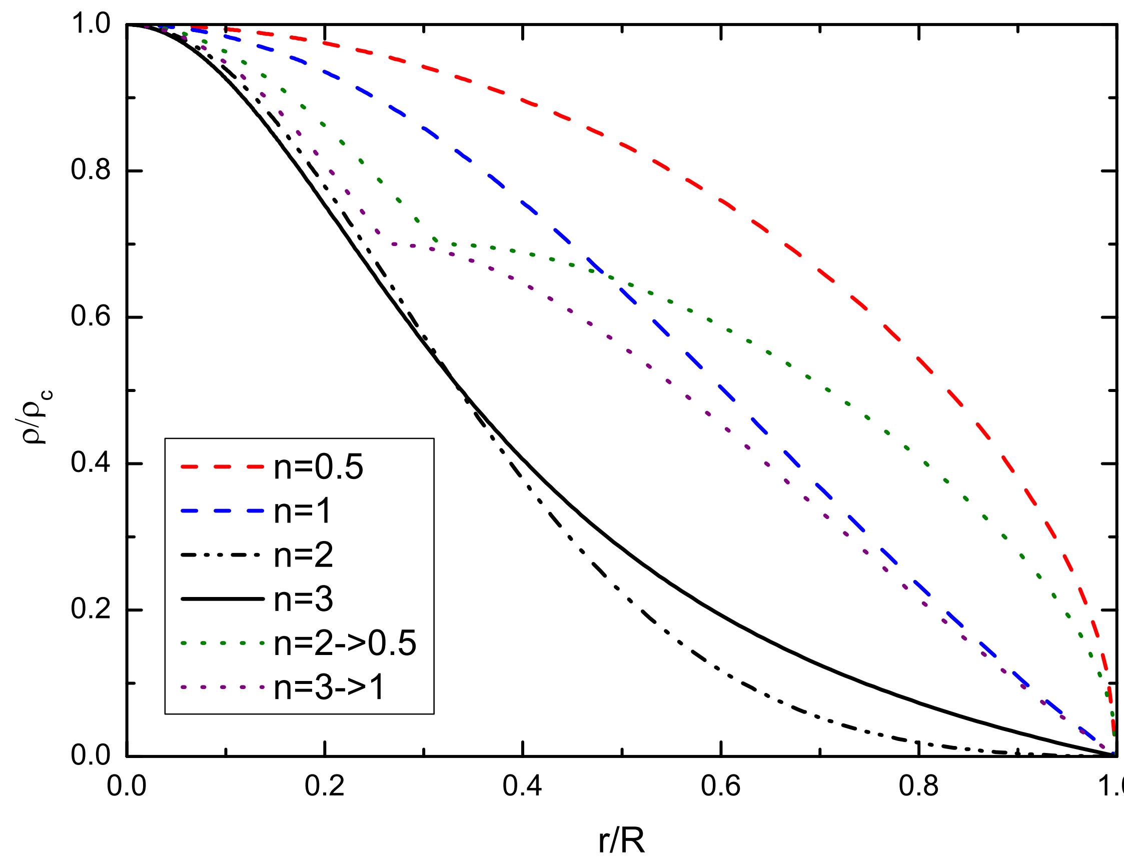

High k2

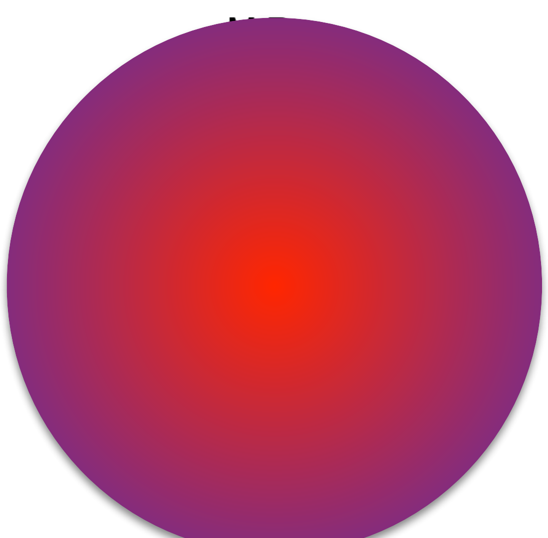

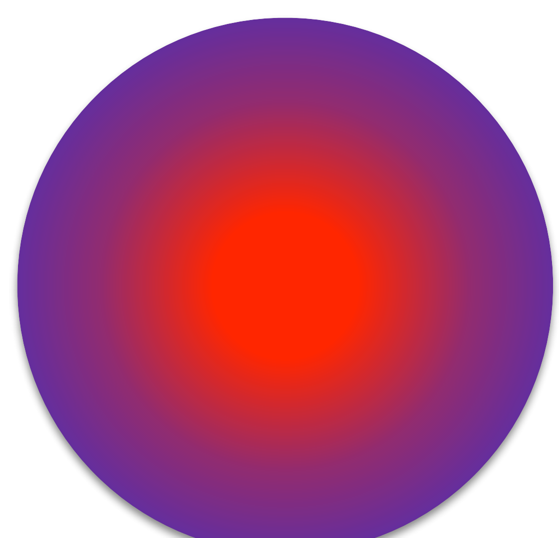

low k2

Tidal Love number, k2

Y.-M. Kim et al. (EPJA 2020)